Theses   Electronic Theses and Dissertations

11-2020

IMPACT OF DIFFERENT ENVIRONMENTAL CONDITIONS ON THE THERMO-MECHANICAL CHARACTERISTICS OF COMPACTED AND NON-COMPACTED CARBON/EPOXY PLAIN WEAVE WOVEN LAMINATED COMPOSITES

Maryam Hamad Helal Thabet Al Kuwaiti

United Arab Emirates University

College of Engineering

Department of Mechanical Engineering

IMPACT OF DIFFERENT ENVIRONMENTAL CONDITIONS ON THE THERMO-MECHANICAL CHARACTERISTICS OF COMPACTED AND NON-COMPACTED CARBON/EPOXY PLAIN WEAVE WOVEN LAMINATED COMPOSITES

Maryam Hamad Helal Thabet Al Kuwaiti

This thesis is submitted in partial fulfillment of the requirements for the degree of Master of Science in Mechanical Engineering

Under the Supervision of Professor Abdel-Hamid Ismail Mourad

November 2020

Declaration of Original Work

I, Maryam Hamad Helal Thabet Al Kuwaiti, the undersigned, a graduate student at the United Arab Emirates University (UAEU), and the author of this thesis entitled "*Impact of Different Environmental Conditions on the Thermo-Mechanical Characteristics of Compacted and Non-Compacted Carbon/Epoxy Plain Weave Woven Laminated Composites*", hereby, solemnly declare that this thesis is my own original research work that has been done and prepared by me under the supervision of Professor Abdel-Hamid Ismail Mourad, in the College of Engineering at UAEU. This work has not previously been presented or published, or formed the basis for the award of any academic degree, diploma or a similar title at this or any other university. Any materials borrowed from other sources (whether published or unpublished) and relied upon or included in my thesis have been properly cited and acknowledged in accordance with appropriate academic conventions. I further declare that there is no potential conflict of interest with respect to the research, data collection, authorship, presentation and/or publication of this thesis.

Student's Signature: _____   Date: 14 January 2021
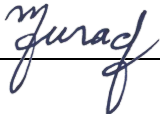
Approval of the Master Thesis

This Master Thesis is approved by the following Examining Committee Members:

1) Advisor (Committee Chair): Prof. Abdel-Hamid Ismail Mourad

   Title: Professor

   Department of Mechanical Engineering

   College of Engineering

   Signature _____ Date 14/01/2021

2) Member: Dr. Kassim Abdullah

   Title: Associate Professor

   Department of Mechanical Engineering

   College of Engineering

   Signature _____ Date 14/1/2021

3) Member (External Examiner): Dr. Manoj Gupta

   Title: Associate Professor

   Department of Mechanical Engineering

   Institution: National University of Singapore, Singapore

   Signature _____ Date 14/1/2021

This Master Thesis is accepted by:

Acting Dean of the College of Engineering: Professor Mohamed Al-Marzouqi

Signature _Mohamed AlMarzouqi_   Date _January 25, 2021_

Dean of the College of Graduate Studies: Professor Ali Al-Marzouqi

Signature _Ali Hassan_   Date _Janurary 25, 2021_

Copy ____ of ____

Abstract

Fiber reinforced polymeric composites used for aerospace applications are subjected to different environmental conditions during their operational life, such as moisture and temperature, which can adversely affect their performance over time. On the other hand, the standard fabrication process of these composite aircraft components requires a certain level of in-process vacuum compaction during the composite lay-up process to ensure the escape of entrapped air between the composite layers to prevent the formation of voids, through the application of bleeders/breathers around the composite laminate known for creating a channel for air to escape through. The aim of this study is to evaluate the effect of moisture and temperature on the integrity of plain weave woven carbon/epoxy laminated composites for both compacted and non-compacted groups, where the compacted group included the application of both in-process compactions during the composite lay-up process and the use of bleeders/breathers around the laminate, while the non-compacted group did not. Twelve-ply specimens were fabricated and immersed in water heating chambers maintained at different immersion temperatures of 40°C, 70°C and 95°C for a period of time that varied from one to 10 months. Mechanical, physical and thermal properties were experimentally investigated, and the effects of temperature, moisture, and immersion time on the deterioration of the composite material were studied against both compacted and non-compacted groups. Results revealed that moisture and temperature have a deteriorative impact on the performance of the composite, and it was observed that high temperatures accelerate the degradation mechanism in the composite. An insignificant difference was observed on the thermomechanical properties between compacted and non-compacted specimens at the immersion temperatures of 40°C and 70°C, but slight degradation was observed at the immersion temperature of 95°C, which indicates that in-process compaction and application of bleeders/breathers for twelve-ply monolithic laminates may be required at high temperature applications.

Keywords: Carbon/epoxy woven laminated composites, Effect of moisture and temperature, Mechanical and thermal properties, Comparison between compacted and non-compacted composites.

Title and Abstract (in Arabic)

تأثير الظروف البيئية المختلفة على الخصائص الميكانيكية والحرارية للمواد المركبة المضغوطة وغير المضغوطة المصنوعة من صفائح الكربون/الإيبوكسي المنسوج

الملخص

تتعرض المواد المركبة البوليمرية المقواة بالألياف (Fiber reinforced polymeric composites) المستخدمة في تطبيقات قطاع الطيران و الفضاء الجوي لظروف بيئية مختلفة خلال حياتها التشغيلية، مثل الرطوبة ودرجة الحرارة، والتي يمكن أن تؤثر سلبًا على أدائها بمرور الوقت. ومن جهة أخرى، تتطلب عملية تصنيع أجزاء هياكل الطائرات المصنوعة من المواد المركبة هذه على مستوى معيّن من الضغط و تفريغ الهواء (in-process vacuum compaction) أثناء عملية التصنيع (lay-up process) لضمان خروج الهواء المحتبس بين طبقات المادة المركبة لمنع تَكَوّن الفراغات (voids/porosity) فيها، من خلال تطبيق النازفات/المتنفسات (bleeders/breathers) حول الصفيحة المركبة التي تعرف بإنشاء قناة لخروج الهواء من خلالها. الهدف من هذه الدراسة هو تقييم تأثير الرطوبة ودرجة الحرارة على سلامة المواد المركبة المنسوجة من صفائح الكربون/ الايبوكسي لكل من المجموعتين المضغوطة وغير المضغوطة (compacted and non-compacted)، حيث تضمنت المجموعة المضغوطة تطبيق كل من عمليات الضغط أثناء عملية التصنيع، كما تضمنت استخدام النازفات/المتنفسات حول الصفائح، بينما لم تتضمنها المجموعة غير المضغوطة. تم تصنيع عينات مكونة من اثنتي عشرة طبقة وتم غمرها في غرف تسخين المياه محفوظة بدرجات حرارة مختلفة من: 40 درجة مئوية، 70 درجة مئوية، و 95 درجة مئوية لفترة زمنية تتراوح من شهر إلى 10 أشهر. تمت دراسة الخواص الميكانيكية والفيزيائية والحرارية اختباريا ودراسة تأثيرات درجة الحرارة والرطوبة وزمن الانغماس على تدهور المادة المركبة ضد كل من المجموعتين المضغوطة وغير المضغوطة. أظهرت النتائج أن الرطوبة ودرجة الحرارة لهما تأثير سلبي على أداء المواد المركبة، كما لوحظ أن ارتفاع درجات الحرارة تسرع من آلية التحلل في المواد المركبة. أشارت النتائج إلى وجود اختلاف ضئيل في الخواص الحرارية الميكانيكية بين العينات المضغوطة وغير المضغوطة عند درجات حرارة الغمر البالغة 40 درجة مئوية و70 درجة مئوية، ولكن لوحظ تدهور طفيف عند درجة حرارة الغمر البالغة 95 درجة مئوية، مما يشير إلى

أن الضغط أثناء عملية التصنيع وتطبيق النازفات/المتنفسات للصفائح المكونة من اثني عشر طبقة قد يكون مطلوبًا في تطبيقات درجات الحرارة العالية.

مفاهيم البحث الرئيسية: المواد المركبة من صفائح الكربون/الإيبوكسي المنسوج، تأثير الرطوبة ودرجة الحرارة، الخصائص الميكانيكية والحرارية، مقارنه بين المواد المركبة المضغوطة وغير المضغوطة.

Acknowledgements

Dedication

To my beloved mom and dad

Table of Contents

List of Tables

List of Figures

List of Abbreviations

BMI	Bismaleimide
C	Compacted (test group)
C/C	Carbon/Carbon Composites
CMC	Ceramic Matrix Composites
CNC	Computer Numerical Control
DMA	Dynamic Mechanical Analysis
DSC	Differential Scanning Calorimetry
FOD	Foreign Object Debris
FRP	Fiber Reinforced Polymers
HT	High Temperature
ILSS	Interlaminar Shear Strength
MMC	Metal Matrix Composites
MPE	Manual Pulse Echo
NC	Non-Compacted (test group)
NC	Numerically Controlled
NDT	Non Destructive Testing
PE	Pulse Echo
PMC	Polymer Matrix Composites
PMMA	Poly Methyl Methacrylate
ROI	Region of Interest
RT	Room Temperature
SEM	Scanning Electron Microscopy
Tg	Glass Transition Temperature

TT   Through Transmission

UD   Unidirectional

UT   Ultrasonic Testing

Chapter 1: Introduction

1.1 Overview of Composites Use in Aerospace

Fiber Reinforced Polymeric (FRP) composite materials have been increasingly used in advanced structural applications due to their high performance characteristics over extended period of time [1]. The aerospace industry has been one of the primary drivers in the development of lightweight high-performance composites materials over the last few decades. The significant growth in the use of FRPs in aerospace applications is due to the fact that advanced composite systems offer an advantage over traditional metallic aircraft materials, as they tend to demonstrate higher strength-to-weight and stiffness-to-weight ratios, and show less sensitivity to fatigue and corrosion, thus reducing aircraft weight and improving performance [2].

Commercial aircrafts have experienced substantial growth in the use of composites over the decades since the late 1950s, as shown in Figure 1; however the implementation of it occurred gradually overtime in three phases due to high airworthiness safety standards [3]. Composite materials were first used on tertiary components such as interior parts, which do not impact the aircraft's flying capability. In the late 1960s, composites (mainly fiberglass) were incorporated into secondary aircraft structures such as ailerons, spoilers, flaps, and rudders, only after the composite interior parts have proven to be efficient, although fiberglass was later on replaced by carbon in most of these secondary structures in the 1970s. The most important implementation is with the introduction of composites into primary airframe structures of commercial aircrafts such as the fuselage, vertical and horizontal stabilizers and wings, which took place gradually over the past 30 years. Figure 2

shows the increasing use of composites in Boeing's commercial aircrafts, where composites on the 787 Dreamliner account for 50% of the aircraft's structural weight, in contrast to the 747 aircraft which consists of only 1% [3].
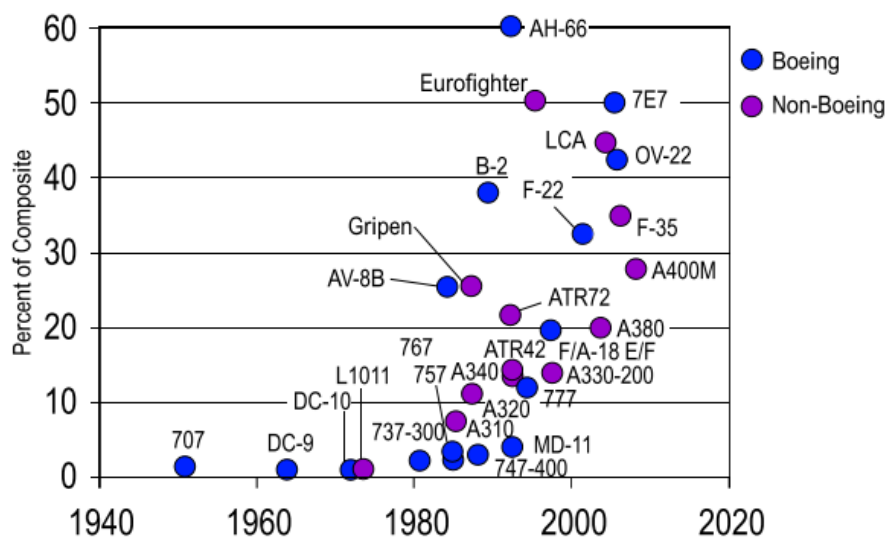
Figure 1: Increase in the use of composites in aircraft components [3]
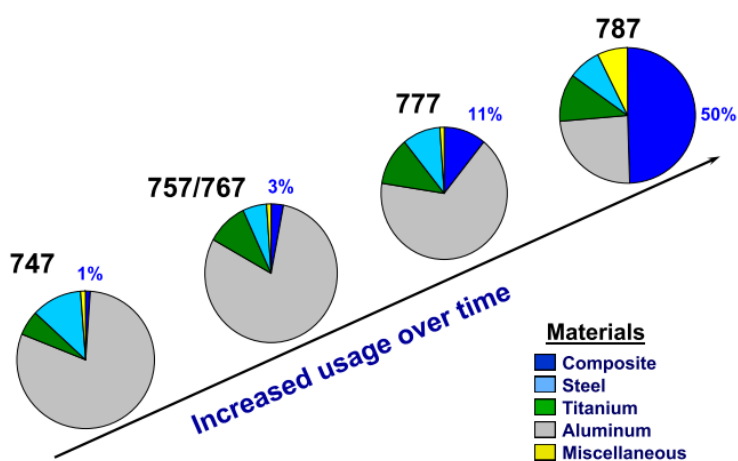
Figure 2: Increased composite usage in Boeing's commercial aircrafts over time [3]

Pre-impregnated carbon fiber fabric laminate is the main composite material used in the fabrication of aircraft components [4]. As shown in Figure 3, carbon

laminate is the primary composite applied in the manufacturing of the 787 Dreamliner, in addition to carbon sandwich and other types of composite materials such as glass fiber.
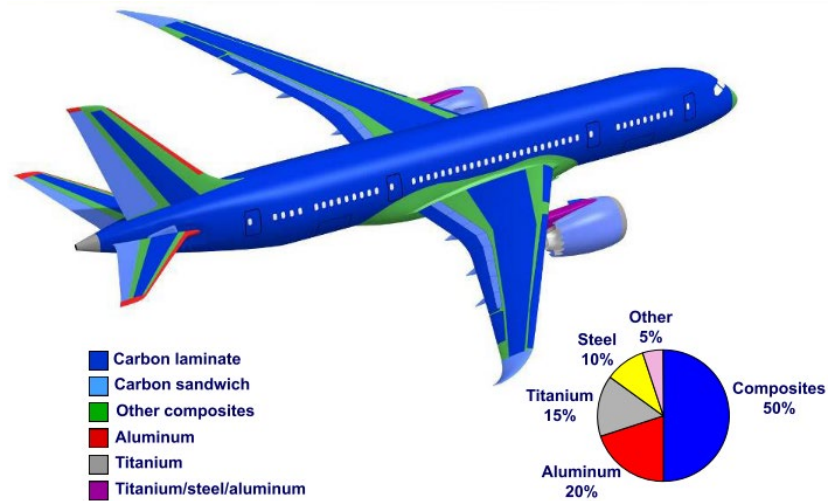
Figure 3: Application of composite materials in the 787 Dreamliner [3]

Laminated composites are the most commonly used composite materials in the different aerospace applications. This type of composites is fabricated through the lay-up process of assembling a number of composite layers to construct the laminate as shown as shown in Figure 4 [5]. When pre-impregnated composite layers are used to fabricate the laminate, the process is known as the dry lay-up process [6].
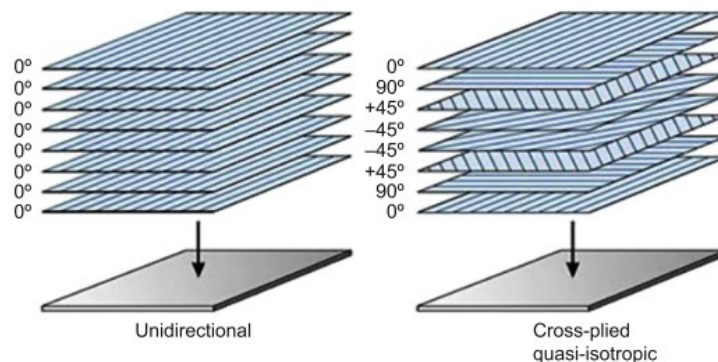
Figure 4: Schematic representation of laminated composites [5]

The standard fabrication process of composite aircraft components requires a certain level of vacuum compaction (debulking) during the composite lay-up process. Compaction is the process of applying vacuum by placing a vacuum bag around the composite lay-up for a specified period of time. Compaction is performed during the composite lay-up process to ensure the escape of entrapped air between the composite layers, which if trapped, would cause voids in the composite component known as porosity, that would generally be detected by non-destructive testing [6]–[8].

Performing compaction during the lay-up process is referred to as "In-Process" compaction and is repeated a number of times depending on different parameters such as the number of plies, plies thickness, and the shape of the laminate. "Final" compaction is performed when all the composite layers of the laminate have been laid, where pressure is applied and maintained throughout the cure cycle. Figure 5 shows a conventionally vacuum bagged part, where the laminate is sealed in an air-tight environment using a vacuum bag connected to a vacuum source. Applying vacuum removes the air within the bag and exerts pressure on the laminate, therefore compacting and consolidating it [9].
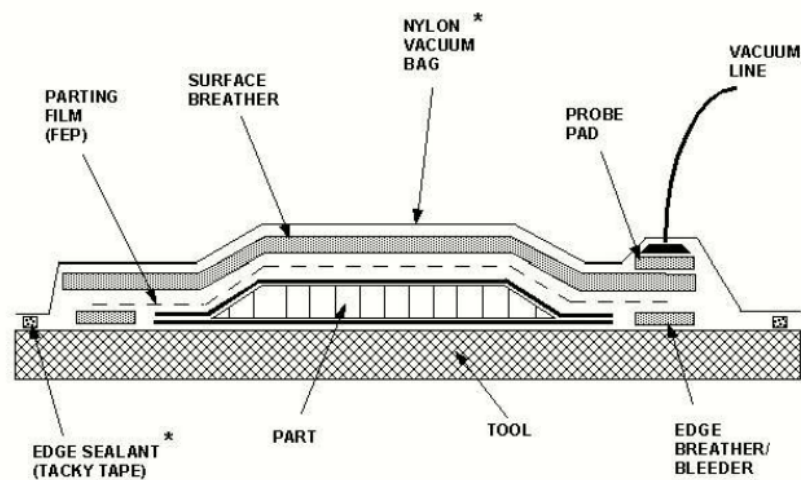
Figure 5: Traditional vacuum bag with edge and surface breathers/bleeders [7]

Epoxy resins release gases and volatiles during cure, and breathers/bleeders have been typically used, as embodied in current aerospace specifications, to remove the evolved volatiles from the composite to prevent porosity. Edge and surface breathers/bleeders are non-structural porous materials that are used during the compaction process to create a continuous air channel (path) within the vacuum bag to allow gasses inside the bag to escape through. A bleeder is used when composite components are manufactured to allow excess gas and resin around the periphery of the composite part to escape during the cure cycle, and serves as a vacuum contact between the part and breather during the curing process, as shown in Figure 5. A breather is a loosely woven material, which serves as a continuous vacuum path over a part but does not come in contact with the pre-impregnated material. Both bleeder and breather cloths are not part of the final composite, and are disposed after the cure [6], [7].

1.2 Statement of the Problem

Composite materials have been widely recognized for playing a major role in weight reduction over the last decades, however the novel and unconventional nature of composites (compared to metals) has undeniably brought on their own challenges and complexities. Satisfying the high degree of reliability and safety requirements of aerospace structures is of a particular concern for composites, due to their unconventional complex structure, the limited information on their complex behavior due to less experience on composites compared to metals [5], and the challenges in creating accurate and reliable prediction models. Composites are anisotropic, non-homogeneous, and exhibit complex material behavior under load, which is not always analytically predictable. Although advanced computational technology and numerical

methods have played a vital role in overcoming such challenges [10], the long-term durability of composites with regards to environmental degradation and impact damage is generally not understood and has therefore created an unavoidable reliance and need for excessive material testing.

During their operational life, these FRP composite structures are typically exposed to different environmental conditions, such as moisture, humidity and temperature, which can affect their long-term mechanical, thermal and physical properties. Therefore, in order to use these materials, it is important to evaluate what adverse effects these conditions would have on the performance and durability of the composites [1].

Impact of environmental factors such as temperature and humidity on fiber reinforced polymers behavior is of a significant concern for aircraft applications, since operational and storage conditions differ considerably and can add to the wear and tear of the aircraft's structural components [11]. Literature has shown that both physical and mechanical properties of composite materials can be strongly affected when exposed to deteriorative environmental conditions involving temperature and humidity, affecting the composite performance [12]. Water absorption in FRPs generally leads to swelling and plasticization of the polymer, which leads to a decrease of the glass transition temperature and deterioration of the mechanical properties [13]. Higher temperatures are also known to accelerate the moisture absorption and degradation process [14]. Characterizing these effects are required and critical to prevent unexpected failures, and with the increasing applications of these materials, there is a pressing need to evaluate and quantify the extent of environmental

degradation on the deviation of mechanical, thermal and physical properties of fiber/polymer composites [11].

On the other hand, when composite parts are manufactured, vacuum compaction is applied to remove air between the composite plies to prevent porosity and void formation by means of using surface and edge bleeders/breathers. Vacuum compaction process is particularly important when thick laminates are manufactured, or complex shaped geometries are involved [15]. In-process compaction is a repetitive, and time-consuming process due to the compaction waiting time required, and the time and effort involved in preparing the vacuum bag. Traditional vacuum bagging processes for autoclave cured composite parts require all the components of the vacuum bag to be custom made for every part which typically include: edge breather/bleeder, surface breather, edge sealant, release/parting film, and nylon vacuum bag. These components are prepared and cut manually by hand to fit the specific composite part being bagged, applied over the part, and then disposed once the part is cured. Although in-process compactions are essential for thick laminates, it might be unnecessary for components with a low number of laminas, as one final vacuum compaction could be sufficient rather than multiple in process compactions during the fabrication process. Understanding the effect of removing in-process vacuum compactions and compaction breathers/bleeders is important in potentially reducing material cost, manual effort and process time, and therefore requires further investigation [7], [8].

Fiber reinforced polymer composite structures are expected to experience a range of environmental conditions during its operational life. Since temperature and absorbed moisture can influence the composite performance by degrading the

materials properties, understanding of the behavior is critical for predicting structural performance. Moreover, no published work was found that deals extensively with studying the environmental effects on the durability of plain weave woven carbon/epoxy composite in combination to studying the effect of eliminating in process vacuum compaction and usage of breathers/bleeders in the composite manufacturing process.

Therefore, to improve reliability of aerospace structures and sustain a steady growth in the use of composites, future efforts should be geared towards attaining a better understanding of the compaction processes in composite fabrication, in addition to attaining a better understanding of degradation mechanisms resulting from long term exposure to different environmental conditions [5].

1.3 Significance of the Study

The standard fabrication process of composite aircraft components requires a certain level of vacuum compaction during the composite lay-up process, in addition to the application of edge and surface breathers/bleeders around the part in order to aid the air removal process of entrapped air between the composite layers, that if trapped would result in voids/porosity. Vacuum compaction and the use of edge/surface breathers/bleeders are factors that affect the formation of voids/porosity in composites and is associated with the material performance and characteristics. Most work on the effects of voids in the literature deals with studying the performance of composite laminates; however little experimental data are available on the impact of voids (or compaction and use of bleeders/breathers) on the performance and durability of composite materials that are exposed to long-term environmental conditions such as temperature and moisture. This work aims to study the impact of long-term

environmental exposure on compacted and non-compacted woven laminated composites, and to compare between the two groups.

This study aims to fill the existing literature gap relating to the impact of long-term environmental exposure on compacted and non-compacted composites, as it aims to provide knowledge of the composite material behavior and contribute to the composites research area. This work findings will provide industrial companies and sectors, in which composite materials are utilized, such as STRATA with data and knowledge of such materials for designing and manufacturing better products.

1.4 Project Objective

The objective of this study is to evaluate the impact of long-term effects of different environmental conditions on the durability of compacted and non-compacted plain weave woven carbon/epoxy laminated composites. In this study, durability is defined as the ability of a composite material to maintain its original physical, thermal and mechanical properties when exposed to different environmental conditions of temperature and moisture/humidity. The material studied is representative of composite material used in the manufacturing of aircraft structural components.

The effect of compaction and use of bleeders is also investigated in this study, where the composites specimens were divided into two groups, compacted and non-compacted. The difference between the two test groups is that the compacted group had undergone: (i) In-process compactions between the composite layers during lay-up, and (ii) Used glass fiber edge and surface bleeders in the final bagging of the test panels, whereas the non-compacted group did not [8].

To study the impact of different environmental conditions on the integrity of plain weave woven laminated composites, both compacted and non-compacted composite specimens were immersed in water heating chambers maintained at different temperatures of 40°C, 70°C and 95°C for a period of time that varied from one month up to 10 months. Mechanical, physical and thermal properties were experimentally investigated on a twelve-ply laminate, and the effects of temperature, moisture, and immersion time on the deterioration of the material were studied against both compacted and non-compacted groups [16].

This study will be mainly focusing on the specific objectives mentioned below:

- Evaluate the impact of removing both "in-process" compactions and the use of edge and surface bleeders/breather on the integrity of the laminate, porosity/void level, mechanical, thermal and physical microstructural properties by comparing the material properties of exposed compacted and non-compacted test results.

- Evaluate the weight change of compacted and non-compacted samples due to long-term water immersion at different immersion temperatures of 40°C, 70°C and 95°C.

- Evaluate the impact of long-term water immersion exposure (at different immersion temperatures of 40°C, 70°C and 95°C) on the degradation of mechanical properties of compacted and non-compacted samples by conducting the following tests:
    - Tensile at RT.
    - Tensile at HT (For control compacted samples at testing temperatures of 70°C and 90°C).

- ▪ Flexural.

- ▪ Interlaminar Shear Strength (ILSS).

- Evaluate the impact of long-term water immersion exposure (at different immersion temperatures of 40°C, 70°C and 95°C) on the thermal properties (glass transition temperature) of compacted and non-compacted samples by conducting the following tests:

  - ▪ DSC.

  - ▪ DMA.

- Evaluate the impact of long-term exposure on the physical and microstructural properties of compacted and non-compacted samples by conducting the following tests:

  - ▪ Ultrasonic Non-Destructive Testing.

  - ▪ Microsections void %.

  - ▪ Water Absorption Test.

  - ▪ Scanning Electron Microscopy.

- Evaluate the actual need for compaction and usage of bleeders/breathers on a twelve-layer flat composite panel, based on the test results obtained due to the combined effect of long-term water exposure at different immersion temperatures, and the implementation of both "in process" compactions and edge and surface breathers on the composite performance.

1.5 Thesis Outline

This thesis consists of five chapters and the focus of each chapter is described in this section. The flow of the thesis work presented in this report follows the sequence outlined herein:

Chapter 1: Introduction

This chapter discusses the overview and background of the use of composites in aerospace industry, and the project's main objectives.

Chapter 2: Literature Review

This chapter provides a literature review to outline and summarize the research conducted and relative literature available about the topic of interest.

Chapter 3: Materials and Research Methods

This chapter provides information about the materials, fabrication process, samples preparation, and characterization testing techniques used in this study.

Chapter 4: Results and Discussion

This chapter discusses the main findings of this study, the analysis and discussion of the experimental results.

Chapter 5: Conclusion

This chapter provides a summary of the important findings and conclusions derived from the experimental results.

Chapter 2: Literature Review

The aim of this literature review is to provide background information on the topics to be considered in this thesis and to highlight the importance of the present research. The topics covered in this review include:

1. Overview of fiber reinforced composites in aerospace.

2. Effect of combined temperature and moisture on carbon/epoxy composites.

3. Formation of voids in composites.

2.1 Overview of Fiber Reinforced Composites in Aerospace

A composite material is a material that is made from at least two constituent materials that differ significantly in their physical and chemical composition, that when combined produce a material with unique characteristics different from the individual constituent materials. The constituent materials are typically referred to as the matrix and the reinforcement. They don't blend nor lose their individual properties, they remain distinct and work together to contribute their unique features to give the composite material it's desired properties [17], which can be tailored for desired applications.

Fiber-Reinforced Polymeric (FRP) composites are made from a polymer matrix (such as epoxy or bismaleimide) that is reinforced with fibers like carbon, glass, aramid or other reinforcing material. The matrix serves as an adhesive that binds the fibers together [18], and protects the fibers from environmental exposure and transfers the load among the fibers. The fibers, in exchange, provide stiffness and strength to reinforce and strengthen the matrix and allows it to withstand cracks and fractures [17].

2.1.1 FRP Classifications

As shown in Figure 6, Erden and Ho [19] illustrated that fiber reinforced composites can be classified into four categories according to their matrix (or resin) group: Metal Matrix Composites (MMCs), Ceramic Matrix Composites (CMCs), Polymer Matrix Composites (PMCs), and Carbon/Carbon composites (C/C).
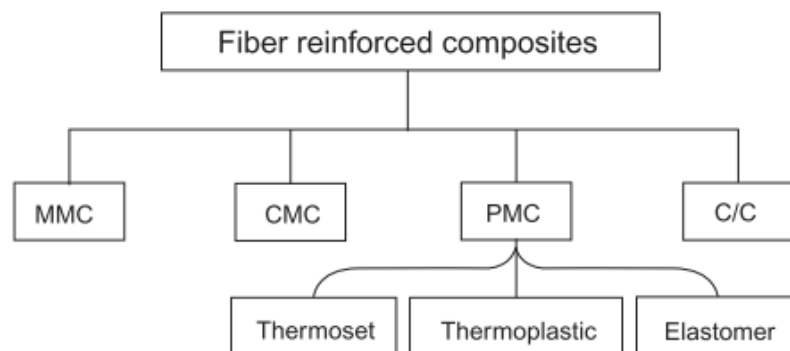
Figure 6: Classification of composites according to matrix type [19]

2.1.2 Polymers in Aerospace

PMCs are particularly known for their lightweight among the other matrix group types and have proven valuable across a wide range of aerospace applications. Thermosets, thermoplastics and elastomers are the three main classes of polymers. Thermosets, such as epoxy resins and bismaleimides, are the most commonly used polymers in aircraft applications due to their high mechanical performance and are used as the matrix in fiber composites and as an adhesive in structural joints and repairs. Thermoplastics and elastomers, on the other hand, are less common in aerospace applications. Elastomers lacks the required stiffness and strength for aerospace applications, as shown in Figure 7. Thermosets demonstrate better

mechanical performance (strength, stiffness, and creep resistance) compared to thermoplastics as shown in Figure 7, since it has molecular chains that are crosslinked which prevent the chains from sliding under stress and therefore increase the mechanical properties [18].
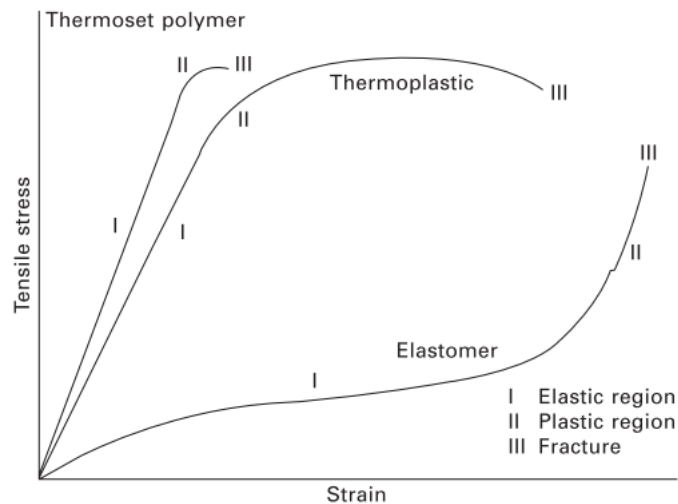
Figure 7: Typical stress–strain curves for a thermoplastic, thermoset polymer and elastomer [18].

As shown in Figure 8, the mechanical performance of most polymers declines sharply with elevated temperatures (above 100–150°C), and therefore their use in composite applications must be limited to lower temperatures. Bismaleimides, cyanates, and polyimides are polymer systems that can operate at elevated temperatures (below 200–220°C). Thermosets do not experience melting at elevated temperatures, due to the crosslinking of the molecular chains and therefore they can retain their structural rigidity and shape, however thermosets experience decomposition when further heated [18].
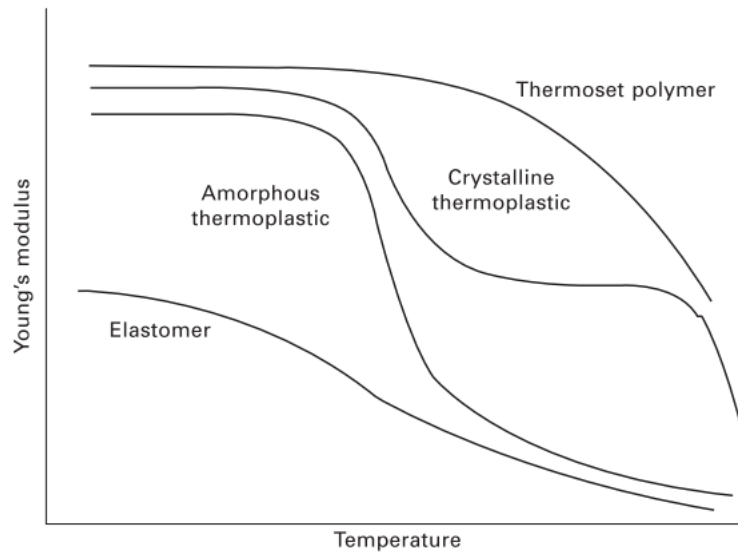
Figure 8: Variation of Young's modulus with temperature [18]

2.1.3 Epoxy Resins

Epoxy resin is the most common thermosetting polymer in aerospace structures and is the most common matrix used in high performance advanced polymer composites, such as carbon/epoxy composites. Its chemical compound consists of two or more C—O—C ring structures per monomer, as shown in Figure 9. During cure, the polymerization process occurs through the crosslinking of the C—O—C ring forming a three dimensional network of crosslinked polymer chains, as shown in Figure 10 [18].
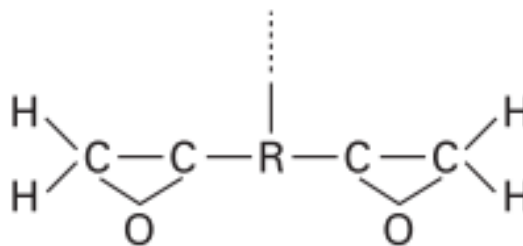
Figure 9: Functional unit of epoxy resins used in aircraft composite materials [18]
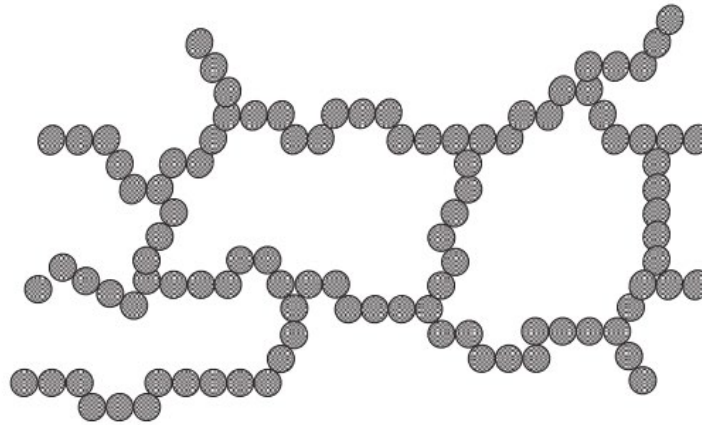
Figure 10: Schematic illustration of the molecular structure of crosslinked polymers [18]

Epoxy resins are the polymer of choice in many aircraft applications because of their low shrinkage and low volatility during curing, good durability in hot and moist environments, and superior mechanical properties such as high strength [18], which is attributed to the densely crosslinked molecular structures. Epoxy resins are considered to be brittle due to the high degree of crosslinking, and may undergo irreversible degradation due to induced stresses caused by environmental effects which may lead to a loss in the load bearing capacity of the polymeric composite [11].

2.1.4 Reinforcements in Aerospace

Fiber reinforcements are classified as natural and synthetic fibers as shown in Figure 11. Carbon, glass, and aramid fibers are considered synthetic fibers, and consist of tens to thousands of single filaments of different diameters and strengths. Fibers generally come in the form of a fabric or cloth, which can be further classified as woven, nonwoven, braided or knitted. Woven fabrics are produced by interlacing two sets of yarns (warp and weft), and the method in which the yarns are interlaced defines

the style of weave like: plain, satin, twill, etc, which has an effect on the properties of the fabric, such as smoothness and drapability [19].
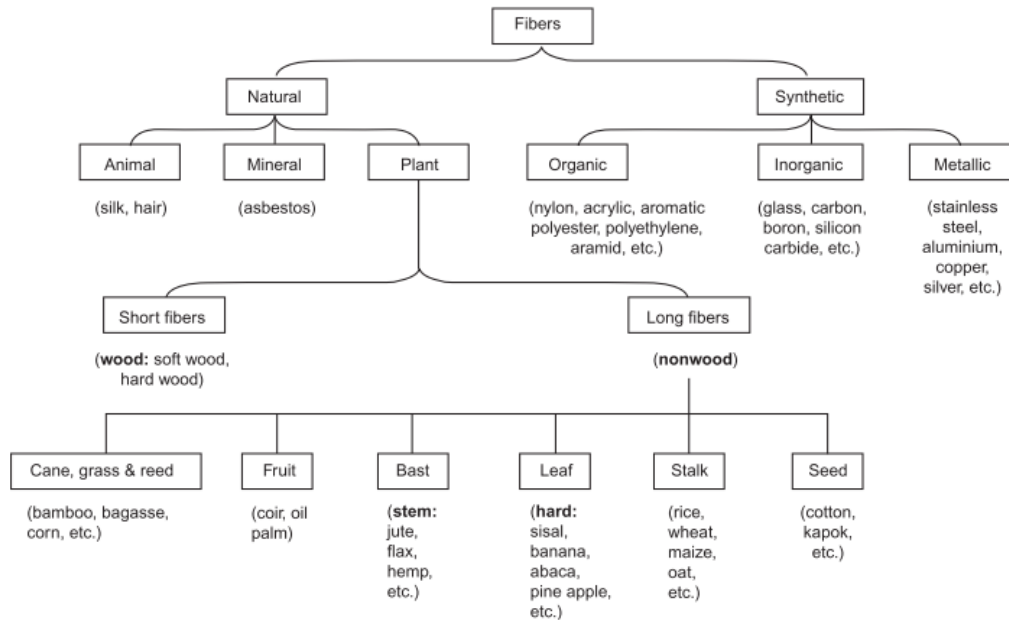
Figure 11: Classifications of fibers [19]

Carbon fiber reinforced polymeric composites are widely used in the aerospace industry compared to the other fibers for their high performance. Glass and aramid have gained, on the other hand, relatively limited use in the aerospace sector due to the lower strength and stiffness to weight ratios of glass to that of carbon, and to the issue of moisture absorption susceptibility with respect to aramid [4]. Carbon and glass reinforcements are inherently not susceptible to moisture absorption because of the fibers good hydrolytic stability [20]

2.2 Moisture Induced and Temperature Degradation

Fiber reinforced polymeric composites used for aerospace applications are subjected to different environmental conditions during their operational life, such as

varying moisture, humidity and temperature, which can adversely affect their performance over time.

There has been a large number of experimental evidence in the literature that demonstrated the unfavorable effects of combined moisture and temperature on the physical and mechanical properties of polymeric composite materials, influencing the composite's performance and limiting its functionality [2], [12], [20]–[23].

The moisture absorption of composite materials depends on factors such as temperature, fiber orientation, fiber volume fraction, fiber type and sizing, matrix type, contact area, void content, and water type such as sea water, or demineralized water [12], [14].

The extent of deterioration that takes place in fiber reinforced polymers due to environmental exposure is associated with the amount of moisture absorbed, which occurs through diffusive and/or capillary processes [11], [24]. Diffusion is considered a key process under which moisture penetrates polymeric composites and is known to be a matrix-dominated phenomenon in which water is mainly diffused in the matrix [11], [12], while moisture diffusion through the fibers is considered negligible [25], [26]. The capillary process involves moisture being drawn into voids and microcracks at the fiber/matrix interfaces, in which the cracks provide a transport system for moisture penetration [25], [27].

The downside of polymer-based composites is the deterioration of the polymer matrix and the fiber/matrix interface when subjected to moist conditions by reacting with water in a hydrolysis process that has an effect on their mechanical performance [14], [28]. The influence of water absorption is known to effect the mechanical

properties of thermoset polymers, demonstrated by both reversible and irreversible changes [11], [14].

Plasticization, swelling and degradation of the fiber/matrix interface are among the adverse effects of absorbed water. Moisture absorption has a plasticizing effect and induces plastic deformation in the matrix, which results in lowering of the glass gransition temperature (Tg) of the matrix [11], [12] due to the disruption of the hydrogen bonds in the epoxy resin [25]. This effect is generally reversible when the absorbed water is removed, however exposure to water at elevated temperatures can cause irreversible impacts, due to the chemical degradation of the matrix and to the deteriorative effect on the fiber/resin interface [12], [28] which increases internal voids and promotes microcrack formation [12].

Swelling is due to the induced differential strain resulting from the significant difference of the amount of moisture absorbed by the matrix resin relative to that of the reinforcement fibers [11]. Polymers are known to swell when they absorb moisture, while the reinforcement typically does not, and therefore the reinforcement inhibits the swelling of the matrix and causes internal strains and stresses in the polymeric composite [12]. Swelling can stimulate the propagation of microcracks in the composite which may accelerate the absorption of water into the composite [25], [29].

The structural integrity and lifetime performance of FRP composites are highly dependent on the stability of the fiber/matrix interfacial region, since it is most likely to control and influence the overall mechanical behavior of the composites [11] [20].The strength of the interface determines the applied stress transmissibility to the load carrying fibers, which is a function of the level of adhesion at the fiber/matrix

interface [12], which is adversely affected when exposed to the environment due to the plasticization of the matrix, chemical and mechanical degradation [11].

Increased temperatures can cause significant reductions in the strength and stiffness of the epoxy. Such reductions can begin to occur at temperatures well below Tg. The reduction in the mechanical properties may be permanent at high enough temperatures. Moreover, the effects are magnified with increased time-at-temperature and moisture content [2], [22].

In a literature survey conducted by Weitsman [30] on the effects hygrothermal (combined moisture and temperature) conditioning on fibrous composites, the following observations and major conclusions were found:

1. If a moisture saturation level exists, it depends mostly on the ambient relative humidity, and may be less on temperature.

2. Moisture diffusivity is highly sensitive to temperature.

3. Moisture enhances creep under external loads.

4. Moisture induces swelling strains, which can lead to internal stresses.

5. Moisture lowers the glass transition temperature (Tg) of PMCs, which may impose severe restrictions on the use of specific composites in hot wet environments.

6. Moisture causes the deterioration of mechanical properties, especially in shear and compression.

7. The details of all the above observations vary quantitatively — some most significantly, among different material systems.

Previous researchers have studied the effects of moisture and temperature on the properties of carbon/epoxy materials and have shown the deteriorative effects it has on the mechanical, physical and thermal properties of carbon/epoxy composites.

For instance, Khan et al. showed that long term hygrothermal conditioning (combined heat and moisture) had an adverse impact on the flexural, interlaminar shear strength and glass transition behaviors of an aerospace grade carbon/epoxy material. Reduction in ILSS was suspected to be due to matrix plasticization and micro cracking, however the latter was eliminated as a second moisture saturation level was not detected and therefore ruling out microcracking as a cause. Reduction in flexural strength was attributed to the swelling of the epoxy due to moisture absorbed, opposite to the fibers which don't absorb water nor swell, and therefore damaging the carbon/epoxy interfaces as the result of unmatched swelling effecting the ability of the matrix to transfer the loads to the fiber [20].

Ray [11] studied the effect of temperature on the interlaminar shear strength of unidirectional carbon/epoxy when exposed to thermal and humid environments, and found that higher temperatures increased the rate of moisture uptake due to higher diffusion rate. Ray reported the absence of the anomalous Fickian behavior at higher temperatures and interpreted it as the result of the surface induced crystallization of the carbon fiber in the epoxy matrix, which indicates that moisture penetration was the result of only diffusion and not by capillary process. Moreover, for the same amount of moisture absorbed by the laminates, higher degradation in shear strength was experienced at higher conditioning temperatures for longer exposures. This behavior is due to the deteriorating effect of temperature in generating thermal stress that may stimulate the initiation and propagation of cracks at the carbon/epoxy interface, due to

the difference in the moisture-induced volumetric expansion rate between the epoxy matrix and reinforcement carbon fiber, since the amount of moisture absorbed by the carbon fibers is significantly less than that by the epoxy matrix [11].

2.3 Formation of Voids in Composites

Voids are considered as one of the most common defects encountered during the fabrication of fibers reinforced polymer composites [31]. A large number of studies have been conducted to characterize voids due to their complex phenomena and adverse effects on the composite properties [31]–[34] . It is known that manufacturing induced defects, such as voids and delamination, have an unfavorable effect on the mechanical performance of composite laminates [35]. Researchers have shown that the mechanical properties of fiber reinforced composites are affected by the presence of voids (porosity). Generally, such defects lower the static and fatigue strength of the composite laminate and lead to higher susceptibility to water absorption and environmental effects [35]. Interlaminar Shear Strength (ILSS) has been the mechanical property most often studied to assess void content due to its high void sensitivity [34], where literature has shown that ILSS decreases with increasing void content [31], [32], [34]. NDT and ultrasonic techniques have been used in order to determine the void content of composite laminates, through the ultrasonic absorption coefficient from which the mechanical properties (i.e. ILSS) are correlated [32], [33], [36], [37].

There are many causes of void formation, however the focus of the literature has been on the following two reasons: first, the entrapment of gases during impregnation process of fiber reinforcement with resin or during the lay-up due to the presence of moisture in the air, and second volatiles arising from the resin during the

cure[34]. There appears to be a lack of analysis in the literature on the mechanisms by which air can be trapped during the lay-up process between prepreg plies forming porosity or voids in the composites.

Bloom et al. [38] investigated the formation and evolution of entrapped air at the tool-ply interface, between the tool surface and the first ply, during lay-up and debulking (compaction) process, which is considered a major contributor to surface porosity. Different layup and bagging schemes were studied to visually characterize the void behavior during layup and compaction, which showed that the process is a complex phenomenon involving the topology and viscoelastic mechanical response of the composite prepreg. Lower void fractions were noticed for woven prepreg in comparison with Uni-Directional (UD) prepreg, which might be related to the structure of the woven fibers that would facilitate a higher degree of through-thickness permeability due to the gaps at crossover points providing a mode of gas transport, which is not the case in the closely packed UD fibers, where air must be removed across the plane of the ply. Moreover, the study showed that the majority of the air extraction from the plies occurred within the first 10 minutes, which is in line with the general manufacturing procedures that considers the same amount of compaction time to be sufficient. On the other hand, it was indicated that simple laminates consisting of one ply could experience variation in the air removal rates at the early stages of vacuum compaction, which leads to the conclusion that compaction processes may need to be tailored in the case of larger, more complex parts. The variability in the results indicates that further studies are needed before any relationship can be quantitatively defined [38].

2.3.1 Usage of Breathers and Bleeders

It has been generally understood in aerospace that the use of surface breathers and edge bleeders/breathers is essential when vacuum bagging components that are autoclave cured, as they are known to create air passages within the bag for air to flow and escape through in order to prevent the occurrence of porosity or void formation during the lay-up process and during the cure. Thompson [7] challenged this concept in his investigation and demonstrated that for the net resin systems typically used in the aerospace industry, the gas transfer capability of conventional breather materials is not important in the manufacture of composite aircraft parts. He investigated the air flow through breather in the autoclave and concluded that gas flow through breathers at cure conditions, while probably not truly zero, is very small. Thompson demonstrated the concept of a breather-less "Silicone-Viton" re-usable vacuum bag (without the use of surface breathers or edge bleeder/breathers) that may be used to fabricate high quality porosity-free composite parts, and has proven successful for sandwich panels and laminates up to 70 plies thick and in a number of modified parts. The mechanical properties and thicknesses for parts produced with the breather-less bagging system were equivalent to those for part produced with standard bagging systems. Application of the breathers and bleeders typically requires 15-60 minutes per part, as they are manually cut and prepared for each composite part, however the re-usable bag allows parts to be vacuum bagged in less than five minutes providing labor and material savings. Moreover, Thompson made the following conclusion, among others: that edge breathers, edge bleeders, and string bleeders are generally unnecessary and should be made optional, regardless of the bagging system used [7].

Chapter 3: Materials and Research Methods

This chapter provides information about the materials, fabrication process, samples preparation, and characterization testing techniques used in this study. The general experimental work plan is described at the end of the chapter.

3.1 Materials

The composite material used in this study and was sponsored by Strata Manufacturing, an advanced composite aero-structures manufacturing facility in the United Arab Emirates, that produces high-quality composite aircraft parts and components for global aircraft manufacturers [39].

The composite material examined in this study is a thermoset carbon fiber prepreg commercially known as CYCOM 970 Epoxy Resin, manufactured by Solvay. The carbon fiber material is supplied which is already pre-impregnated with resin and having a nominal resin content of 40% by weight, and nominal curing temperature of 177°C (350°F). As shown in Figure 12, the carbon prepreg material is a plain weave, woven fabric, and is supplied in the form of rolls and stored at -18°C (0°F) [40].
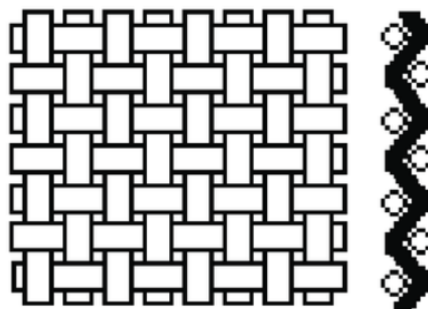
Figure 12: 1x1 Plain weave carbon fabric

3.2 The Composite Panels Fabrication Process

This section describes the detailed fabrication process of the composite panels used in this study. The fabrication process was carried out at Strata Manufacturing facility, which provided the materials, tools, and equipment required to manufacture the test specimens.

3.2.1 The Fabrication Process Overview

CYCOM 970 plain weave prepreg was used to fabricate monolithic composite laminates using the manual lamination process. Flat quasi-isotropic laminates of dimensions 350 mm x 600 mm were fabricated from the prepreg, consisting of twelve plies each, with a layup stacking sequence of $[(0^o/90^o)]_{6S}$, as shown in Figure 13.
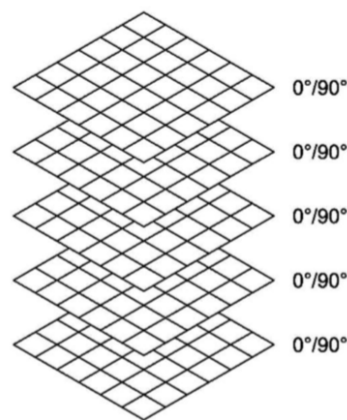
Figure 13: Fabric layup stacking sequence [41]

During the lay-up process, the test panels were divided into two groups: compacted and non-compacted. The composite panels were cured in an autoclave dwelling at 180 ±5°C for approximately 3 hours, where temperature, pressure, and vacuum levels were controlled and monitored. All test panels were cured in the same autoclave cycle to ensure similar material properties between the test panels/laminates.

Non-Destructive testing was performed on the test panels after curing to inspect and ensure the integrity of the fabricated test panels.

3.2.2 Thawing of the Prepreg Material

The pre-impregnated carbon roll was removed from the freezer to allow it to thaw while sealed in its moisture-proof bag as shown in Figure 14. The prepreg material was kept sealed until the temperature of the material has sufficiently adapted to the ambient temperature and no more moisture forms on the outside or the inside of the bag. This step is required to prevent any condensation on the material after the opening of the sealed bag.

Figure 14: Thawing of the pre-impregnated carbon roll

3.2.3 Ply Cutting Carbon

An automated 2-axis NC machine (LECTRA) was used to cut the carbon prepreg into the desired ply dimensions to produce the test laminates, as shown in Figure 15. The carbon prepreg was cut into rectangular laminas of the size 350 mm x 600 mm to an orientation of $0^\circ/90^\circ$ using a nesting program as shown in Figure 16 (a) and (b). The nesting program is a numerically controlled program designed to optimize material usage and reduce material waste.

Figure 15: LECTRA ply cutting machine
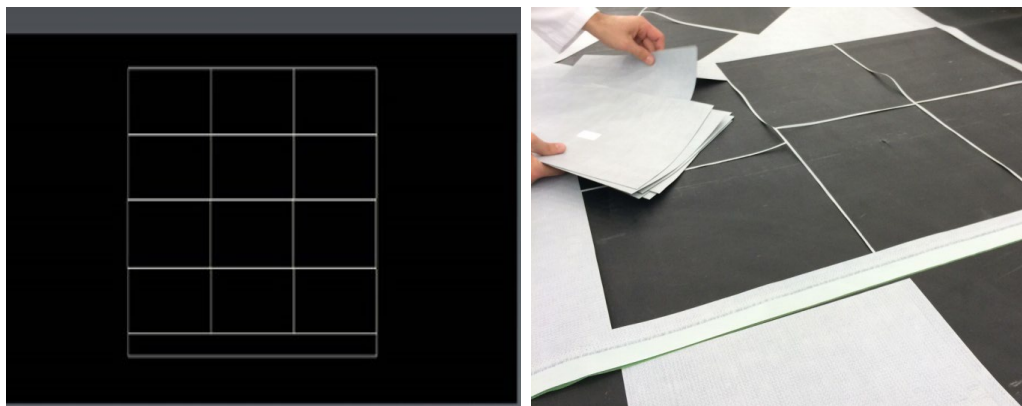
(a)   (b)

Figure 16: Ply cutting using nesting file. (a) Nesting file (b) Carbon laminas after cutting

3.2.4 Tool Preparation

A flat aluminum tool was used to fabricate the test panels, as shown in Figure 17 (a). The surface of the tool was coated with Loctite Frekote 700NC (Shown in Figure 17 (b)), a release agent, to prevent the test panels from sticking on the tool when cured. The applied release agent was left to dry for a minimum of 30 minutes before the start of the layup process.

(a)   (b)
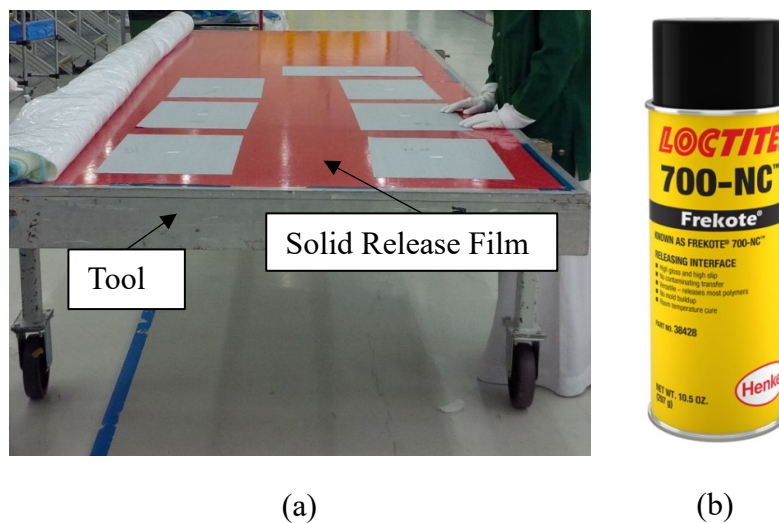
Figure 17: Tool preparation. (a) Flat aluminum tool (b) Loctite Frekote 700NC (Release agent)

A layer of solid release film was applied to the entire tool surface using high-temperature tape to keep it in its place. The application of the release film aids in the debagging process, however it is not mandatory, as the tool surface was initially coated with the release agent.

3.2.5 Lay-Up Process

The manual lamination process (hand lay-up) was followed to fabricate the test panels. Flat test panels of dimensions 350 mm x 600 mm were manufactured consisting of 12 carbon layers each, with plies oriented at 0°/90°.

The prepreg plies were covered with colored backing paper on either side, which was removed when the plies were applied on the tool. The colored backing paper typically indicates different fiber orientation, fiber style, or resin content, however in this study, all plies were a plain weave of 0°/90° orientation. The backing paper of the examined prepreg was green on one side, and white on the other side, as shown in Figure 18.
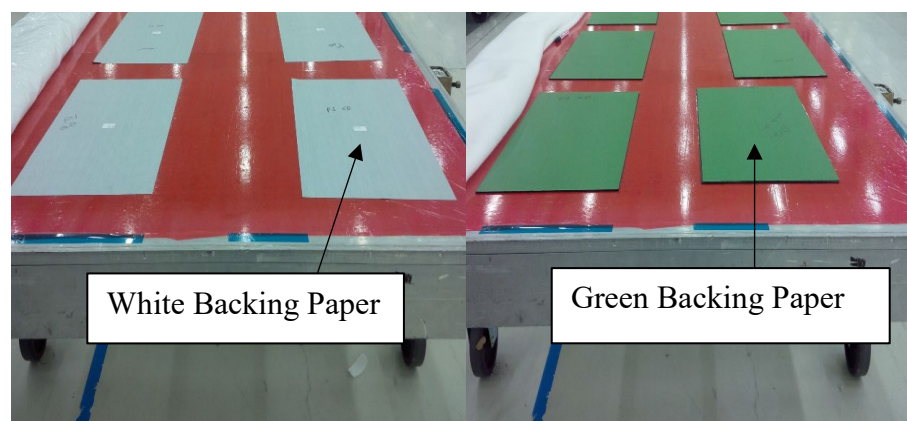
Figure 18: Backing paper on either side of the prepreg plies

There could be a chance that one side of the prepreg roll has more or less resin content than the other side. Therefore, to ensure symmetry within the panel, the first batch of 6 plies were laid down with the green backing paper facing the tool, the second batch of 6 plies were laid down with the white backing paper facing the tool, as shown in the ply lay-up sequencing in Tables 1 and 2.

During the lay-up process, the test panels were divided into two groups: compacted and non-compacted. The difference between the two test groups is that the compacted group had: (i) In-process compactions between the composite layers. (ii) Used glass fiber edge and surface bleeders in the final bagging of the test panels, whereas the non-compacted group did not.

Compacted Group

Table 1 and Figure 19 show the layup sequence and final bagging procedure of the compacted group, respectively. The lay-up of the test panels in the compacted group started with applying the first ply to the tool, getting rid of as much air under the ply as possible by hand. After the first ply, the first in-process compaction was performed to avoid any trapping of air bubble between the tool and ply, as shown in the layup-sequencing in Table 1. To perform the in-process compaction, a compaction bag was prepared using a layer of perforated release film on the ply, followed by a layer of breather, enclosed in a nylon vacuum bag, and sealed using a vacuum sealant tape around the tool periphery. Vacuum ports were inserted before sealing the vacuum bag and 100% vacuum pressure (minimum of 745 millibar/22'Hg) was applied for a minimum of 10 minutes. The bag was removed carefully, as the bagging materials were re-used for the subsequent in-process compaction operations. Plies 2, 3, and 4 were applied, followed by a 2nd 100% vacuum in-process compaction operation for 10 minutes. Plies 5, 6, 7, and 8 were applied followed by a 3rd 100% vacuum in-process compaction for 10 minutes. Plies 9, 10, 11 and 12 were applied, and the final 100% vacuum compaction was performed using the final compaction bag. The final compaction bag was prepared as per the final bagging procedure illustrated in Figure 19, using new bagging material including the edge and surface bleeders as indicated for the compacted samples group.

Table 1: Lay-up sequencing of compacted samples with in-process compactions

Compaction	100% Vacuum untill End of Cure		
P12	CYCOM 970 prepreg (white backing side down)	0º/90º	350 mm x 600 mm
P11	CYCOM 970 prepreg (white backing side down)	0º/90º	350 mm x 600 mm
P10	CYCOM 970 prepreg (white backing side down)	0º/90º	350 mm x 600 mm
P9	CYCOM 970 prepreg (white backing side down)	0º/90º	350 mm x 600 mm
Compaction	100% Vacuum 10 minutes		
P8	CYCOM 970 prepreg (white backing side down)	0º/90º	350 mm x 600 mm
P7	CYCOM 970 prepreg (white backing side down)	0º/90º	350 mm x 600 mm
P6	CYCOM 970 prepreg (green backing side down)	0º/90º	350 mm x 600 mm
P5	CYCOM 970 prepreg (green backing side down)	0º/90º	350 mm x 600 mm
Compaction	100% Vacuum 10 minutes		
P4	CYCOM 970 prepreg (green backing side down)	0º/90º	350 mm x 600 mm
P3	CYCOM 970 prepreg (green backing side down)	0º/90º	350 mm x 600 mm
P2	CYCOM 970 prepreg (green backing side down)	0º/90º	350 mm x 600 mm
Compaction	100% Vacuum 10 minutes		
P1	CYCOM 970 prepreg (green backing side down)	0º/90º	350 mm x 600 mm
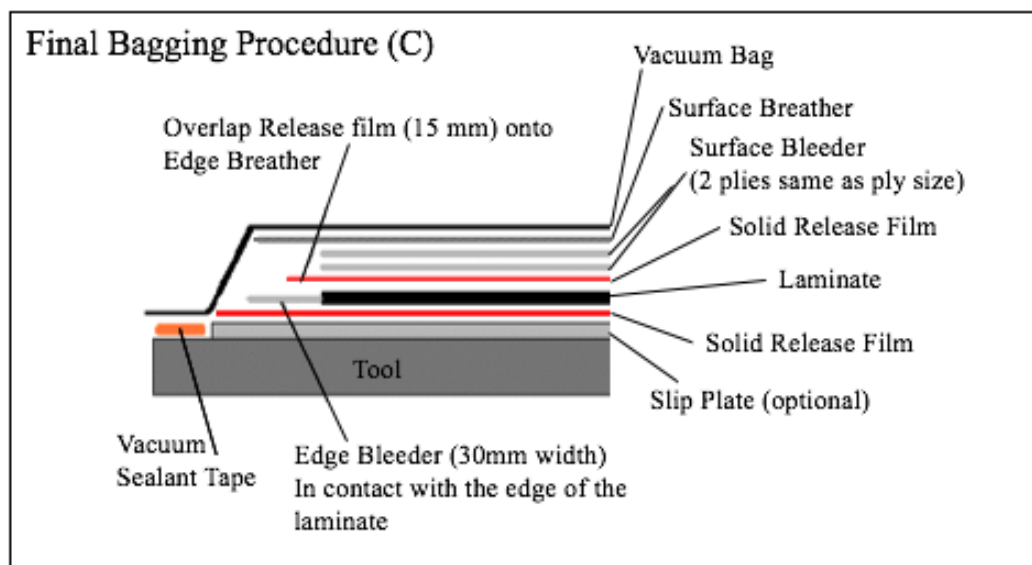
Figure 19: Final bagging procedure for compacted laminates showing the usage of edge and surface bleeders

Non-Compacted Group

Table 2 and Figure 20 shows the layup sequence and final bagging procedure of the non-compacted group, respectively. The lay-up process of the test panels in the non-compacted group was performed without any in-process compaction operations, as shown in the lay-up sequencing in Table 2. Plies 1-12 were applied to the tool, and the final 100% vacuum compaction was performed using the final compaction bag. The final compaction bag was prepared as per the final bagging procedure as illustrated in Figure 20, without using the edge and surface bleeders as indicated for the non-compacted samples group.

Table 2: Lay-up sequencing of non-compacted samples with no in-process compactions

Ply sequence number	Material Description	Orientation degree	Size
Compaction	100% Vacuum until End of Cure		
P12	CYCOM 970 prepreg (white backing side down)	0º/90º	350 mm x 600 mm
P11	CYCOM 970 prepreg (white backing side down)	0º/90º	350 mm x 600 mm
P10	CYCOM 970 prepreg (white backing side down)	0º/90º	350 mm x 600 mm
P9	CYCOM 970 prepreg (white backing side down)	0º/90º	350 mm x 600 mm
P8	CYCOM 970 prepreg (white backing side down)	0º/90º	350 mm x 600 mm
P7	CYCOM 970 prepreg (white backing side down)	0º/90º	350 mm x 600 mm
P6	CYCOM 970 prepreg (green backing side down)	0º/90º	350 mm x 600 mm
P5	CYCOM 970 prepreg (green backing side down)	0º/90º	350 mm x 600 mm
P4	CYCOM 970 prepreg (green backing side down)	0º/90º	350 mm x 600 mm
P3	CYCOM 970 prepreg (green backing side down)	0º/90º	350 mm x 600 mm
P2	CYCOM 970 prepreg (green backing side down)	0º/90º	350 mm x 600 mm
P1	CYCOM 970 prepreg (green backing side down)	0º/90º	350 mm x 600 mm
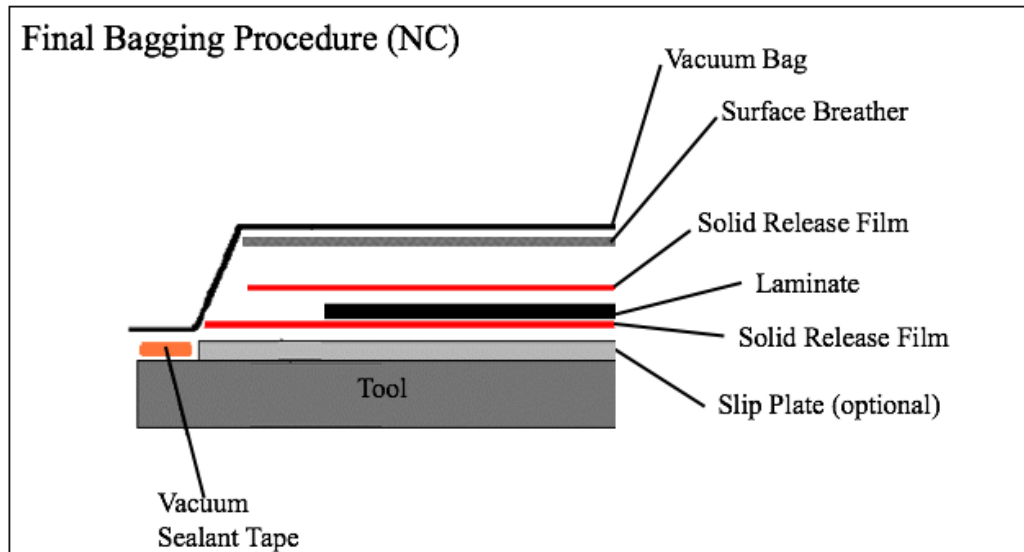
Figure 20: Final bagging procedure for non-compacted laminates showing no usage of edge and surface bleeders

3.2.6 Final Bagging and Final Compaction

The final bagging used for both groups was done in accordance to the final bagging procedure illustrated in Figure 19 and 20, and is shown in the Figure 21 (a), (b), and (c).

As shown in Figure 21 (c), standard K-type thermocouples were used to monitor the temperature within the laminates in the autoclave during the cure cycle. Two thermocouples were positioned, on opposite sides of each test panel, between the ply stack ensuring that the tip of the thermocouple is secured between the carbon plies. The wires of the thermocouple were taped on the tool to keep them in place.

To ensure that the final bag was sealed efficiently, a leak test was performed. Prior to performing the leak check, 100% vacuum pressure of a minimum 745 millibar/22" Hg was applied for at least 15 minutes, then the vacuum system was turned off and the drop in the vacuum level was monitored using a vacuum gauge, as

shown in Figure 21 (c). The leak test showed a vacuum drop of less than 169 milllibar (5" Hg) in 5 minutes, which is considered acceptable.
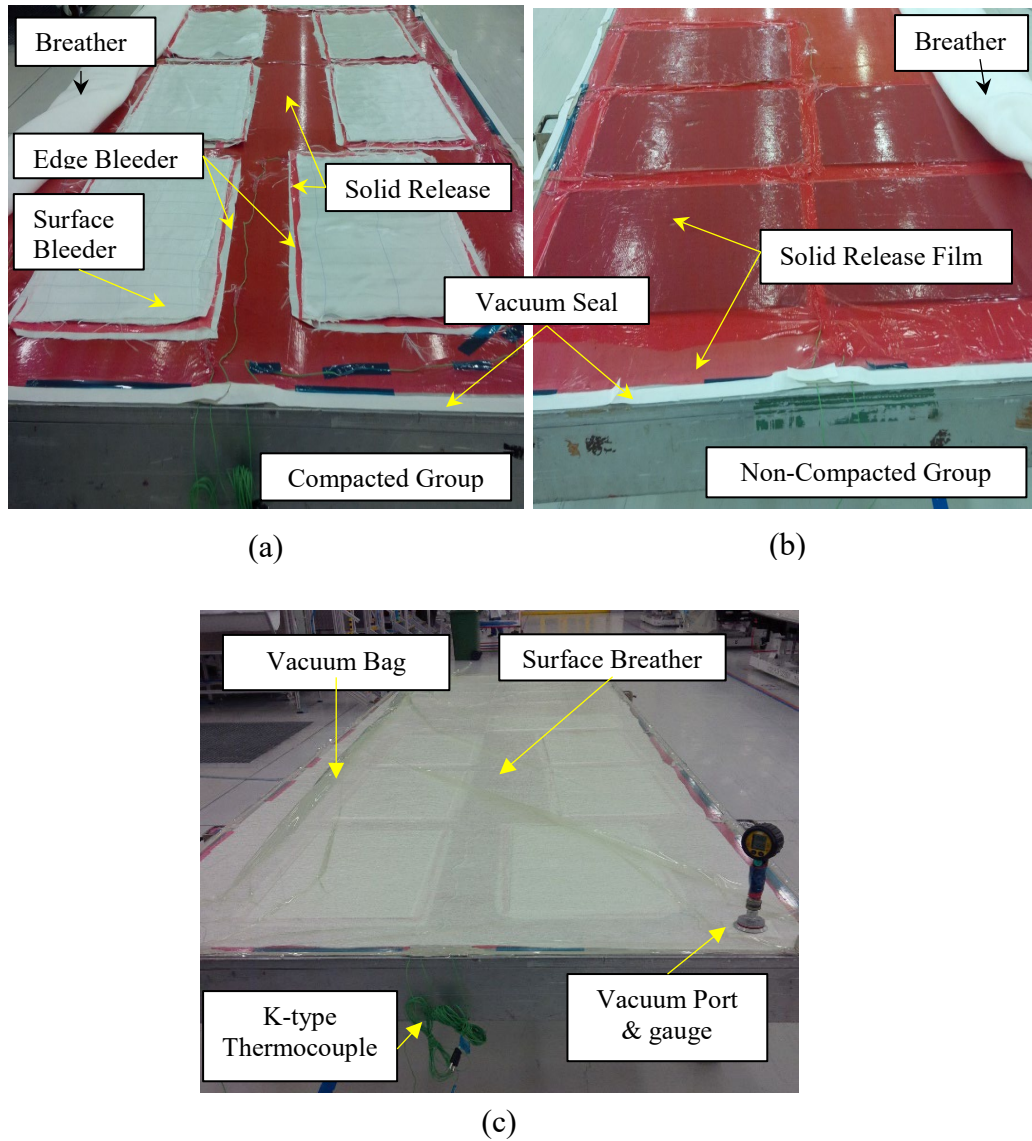
Figure 21: Final bagging and compaction materials. (a) Bagging material for compacted panels (b) Bagging materials for non-compacted panels (c) Final compaction materials

3.2.7 Autoclave Curing Process and Debagging

The composite panels were cured in an autoclave where temperature, pressure, and vacuum levels were controlled and monitored as per the cure cycle shown in Figure 22.
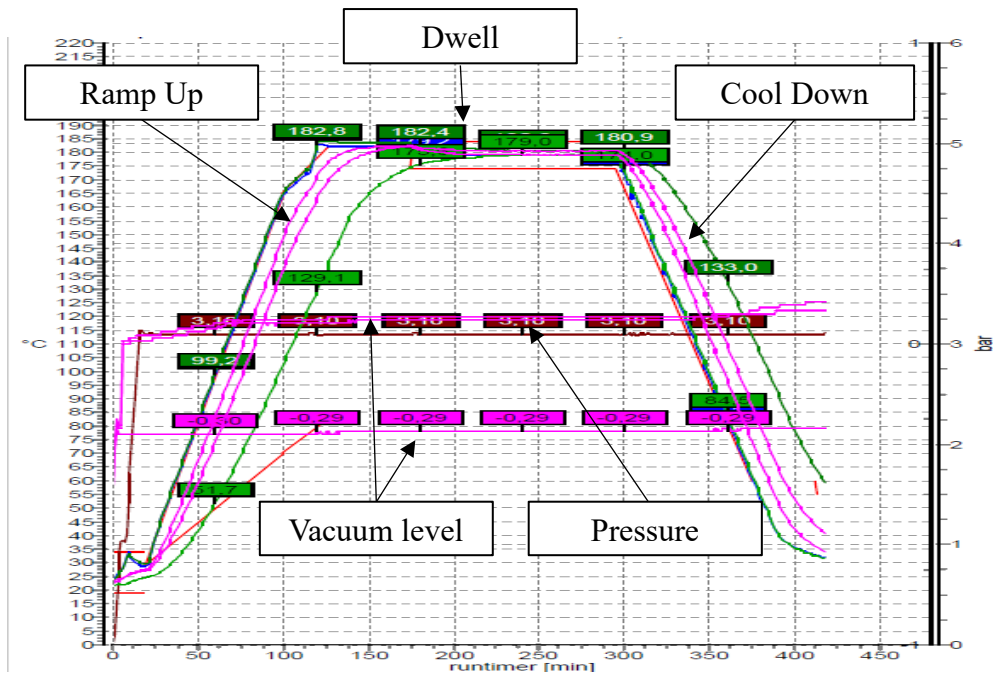
Figure 22: Autoclave cure cycle

The test panels were cured in the same autoclave cycle to ensure similar material properties between the test panels and eliminate the variability associated with curing in different cure cycles.

Figure 22 shows the actual cure cycle of the test panels. The pink lines represent the temperature of the thermocouples showing an average ramp-up of 1.6 °C/min and a dwell at 180°C for approximately 3 hours, followed by an average cool down of 1.2°C/min in accordance with the set values, shown in red, as per the recommended material specification.

A pressure of 3.1 bars was applied over the entire period of the cure cycle of around 7 hours. The vacuum level was maintained at 30% (minimum of 225 millibar) until the end of the cure cycle, without any vacuum leak or seal off.

The tool was removed from the autoclave and debagging process was performed after cooling, as shown in Figure 23 (a). The vacuum bag was detached from the tool ensuring no damage to the thermocouples and panels. Protective gloves were worn to prevent any injuries, as the carbon panels can be sharp around the edges. Figure 23 (b) shows the cured test panels after debagging. The test panels were marked for testing traceability.

(a)   (b)

Figure 23: Debagging of test panels. (a) Tool after being removed from the autoclave (b) Cured test panels after debagging

3.2.8 Non-Destructive Testing (NDT)

The integrity of the panels were investigated after curing using non-destructive testing (NDT) methods. Ultrasonic Testing (UT) is an NDT (Non Destructive Test) technique that transmits high frequency sound into a material to interact with features within the material that reflect or attenuate it, therefore it can be used to detect porosity,

delamination, defects, bonding voids, and foreign materials in composite structures. Through transmission (TT) and Pulse Echo (PE) are the two ultrasonic techniques followed to scan the test panels in accordance with the 6 dB drop method, a widely used method to evaluate composites ultrasonically. The -6 dB method is achieved by implementing Equation (3.0) below:

$$\Delta I \ (dB) = \ 20\log(\frac{V_2}{V_1}) \ \ (3.0)$$

Where,

$\Delta I \ (dB)$= The change in the sound intensity between two measurements, dB.

V_1 / V_2= The ratio between two different transducer output voltages (or readings) = 0.5 to achieve -6 dB drop in sound intensity.

Porosity is known as the trapped air bubbles between the carbon layers, and would be detected by ultrasonic inspection; hence, this step was critical to determine the impact of removing both in-process compactions and the usage of bleeders during the fabrication process on the integrity of the non-compacted composite panels group in terms of porosity or voids.

In this study, the ultrasonic scans performed on the panels were represented by both the A-Scan and C-Scan. C-Scan was the primary inspection method performed using the automated Through Transmission (TT) technique, while the A-Scan was the secondary inspection method performed using the Manual Pulse Echo (MPE) technique. The secondary method (A-Scan) was used in case additional verification was required following any indications from the C-Scan. The 6 dB drop method was

used for evaluation as it is the most common Ultrasonic Testing (UT) evaluation technique.

i. Primary technique: Automatic through transmission method (C-scan)

Midas Automated Ultrasonic Squirter, an automatic through transmission device supplied by Midas (UK), was used to perform the C-Scan on the cured composite panels, as shown in Figure 24 (a). The Midas system is a fully automated system used for non-destructive testing to detect defects and indications in the composite specimen. Midas uses a closed loop water system as couplant, 2.25 MHz probe, and a 6 mm nozzle.

The C-scan was performed against a reference standard panel, as shown in Figure 24 (b). The reference panel is a panel that is used to define the material, thickness and possible defect types for the inspection equipment or machine. ZEUS v3 Midas software has been used to capture and evaluate the C-Scan images in accordance to the 6 dB drop method.

(a)   (b)
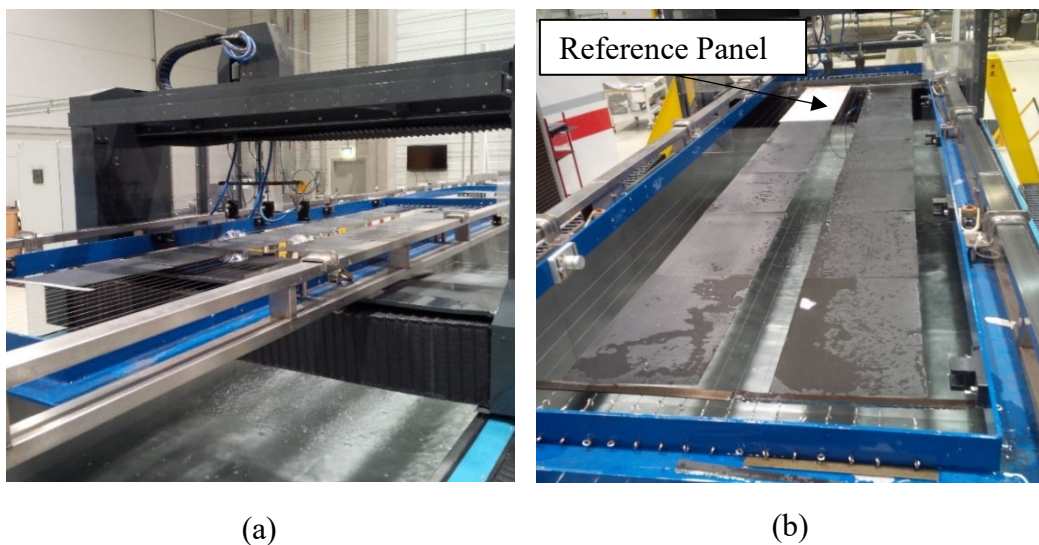
Figure 24: C-scan of test panels. (a) Midas Automated Ultrasonic Squirter (b) C-scan of the panels against reference panel

ii. Secondary technique: Pulse-Echo method (A-scan Conventional)

Epoch XT Ultrasonic Flaw Detector was used to perform a manual A-Scan on the cured composite test panels to investigate the integrity of the panels as shown in Figure 25.
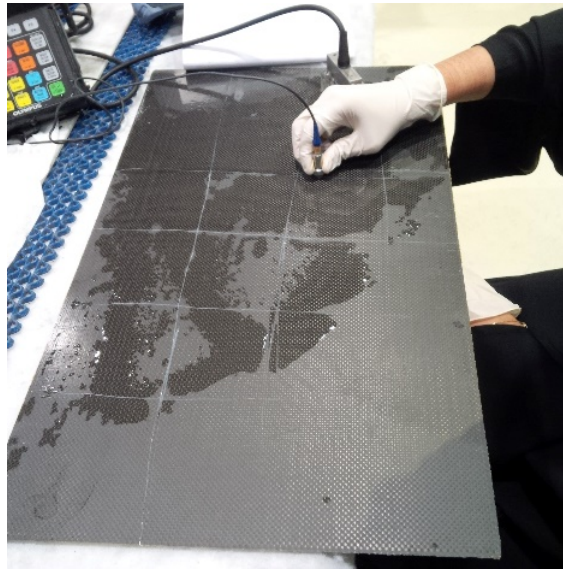
Figure 25: Manual A-scan process of a composite Panel

Epoch XT Ultrasonic Flaw Detector, a Manual Pulse Echo (MPE) device supplied by OLYMPUS, was used to perform the A-Scan on the cured composite panels as shown in Figure 26. Epoch XT uses a BNC/Micro dot coaxial cable, 5MHz transducer, and water as a couplant. The display screen presents data in real-time while scanning. The horizontal axis (X-Axis) of the graph shows Time/Distance and the vertical axis (Y-Axis) displays the signal amplitude.

Figure 26: Epoch XT Ultrasonic Flaw Detector

The Pulse-Echo (PE) method was a secondary scan used for verification to inspect indications or any suspicious areas indicated by the C-scan. The Pulse-Echo (PE) method uses ultrasonic waves to find defects in an object using the principle of sound travel. The sound travels through the BNC/Microdot, to the ultrasonic transducer (Probe) as pulse or energy in the material through the couplant (water medium). After striking the surface, some of the sound will reflect back to the transducer. Peaks will be generated in the flow detector screen based on the time of receiving the sound signals by the transducer. The height of the generated peak represents the amount of sound reflected.

When a probe sends a sound wave to a defect-free object, the A-scan display screen will display two signal indications. The first signal indication represents the initial peak, the second signal represents the back-wall echo, and the distance between them is the thickness of the tested object, Ep, as shown in Figure 27 - left. In the case of a defect detection, a third signal indication (intermediate echo) would appear at a

distance D from the transducer (the top surface of the object) as shown in Figure 27 - right.
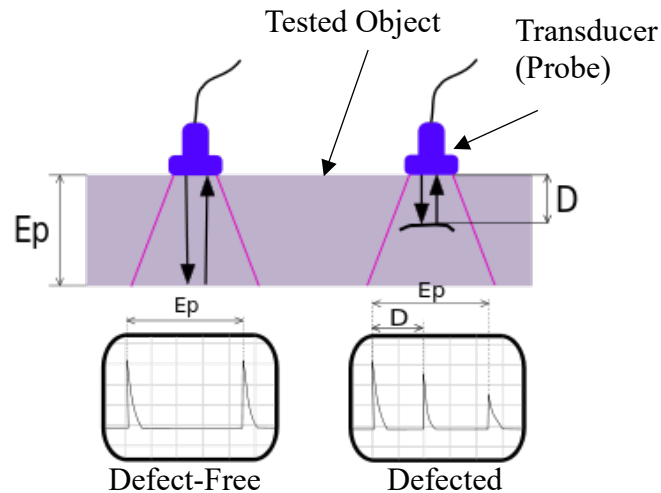
Figure 27: A-Scan display of defected and non-defected objects

3.2.9 Void Calculation of Microsections

Fractography analysis was performed on cured composite samples to determine the void content in both compacted and non-compacted control samples, in accordance to AITM4-0003 (Test Method for Determining the Pore Content of Fiber Reinforced Plastics using Automatic Image Analysis). Olympus BX51M Microscope and Stream Essentials software were used to perform the analysis as shown in Figure 28. Camera adapter used was 0.63x with DP21 Camera. Microsection images were performed with 5x magnification lens.

The void content was calculated using Equation (3.1)

$$\text{Void \%} = \frac{Area\ of\ Void}{Total\ Area} * 100 \qquad (3.1)$$

Where,

$Void\ \%\ =$ Percentage of void (%)

$Area\ of\ Void\ =$ Total area of void in the region of interest (mm^2)

$Total\ Area\ =$ Total area of region of interest (mm^2)

Figure 28: Olympus BX51M Microscope

3.3 Sample Preparation and Testing

This section describes the different tests conducted, testing equipment and parameters and the samples preparation.

3.3.1 Tensile Samples

The tensile strength of the composites was determined for samples exposed to different immersion times and temperatures using the tensile test method standard ASTM D-3039 (Standard Test Method for Tensile Properties of Polymer Matrix Composite Materials).

The cured composite panels were machined using a CNC machine to prepare the tensile samples with the desirable dog bone profile, as shown in Figure 29.
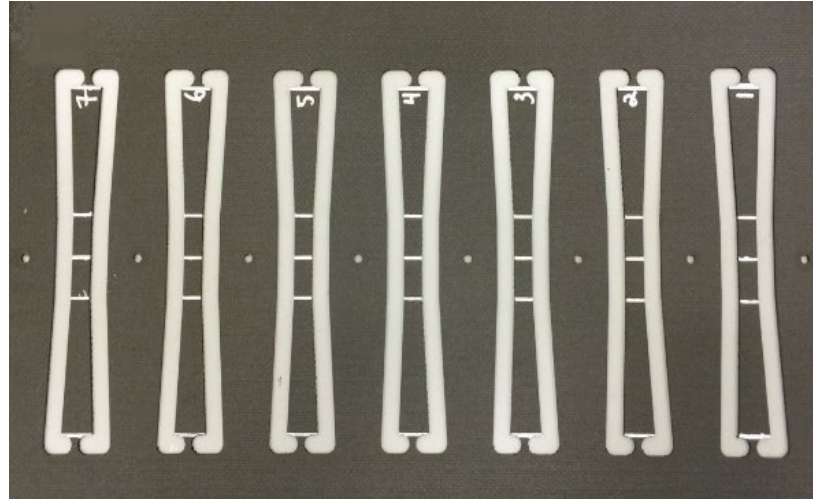
Figure 29: CNC machined panel

A Benetec diamond saw was used to trim the panel into individual tensile samples. The tensile samples were prepared with dimensions of 229 mm in length, a smooth transition in the width from 22 mm to 13 mm, an average thickness of 2.6 mm, and a gauge length of 54 mm gauge, as shown in Figure 30.
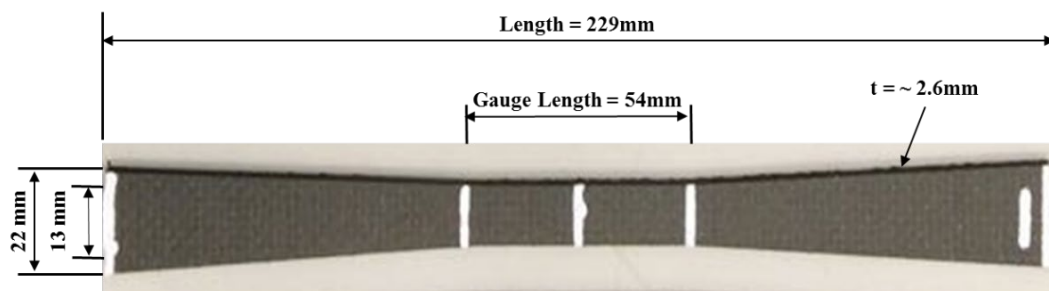
Figure 30: Tensile sample dimensions

Edge surface finish was inspected to be within 125RA in accordance to ANSI B46.1. The edge surface was measured using the Mitutoyo Surface Roughness Tester

SJ 301 shown in Figure 31 to ensure edge surface finish within 125RA. The Roughness test apparatus uses a very fine probe which moves across the edge of the specimen to determine the surface finish. For each specimen, a report was generated by the machine as a proof for passing the roughness test, as shown in Figure 32.

Figure 31: Mitutoyo Surface Roughness Tester SJ 301

Figure 32: Roughness test report

Prior to conditioning, the cut edges of the tensile samples (shoulders) were sealed with a protective layer of teflon tape followed by another layer of aluminum

tape, as shown in Figure 33 and 34, to shield and protect the ends of the samples from water immersion exposure. It also maintains the integrity of the sample shoulders when placed between the tensile testing gripping jaws.
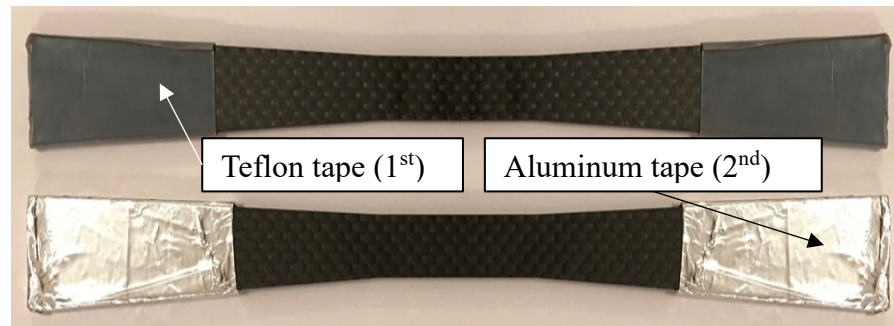
Figure 33: Tensile sample after the application of the protective layers to the shoulders

Figure 34: Tensile samples ready for immersion

The weight of the tensile samples was measured before the addition of the protection layers to record the initial weight of the samples in order to track the moisture intake during water immersion.

Sample Conditioning

To study the impact of different environmental conditions on the integrity of the samples, both compacted and non-compacted tensile samples were immersed in water heating chambers maintained at different temperatures of 40°C, 70°C and 95°C for a period of time varied from one month up to 10 months.

The environmental water chamber system was constructed in the lab using an electric heater and a glass beaker. The electric heater was calibrated to the desired temperatures of 40°C and 70°C and was fixed on a PMMA (plexiglass) plate as shown in Figure 35. The tensile samples were immersed as shown in Figure 35.
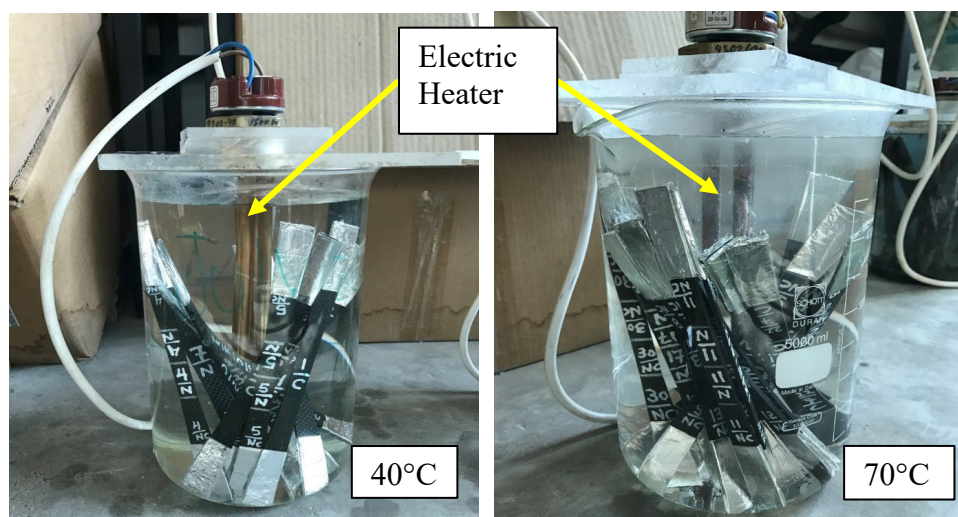
Figure 35: Water heating chamber of 40°C and 70°C

A Fisher Scientific water chamber system was used to achieve the 95°C water temperature. The initial intention was to set the water temperature at 100°C to achieve the harshest water immersion condition of boiling water, however due to the high rate of water loss to evaporation, and the need to top up the water levels on hourly basis, it was decided to set the water temperature on a slightly lower setting of 95°C.

The tensile samples were immersed horizontally, and positioned in layers, as shown in Figure 36 to ensure that the exposed surface area of the samples are all exposed to water in the same manner. Rectangular aluminum spacers were placed between the samples layers to maintain space between the samples and maximize the surface area exposed to the hot water.

Figure 36: Fisher Scientific 95°C water bath

The water chambers were filled with tap water. The water level in the chambers was monitored on a regular basis and required a top up every 2-3 days due to the loss of water loss by evaporation.

Water Absorption

Before tensile testing, samples were extracted from their respective environmental water chamber and were left at room temperature. The weight of the samples was recorded after 24 hours to track the moisture intake of the samples.

To determine the mass change due to water immersion, the tensile samples were withdrawn from the water, wiped dry to remove surface moisture, and then weight was recorded to the nearest 0.0001g, as shown in Figure 37. The percentage mass change of the composite samples (M) was be calculated by Equation (3.2) [28]:

$$M = \frac{M_t - M_o}{M_o} 100[\%] \quad (3.2)$$

Where,

$M =$ Percentage mass change

$M_t =$ Mass of the sample after a given immersion time, g

$M_o =$ Original mass of the sample, g

Figure 37: Sensitive scale with 4 decimal place resolution

Room Temperature Tensile Testing

In preparation for tensile testing, rectangular-shaped aluminum shoulder tabs of dimensions 51.7 mm x 23.5 mm x 2.9 mm were attached to the sample using super glue, as shown in Figure 38.
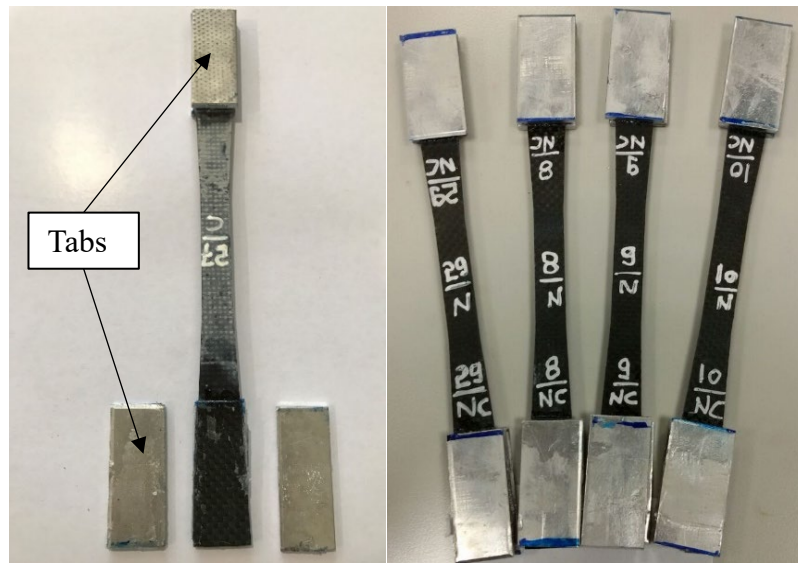
Figure 38: Aluminum shoulder tabs

The shoulder tabs act as a spacer to help with proper alignment and gripping of the samples by the jaws of the tensile testing machine. It also prevents the sample from fracturing under the jaw's grip.

Tensile test was performed at Room Temperature (RT) on control and conditioned cured samples in accordance to ASTM D-3039, as shown in Figure 39. The tensile test was carried out using MTS Universal Testing Machine with 100 kN load cell at a crosshead displacement of 2 mm/min [42], [43] The ultimate tensile strength F^{tu}, and tensile stress σ_i were calculated as per Equations (3.3 and 3.4) :

$$F^{tu} = \frac{P^{max}}{A} \qquad (3.3)$$

$$\sigma_i = \frac{P_i}{A} \qquad (3.4)$$

Where,

F^{tu} = Ultimate tensile strength, MPa

P^{max} = Maximum load before failure, N

σ_i = Tensile stress at ith data point, MPa

P_i = Load at the ith data point, N

A = Avergae cross-sectional area of specimen, mm^2 [44]
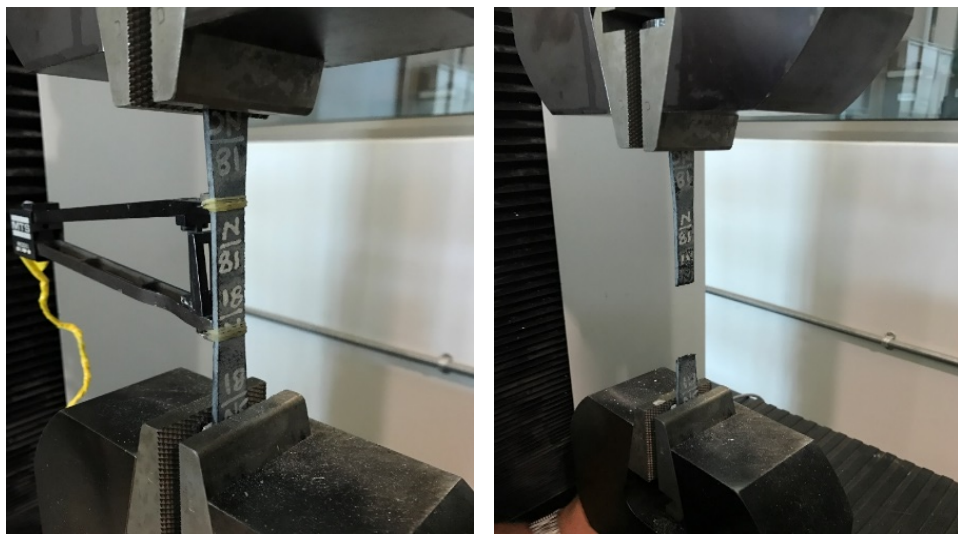
Figure 39: Tensile sample testing at room temperature

High Temperature Tensile Testing

High temperature tensile testing was performed on control compacted tensile samples to study the impact of high temperature testing on the tensile strength of the samples. The high temperature tensile test was performed at different temperatures (70°C, and 90°C ± 5°C) and was achieved by installing a heat chamber around the tensile testing fixture, as shown in Figure 40 (a) and (b). When the required temperature inside the chamber was achieved, an additional time margin of few minutes was given in order to ensure that all the test chamber, the test fixture, and the samples have achieved the desired temperature before starting the test. The high

temperature tensile test was performed in accordance with ASTM D-3039 and was carried out using ZWICK/ROEL of 100 kN load cell at a crosshead displacement of 1.27 mm/min.

(a)   (b)
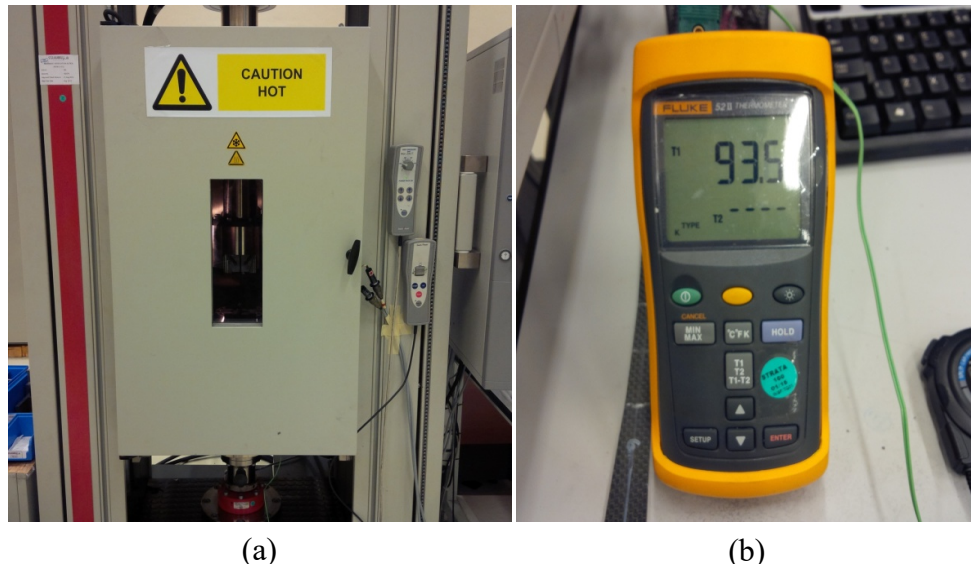
Figure 40: High temperature tensile testing. (a) Tensile test heat chamber (b) Temperature reading inside the heat chamber

3.3.2 Flexural, ILSS, DMA and DSC Samples

After the preparation of the tensile samples, the remaining cutouts from the flat composite panels (compacted and non-compacted test panels) were used to prepare the remaining test samples for the flexural, ILSS, DSC and DMA tests. A milling machine was used to cut out the specified samples dimensions, in addition to using a surface grinder for trimming to achieve the exact required dimensions, as shown in Figure 41 (a) and (b). After cutting the samples, both compacted and non-compacted samples were conditioned by immersion in water baths maintained at 40°C, 70°C and 95°C.

<table>
<tr><td>(a)</td><td>(b)</td></tr>
</table>
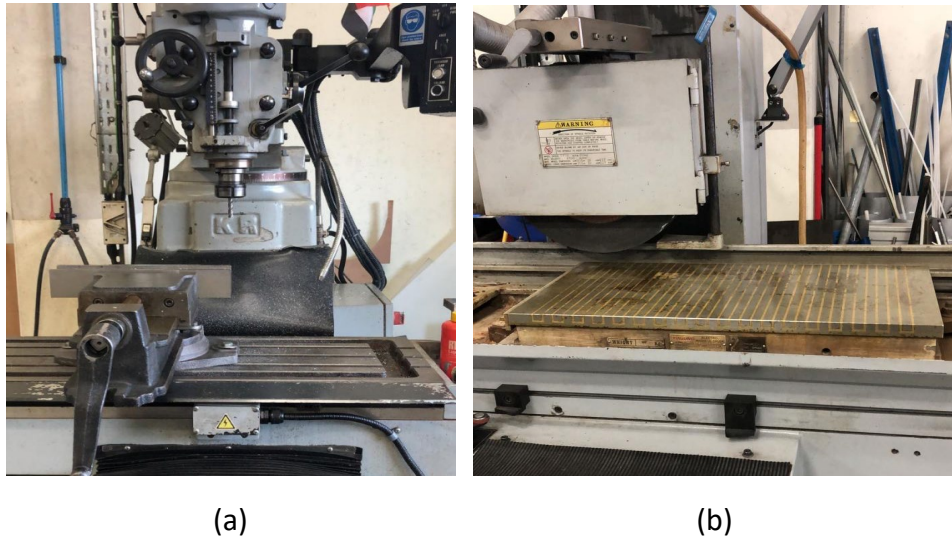
Figure 41: Cutting machines. (a) Milling machine (b) Surface grinder

Flexural Samples

The flexural modulus and strength of the composites were determined for control and conditioned samples using the 3-point bend test method, in accordance to ASTM D790 (Standard Test Methods for Flexural Properties of Unreinforced and Reinforced Plastics and Electrical Insulating Materials). Flexural samples of dimensions 58 mm x 12.7 mm with an average thickness of 2.6 mm were prepared as shown in Figure 42.

Figure 42: Flexural test samples

The specimens were tested with a span length of 41.9 mm, and a cross head displacement rate of 1mm/min. The flexural strength σ_f, and the flexural modulus E_B of the composite was calculated as per Equations (3.5 and 3.6).

$$\sigma_f = \frac{3PL}{2\,bd^2} \qquad (3.5)$$

$$E_B = \frac{L^3 m}{4bd^3} \qquad (3.6)$$

Where,

σ_f= Stress in the outer fibers at midpoint, MPa

P= Load at a given point on the load-deflection curve, N

E_B = Modulus of elasticity in bending, MPa

L = Support span, mm

b = Width of beam tested, mm

d = Depth of beam tested, mm

m = Slope of tangent to the initial straight-line portion of the load-deflection curve, N/mm of deflection [45]

Interlaminar Shear Strength Samples

The Interlaminar Shear Strength (ILSS) test was conducted to examine any change in the laminar shear strength on the control and conditioned test samples, in accordance to EN 2563 (Determination of the Apparent Inter Laminar Shear Strength) standard. The samples preparation was performed as per standard EN 2655 (Aerospace Series Preparation of Carbon Fibre Reinforced Resin Panels for Test Purposes) with

the dimensions of 20 mm x 10 mm and an average thickness of 2.6 mm, as shown in Figure 43.

Figure 43: ILSS test samples

The test was performed on a Zwic/Roell Z010 UTM of 10 kN load cell at a crosshead displacement rate of 1 mm/min, and a span length of ≈12.6 mm. The shear strength was calculated as per Equation (3.7).

$$\tau = \frac{3P_R}{4\,b\,h} \qquad\qquad (3.7)$$

Where,

τ = Apparent interlaminar shear strength, MPa

P_R = Maximum load at the moment of first failure, N

b = Width of specimen, mm

h = Thickness of specimen, mm

Differential Scanning Calorimetry (DSC) Samples

Differential Scanning Calorimetry (DSC) tests were performed on control and conditioned cured samples to determine the glass transition temperature using TA Instrument Q200 series as shown in Figure 44.

Figure 44: TA Instrument Q200 series
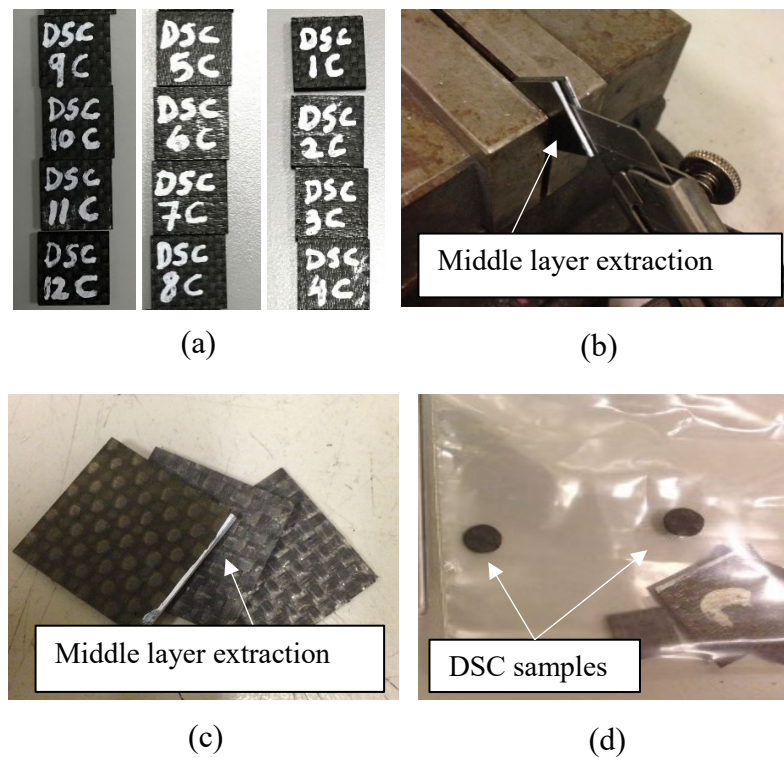
Figure 45: DSC samples preparation

DSC samples were prepared by first cutting out square samples as seen in Figure 45 (a), from which the middle layer was extracted to get the desirable thickness of the sample as shown in Figure 45 (b) and (c). Using a puncher, DSC samples were prepared as shown in Figure 45 (d).

Dynamic Mechanical Analysis (DMA) Samples

In order to compare it with the values obtained by the DSC test, the glass transition temperature of the composites system was also determined by performing Dynamic Mechanical Analysis (DMA) on control and conditioned samples. The DMA tests were conducted in accordance with AITM1-0003 (Determination of Glass Transition Temperatures) using Perkin Elmer DMA8000 system as shown in Figure 46.
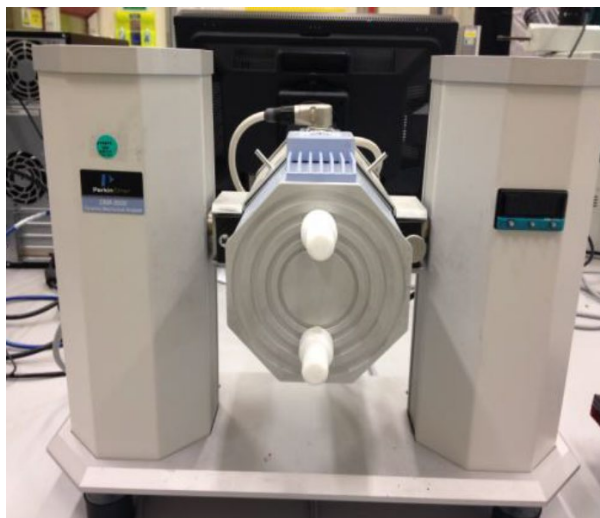
Figure 46: Perkin Elmer DMA8000 system

The test specimens were prepared having dimensions of 35 mm x 10 mm with an average thickness of 2.6 mm, as shown in Figure 47.

Figure 47: DMA test samples

The test was conducted under a constant strain control mode in a single cantilever set-up, using a DMA8000 from Perkin Elmer. The DMA continuously measures force (F), displacement (D) and phase angle (δ) between the stress and strain vectors during tests. The storage modulus E′, loss modulus E″ was calculated using Equations (3.8 and 3.9) [46], [47].

$$E' = \frac{l^3}{wt^3}\frac{F}{D}g \ sin\delta \qquad (3.8)$$

$$E'' = \frac{l^3}{wt^3}\frac{F}{D}g \ cos\delta \qquad (3.9)$$

Where,

l = Length of the sample

w = Width of the sample

t = Thickness of the sample

g = Gravitational constant

A single cantilever arrangement was chosen since it generates data that are closer to the actual mechanical properties of the composite parts during curing [12, 13]. The glass transition temperature was determined using loss modulus.

3.3.3 Scanning Electron Microscope (SEM)

The fracture surfaces of the tensile samples were examined for visible signs of fiber/resin degradation due to the long-term exposure using a Scanning Electron Microscope (SEM) [48] on control and exposed samples, for both compacted and non-compacted. The scanning electron microscope used was JEOL JSM-5600, as shown in Figure 48 (a).

The samples were cut in 1 cm x 1 cm size and fixed vertically on the SEM specimen stub using double-sided conductive carbon tape and were coated with a gold layer using JEOL JFC-1200 Fine Coater, as shown in Figure 48 (b).

| (a) | (b) |
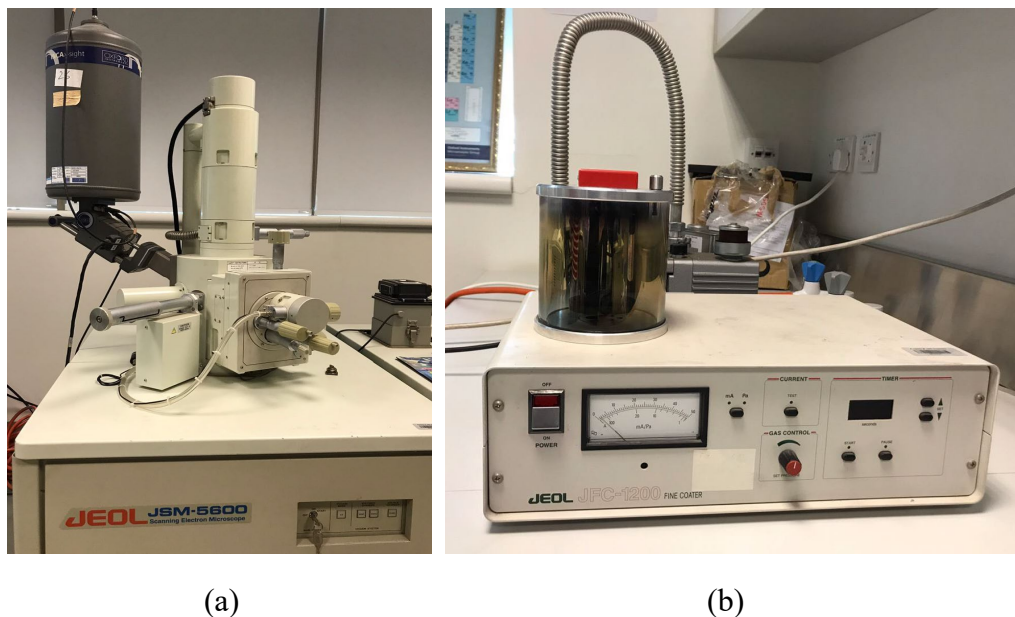
Figure 48: Equipment used for SEM test. (a) Jeol JSM-5600 Scanning Electron Microscope (b) Jeol JFC-1200 Fine Coater

3.3.4 Experimental Work Plan

Rectangular shaped test panels were fabricated from Carbon/epoxy prepregs, using the dry lay-up process. Two groups (compacted and non-compacted) were fabricated and were cured in the same autoclave cycle to ensure similar material properties between the test panels and eliminate the variability associated with curing in different cure cycles. Non-destructive scanning techniques were used to investigate the integrity of the panels after curing, and the impact on porosity as a result of removing both in-process compactions and the usage of bleeders during the fabrication process on the non-compacted composite panels group. The test panels were used to manufacture the test specimens required for mechanical and thermal tests. The test specimens were immersed in water heating baths of 40°C, 70°C and 95°C for different periods of time. The 40°C and 70°C water chamber systems were constructed in the lab using a calibrated electric heater and a glass beaker, while the 95°C water chamber was achieved using a fisher scientific water bath. A number of mechanical, thermal, and microstructural/physical tests were conducted to investigate the effect of long-term immersion on the performance of the composite material. Test results were analyzed to draw the findings and conclusions, which will be discussed in the next chapter.

The experimental work plan followed is shown in Figure 49 flow diagram

```
┌─────────────────────────────────┐
│      Selection of Material       │
└─────────────────────────────────┘
                 │
                 ▼
┌─────────────────────────────────┐
│   Fabrication of Test Panels:    │
│   (compacted and non-compacted   │
│            groups)               │
└─────────────────────────────────┘
                 │
                 ▼
┌─────────────────────────────────┐
│     Non-Destructive Testing      │
└─────────────────────────────────┘
                 │
                 ▼
┌─────────────────────────────────┐
│    Manufacturing of Specimens    │
└─────────────────────────────────┘
                 │
                 ▼
┌─────────────────────────────────┐
│ Construction and set-up of       │
│ conditioning water tanks of      │
│ temperatures 40°C, 70°C and 95°C │
└─────────────────────────────────┘
```

|Room Temperature Conditioning of Specimen (No Immersion)|Conditioning of Specimen at Various Temperatures for Different Time Periods (Immersion)|

Conducting Various Tests

| Mechanical Tests: Tensile at RT&HT Flexural ILSS | Thermal Tests: DMA DSC | Microstructural/Physical Tests: Non destructive Test (UT) Microsections (Void%) Water absorption SEM |

```
                 │
                 ▼
┌─────────────────────────────────┐
│        Analysis of Results       │
└─────────────────────────────────┘
                 │
                 ▼
┌─────────────────────────────────┐
│   Development of Findings and    │
│          Conclusions             │
└─────────────────────────────────┘
```
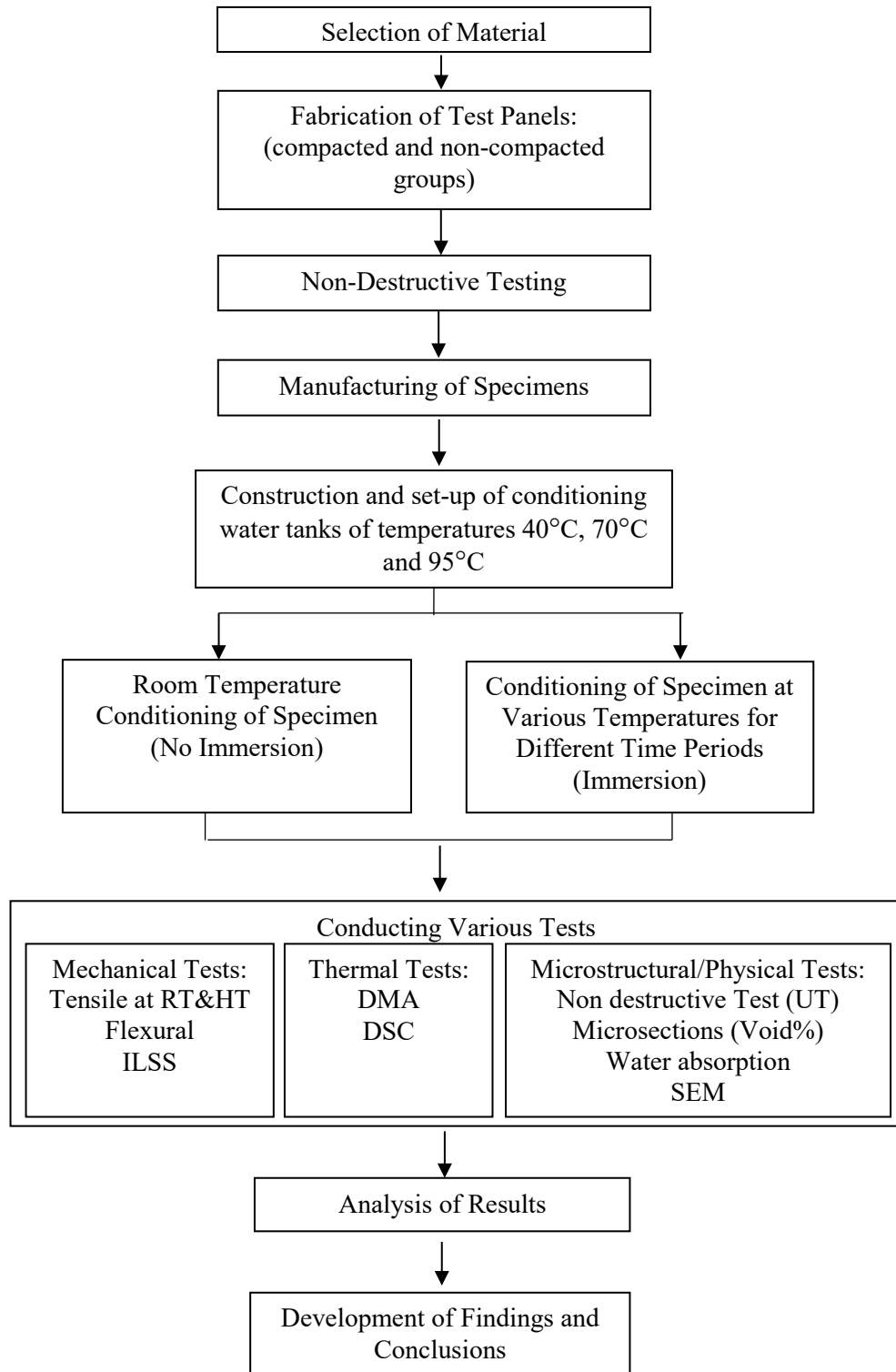
Figure 49: Experimental work plan

Chapter 4: Results and Discussion

4.1 Non-Destructive Testing

To investigate the integrity of the manufactured test panels after curing and to examine the effect of in-process compaction and the use of edge and surface bleeders on porosity, ultrasonic inspection of the test panels was performed by applying both (i) Automatic through transmission method (C-scan) and (ii) the Pulse – Echo method (A-scan).

C-scans were performed for all compacted and non-compacted test panels against a reference standard panel shown in Figure 50. A reference standard panel is a panel that is used to define the material, thickness and possible defect types for the inspection equipment or machine, it is representative of the composite part being tested. It is manufactured with staggered thicknesses and induced artificial defects/discontinuities. The thickness variation in the reference panel is represented by the different shades of grey as shown in Figure 50, and the artificial defects are appearing in red, as shown in Figure 50, which would produce a similar response to that caused by typical defects such as voids, de-bonds, de-lamination and inclusions (FOD) when detected in composites [49]. Figure 51 shows the implementation of the 6 dB drop method to evaluate the C-scans, where a defect-free area was identified on the reference panel at the required panel thickness of 12 layers (identified by the red box) from which a mean value of 10 dB was identified. 6 dB is added to the 10 dB resulting in 16 dB at which the scans were evaluated. The C-scans in Figure 52 and Figure 53 are representative scans of the compacted and non-compacted groups, illustrating that the panels are acceptable since no porosity or defects were detected by the scans as per the 6 dB drop method.
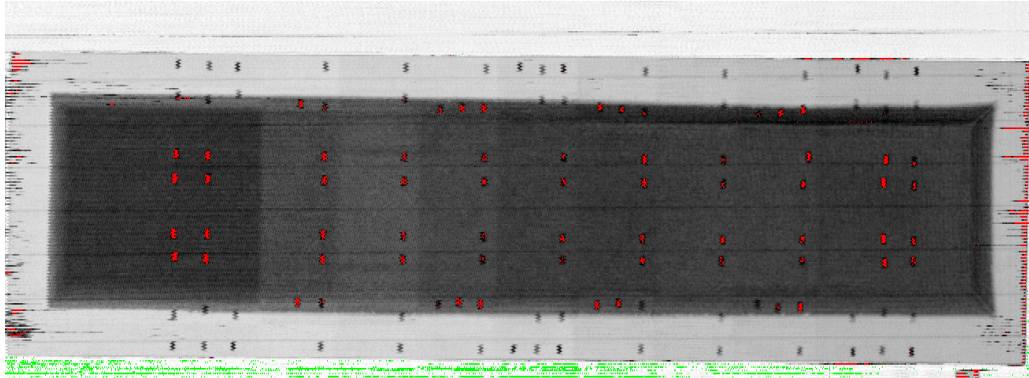
Figure 50: C-scan of reference panel showing thickness variation and artificial defects in the reference panel
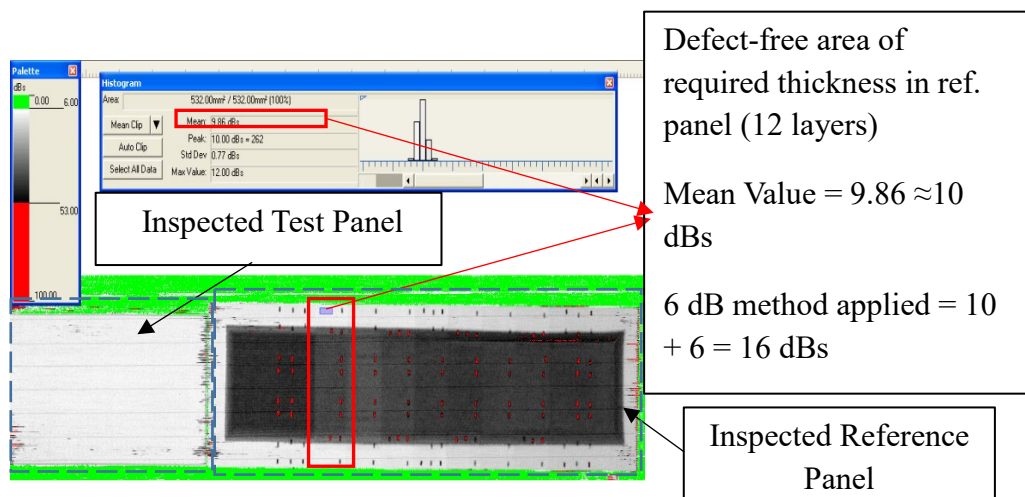

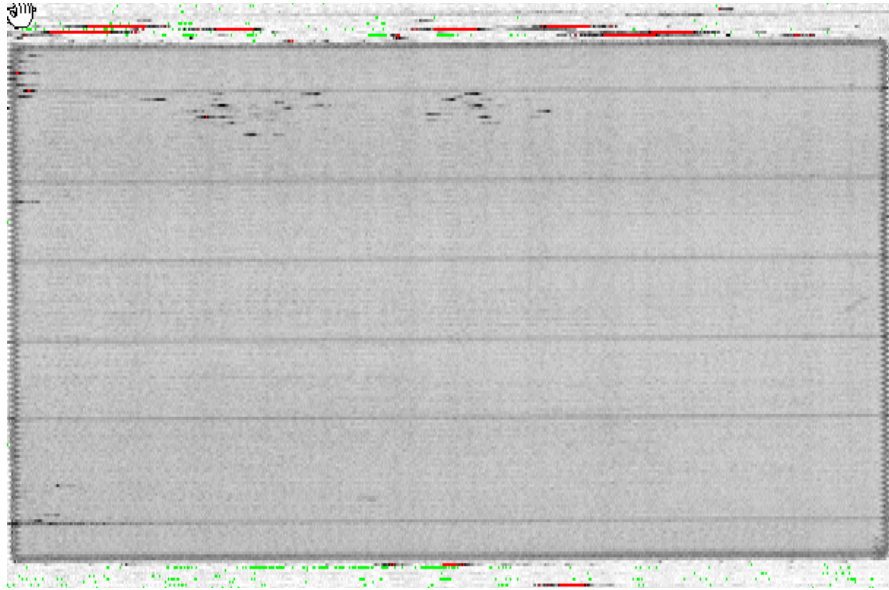Figure 51: Use of reference panel to implement the 6 dB drop method

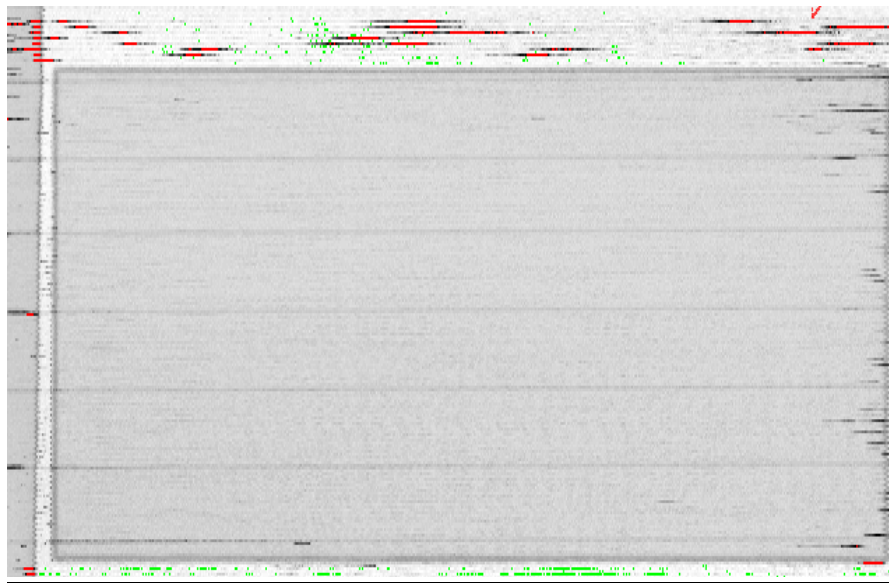Figure 52: Accepted C-scan of a compacted test panel

Figure 53: Accepted C-scan of a non-compacted test panel

A-scans of manufactured compacted and non-compacted test panels were manually performed when required to verify indications from the C-scan. The pulse echo device used to inspect monolithic regions displays raw live data on the display

screen as it scans showing Time/Distance in the horizontal axis, and the signal amplitude in the vertical axis. All panels A-scans (both compacted and non-compacted) reported an acceptable status showing continuous two peaks indicating that the composite panels are porosity/defect-free. Indications that were detected from C-scans where due to water backsplash from the water couplant and were cleared out by the A-scans.

A-scans and C-scans of the test panels indicated that both compacted and non-compacted test panels showed similar results, no porosity or defects were detected by the test equipment as per the 6 dB drop method, which indicate that for a 12 layer composite panel, the removal of in-process compaction and the use of edge and surface breathers has no significant effect. This could be attributed to the low number of composite layers, where the final applied vacuum bag was sufficient to remove the entrapped air if present.

4.2 Microsections Void Volume Fraction Calculation

Further investigation was performed to determine any presence of porosity/voids within the control samples. Fractography was performed on microsections of both compacted and non-compacted control groups with a magnification of 5x, from which the void volume fraction was calculated as presented in Table 3.

The void volume fraction analysis was performed using Stream Essentials software, based on a region of interest (ROI) of ~ 60 mm² for all the examined samples. As presented in Table 3, compacted control samples, C1 and C2, had a void content of

0.085% and 0.052% respectively, while the non-compacted control samples, NC1 and NC2 had slightly higher values of 0.139% and 0.460% respectively.

Table 3: Void volume fraction calculation of control samples

Description	Designation	ROI Area (mm²)	Area of Void (mm²)	Void (%)
Compacted Control	C1	60.2674	0.0510	0.085
Compacted Control	C2	60.4868	0.0314	0.052
Non-Compacted Control	NC1	60.1300	0.0838	0.139
Non-Compacted Control	NC2	60.0470	0.2763	0.460

Figures 54 to 57 show the microsection images of the compacted and non-compacted control samples of which the fractography analysis was performed. The magnified images show the plain weave style of the fabric through the weaving of the in-plane and out-of-plane fibers. Voids (porosity) are represented by the red colored spots and is typically found in the resin area.
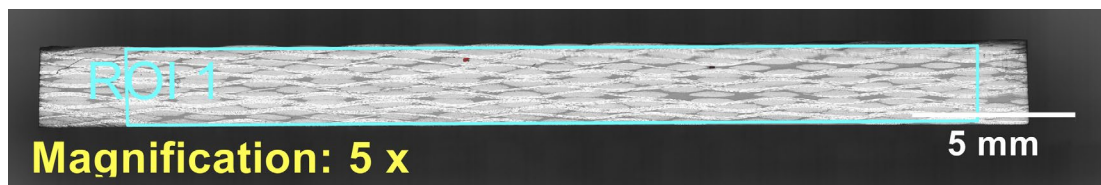

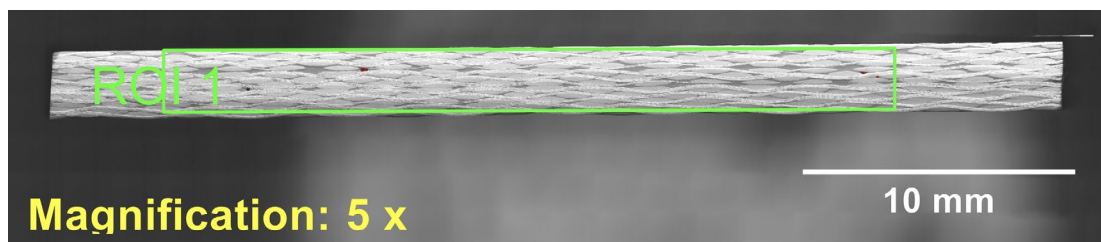Figure 54: Microsection image of compacted control sample – C1

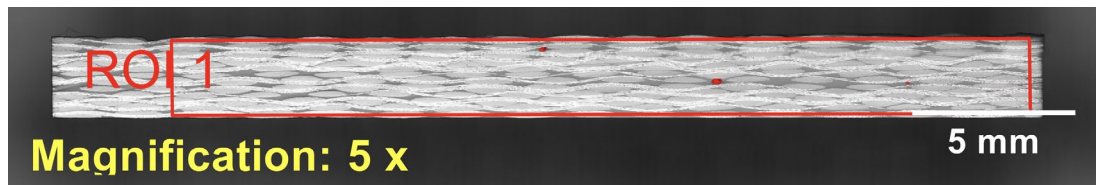Figure 55: Microsection image of compacted control sample – C2

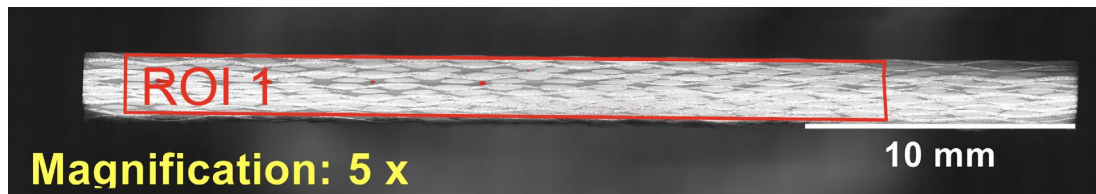Figure 56: Microsection image of non-compacted control sample – NC1

Figure 57: Microsection image of non-compacted control sample – NC2

The higher void content values in the non-compacted control group is explained by the removal of the in-process compactions and the removal of the edge and surface breathers which typically aid in the removal of the entrapped air between the composite layers. Although the non-compacted control group showed a slightly higher void content than the compacted control group, both groups were considered acceptable as indicated by the NDT test results obtained.

4.3 Water Absorption Test

The weight of specimens was taken before immersion into the water at different temperatures. Every month specimens were removed from water tank and re-dried at room temperature for 24 hours to determine the change in the weight. The final weight change percent of specimen after drying was calculated as follows:

$$W\ (\%) = \frac{W_2 - W_1}{W_1} \times 100$$

Where,

W (%) = Weight change percentage, %

W_2 = Weight after drying, g

W_1 = Weight before immersion, g

Figure 58 shows the percentage change in the weight of the specimen after different periods of immersion. An increase in the weight of the specimen was observed at 40°C, 70°C and 95°C for compacted and non-compacted specimens. The water absorption or increase in weight was 1.34%, 1.52% and 2.52% after the immersion of 9 months for compacted specimens at 40°C, 70°C and 95°C respectively. However, the weight of non-compacted specimens increased by 1.41%, 1.64% and 2.82% after the immersion of 9 months at 40°C, 70°C and 95°C, respectively.

The results show that water absorption was higher in non-compacted samples as compared to compacted samples, and this could be due to the slightly higher void content present in the non-compacted group compared to the compacted group, as seen in the previous section (void volume fraction calculation). However, the general increase in weight, for both groups, is due to the water absorption that occurs through diffusive and/or capillary processes. Diffusion is considered a key process under which moisture penetrates polymeric composites and is known to be a matrix-dominated phenomenon in which water is mainly diffused in the matrix [11], [12]. The capillary process involves moisture being drawn into voids and microcracks at the fiber/matrix interfaces, in which the cracks provide a transport system for moisture penetration [25], [27].

Moreover, for all exposure times, it was observed that higher absorption occurs at higher exposure temperatures, for both compacted and non-compacted groups, which therefore indicates that higher temperatures accelerate the absorption process, which could be due to the deteriorating effect of temperature in generating higher degradation (such as micro-voids), which in turn induces higher absorption. Similar findings were reported in the literature, where higher temperatures are observed to have more influence in accelerating the moisture absorption and degradation process in polymers [14].

As seen in the literature, the extent of deterioration that takes place in fiber reinforced polymers due to environmental exposure is associated with the amount of moisture absorbed [11], [24], therefore it is important to highlight that the highest increase in weight due to water absorption reported was less than 3%, observed in the non-compacted group immersed at the highest exposure temperature of 95°C for the longest exposure period of 9 months.
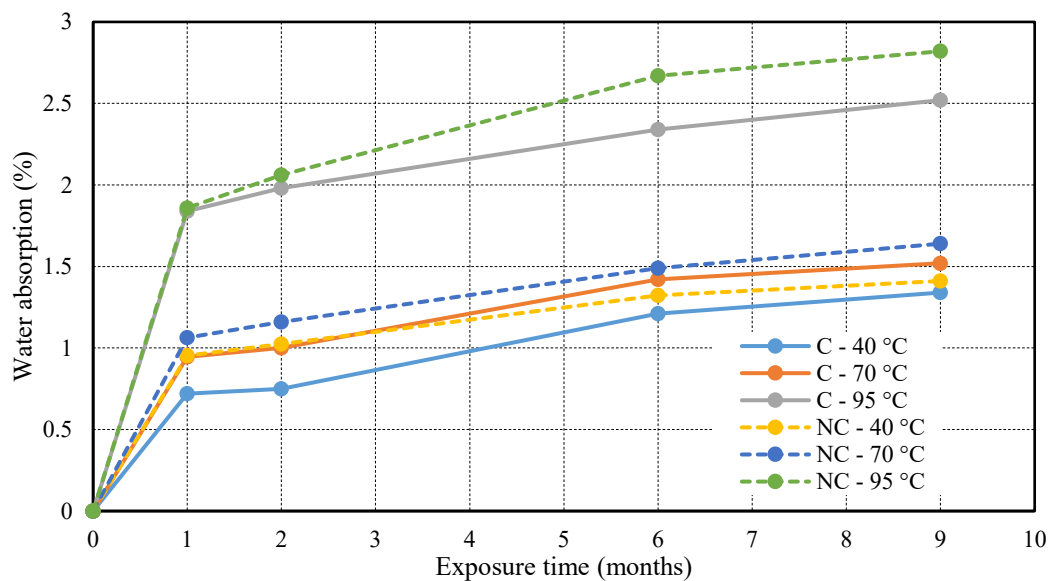

Figure 58: Variation in weight of compacted and non-compacted composite with conditioning duration and temperature

4.4 Tensile Strength Test

Tensile strength of both compacted and non-compacted specimens is shown in Figure 59. The tensile strength of the compacted specimen reduced by only 2.9% at the immersion of 9 months at 40°C, whereas the drop in the strength was higher combatively at 95°C for the same duration of time, where the strength reduced by 6% from 601.8 MPa to 565.9 MPa. Sample immersed at 70°C had the mediate effect of water and high temperature on the durability of composite and it reduced to 95.5%. The trend of reduction in tensile strength of compacted and non-compacted specimen observed to be same for the duration of 9 month at 40°C. Tensile strength of non-compacted specimen reduced by 3% and 6.3% at the immersion of 40°C and 70°C, whereas a significant decrease in the tensile strength was noted at 95°C for non-compacted specimen and it reduced by 14.8% from 593 MPa to 504.8 MPa. The reduction in the tensile strength of compacted specimens was gradual at all temperatures. Same rate of reduction was observed for the non-compacted specimen immersed at 40°C and 70°C, whereas the drop was sharp at 95°C. The reduction was 9% higher at 95°C for non-compacted samples as compared to compacted samples for the same exposure duration of 9 months. For non-compacted specimen immersed at 95°C, the tensile strength sharply reduced by 8% from 593 MPa to 541 MPa within 2 months of immersion and continued to 504.8 MPa with comparatively lesser rate in 9 months.
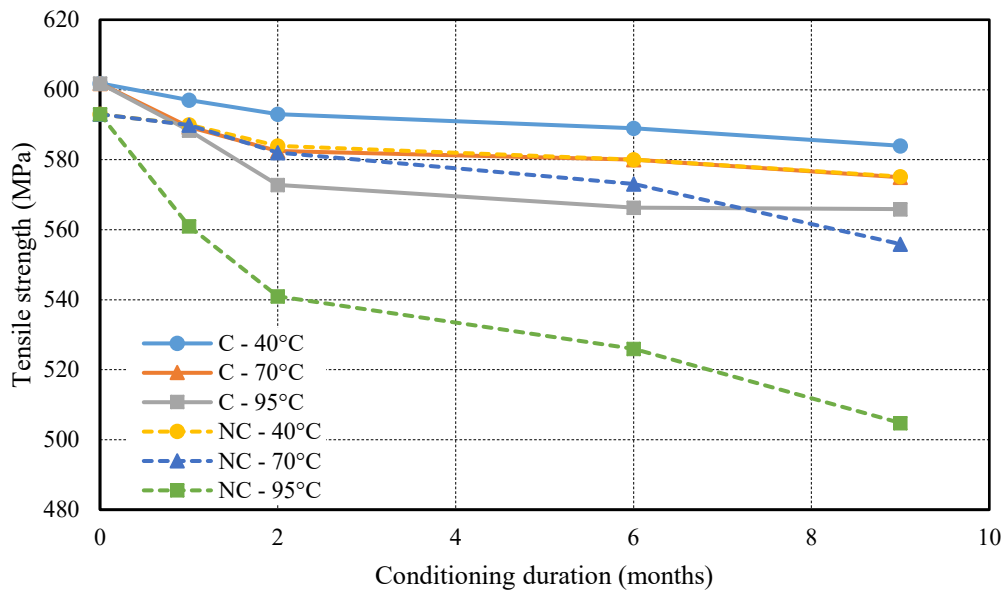
Figure 59: Tensile strength of compacted and non-compacted composite after the immersion of 9 months at different temperatures

The carbon fiber shares most of the load applied to the laminates, and the fiber/matrix interface plays an important role in load transmission [50]. Therefore, the deterioration of the fiber/matrix interface due to water immersion led to a decrease in the fiber/matrix interface load transmission efficiency; as a result, the mechanical properties of the laminates deteriorated. Previous studies have shown a similar behavior in which the strength decreases immediately after immersion and gradually decreases to saturation depending on the amount of water absorbed in the sample [26], [51]. Therefore, it was suggested that the deterioration of the mechanical properties greatly depended on the deterioration of the fiber/matrix interface resulting from water immersion.

The highest reduction in tensile strength was 14.8% observed in the non-compacted group when immersed at the highest exposure temperature of 95°C for the longest exposure period of 9 months. The compacted group experienced a reduction

of 6% for the same conditions. This behavior could be due to the fact that the non-compacted group, at the mentioned conditions, experienced the highest increase in weight due to water absorption of 2.82%, as seen in the previous section. However, the difference in weight change is relatively small compared to the compacted group which experienced a weight increase of 2.52%, at the same conditions. Therefore, another reason for the reduction in strength could be due to the presence of higher amounts of voids in the non-compacted samples compared to the compacted samples, which was initially observed in the control specimen showing a higher tensile strength of 601.8 MPa for the compacted samples, compared to 593 MPa for the non-compacted control samples.

The tensile strength of control compacted samples was also determined by testing at high temperature chamber. The temperature of the chamber was maintained at 70°C and 90°C. The tensile strength of control samples tested in the chamber maintained at 70°C and 90°C was 592.3 MPa and 584.3 MPa, respectively as shown in Figure 60. The reduction in the strength could be due to the plasticization of the fiber/matrix interface at high temperatures.
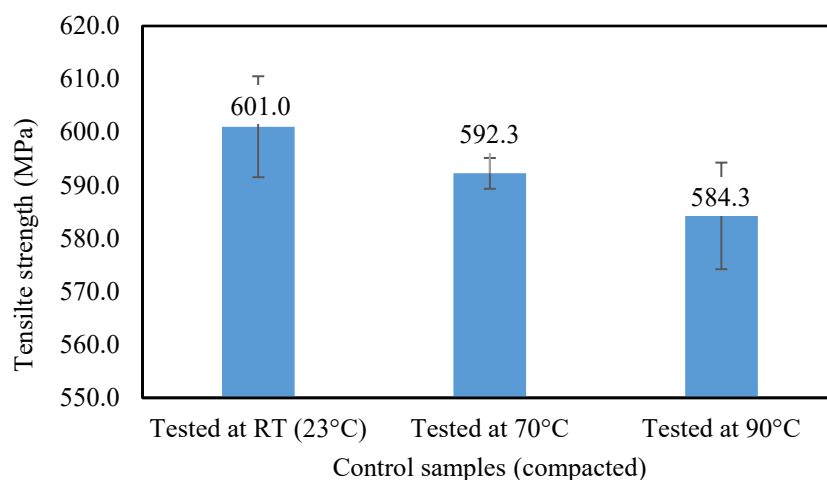

Figure 60: Tensile strength of compacted control samples tested at RT, 70°C and 90°C chamber in ZWICK machine

4.5 Three Point Flexural Test

Similar trend was observed, where the control samples of the compacted group showed a slightly higher initial flexural strength compared to the non-compacted control samples, shown in Figure 61.

A decrease in the flexural strength of the specimens was observed at 40°C, 70°C and 95°C for both compacted and non-compacted samples, as shown in Figure 61. The flexural strength of compacted samples decreased by 4.6%, 6.8% and 10.8% with respect to the control after the immersion period of 10 months at 40°C, 70°C and 95°C respectively. However, for non-compacted samples it decreased by 3.3%, 6.1% and 15.6% for the similar conditions.

The rate of deterioration was significantly high in both compacted and non-compacted sample immersed at 95°C. The compacted samples show the flexural strength of 43.3 MPa and 40.5 MPa for the immersion of 10 months at 40°C and 95°C respectively. The degradation was 6.5% higher in samples immersed at 95°C as compared to 40°C. Similarly, the non-compacted samples show the flexural strength of 42.7 MPa and 37.3 MPa for the immersion of 10 months at 40°C and 95°C respectively. The degradation was 12.6% higher in samples immersed at 95°C as compared to 40°C.

The flexure strength reduced with the higher rate in two months then dropped gradually till 10 months for the compacted specimen for all immersion temperatures as shown in Figure 61. A similar trend was observed for the non-compacted specimens immersed at 40°C. The rate of decrease in flexural strength was significantly high for non-compacted specimen immersed at 95°C in comparison of all other conditions. At

95°C, the flexural strength reduced by almost 12.6% from 44.2 MPa to 37.3 MPa in the immersion period of 10 months, which is similar to the behavior observed for the tensile strength results for the same conditions.

One probable reason could be due to the absorbed moisture diffused into intermolecular chains causing the epoxy in the carbon/epoxy composites to swell, while carbon fiber neither absorbs water nor swells, thus damaging the interfaces between carbon fibers and epoxy resin due to the unmatched swelling effecting the ability of the the matrix to transfer the loads to the fibers effectively, hence resulting in the reduction of flexural strength values [20].
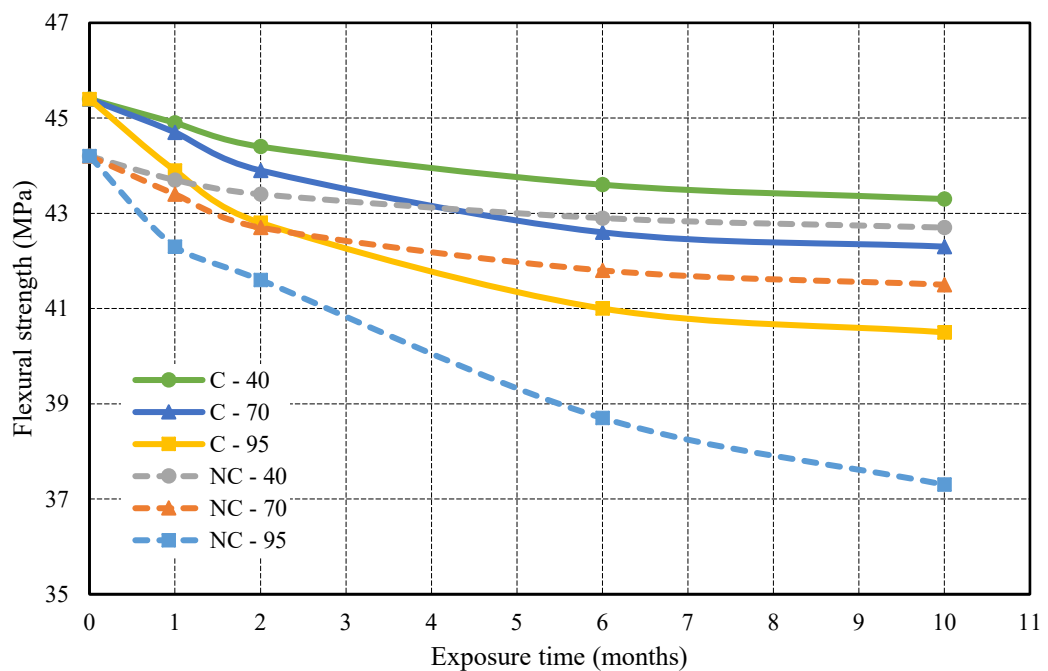

Figure 61: Flexural strength of compacted and non-compacted composite after the immersion of 10 months at different temperatures

Compacted specimens indicated almost same flexural modulus at 40°C, 70°C and 95°C as shown in Figure 62 (a) but slight variation was observed in non-compacted specimens as shown in Figure 62 (b). The force versus displacement are curves shown

in Figure 63 for compacted and non-compacted specimens after 10 months of immersion. The non-compacted specimen immersed at 40°C shows similar behavior as compacted specimens but significant decrease in the flexural modulus and force observed in specimens immersed at 70°C and 95°C after the immersion of 10 months. The decrease in the flexural force of the samples immersed at 95°C was observed to be only 3% (from 1366N to1324N) in compacted specimens whereas it was 7.6% (from 1345N to1243N) for non-compacted specimens with respect to samples immersed at 40°C. This degradation also indicates dominant decrease in the modulus of non-compacted samples as compared to compacted samples.
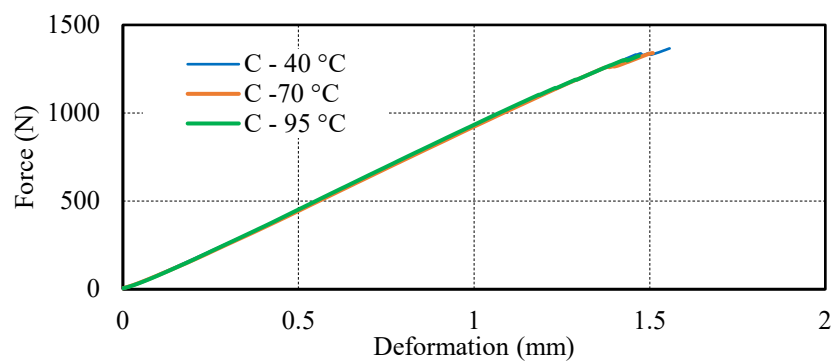
(a)
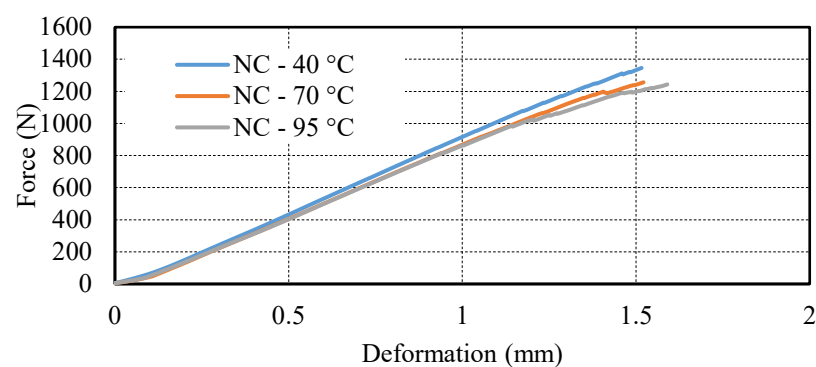
(b)

Figure 62: Force-deformation behavior samples at various temperature for the exposure of 10 months at different temperatures (a) Compacted samples (b) Non-compacted samples
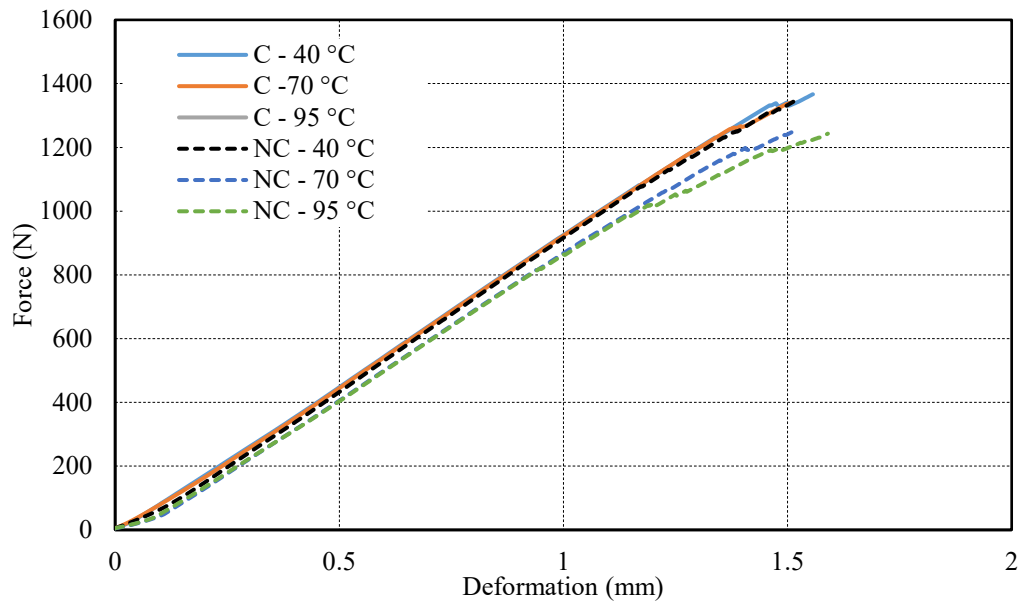
Figure 63: Force-deformation behavior comparison of compacted and non-compacted composite samples at different temperatures for the exposure of 10 months

4.6 Interlaminar Shear Strength (ILSS) Test

Figure 64 presents the variation of Interlaminar Shear Strength (ILSS) against exposure time (up to 10 months) for compacted and non-compacted samples immersed at 40°C, 70°C, 95°C for the immersion period of 10 months. The interlaminar shear strength of the compacted and non-compacted control specimens was 73.8MPa and 71.8 MPa respectively. The results show that the interlaminar shear strength of both composites reduced linearly with respect to time and temperature. The interlaminar shear strength of the compacted samples reduced by 10.3%, 12.4%, and 17.3% whereas it reduced by 11.3%, 12.6% and 17.2% for non-compacted samples after the immersion of 10 months at 40°C, 70°C and 95°C respectively.

Higher degradation in shear strength was experienced at higher conditioning temperatures for longer exposures. This behavior could be due to the deteriorating effect of temperature in generating thermal stress that may stimulate the initiation and propagation of cracks at the carbon/epoxy interface, due to the difference in the moisture-induced volumetric expansion rate between the epoxy matrix and reinforcement carbon fiber, since the amount of moisture absorbed by the carbon fibers is significantly less than that by the epoxy matrix [11].
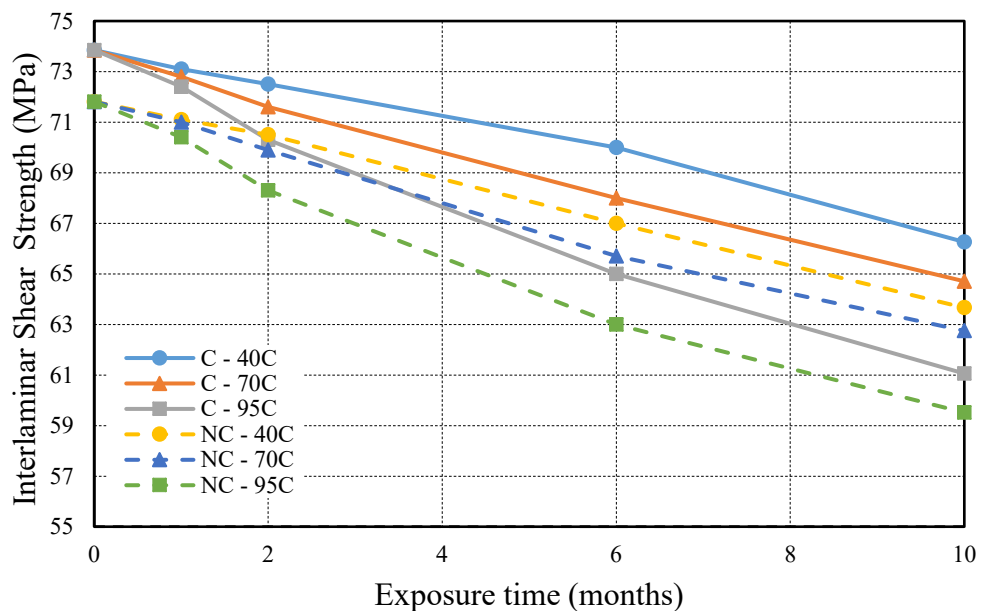

Figure 64: Interlaminar shear strength of compacted and non-compacted composite after the immersion of 10 months

The load versus displacement curves for interlaminar shear strength are shown in Figure 65 for compacted and non-compacted specimens after 10 months of immersion. There is a linear relationship between the load and deformation, then the curves slightly deviate from linearity till the fracture load. The compacted specimen immersed at different temperatures showed same modulus, but significant decrease in

the shear modulus was observed for non-compacted samples with the increase of immersion temperature. The maximum load for compacted samples immersed at 40°C, 70°C and 95°C was 2208.1N, 2146.5N and 2050.7N respectively whereas it was 2187.8N, 2030.4 and 1994.5N for non-compacted samples.
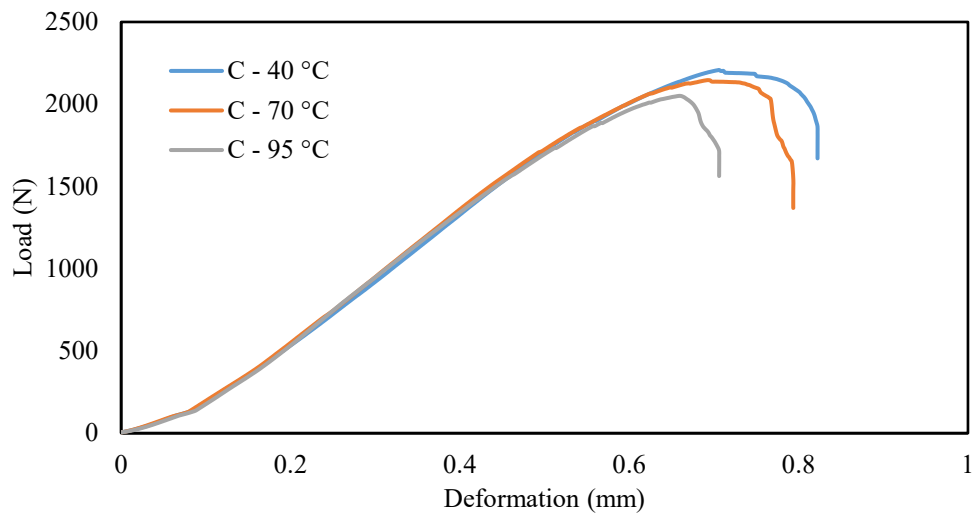

(a)
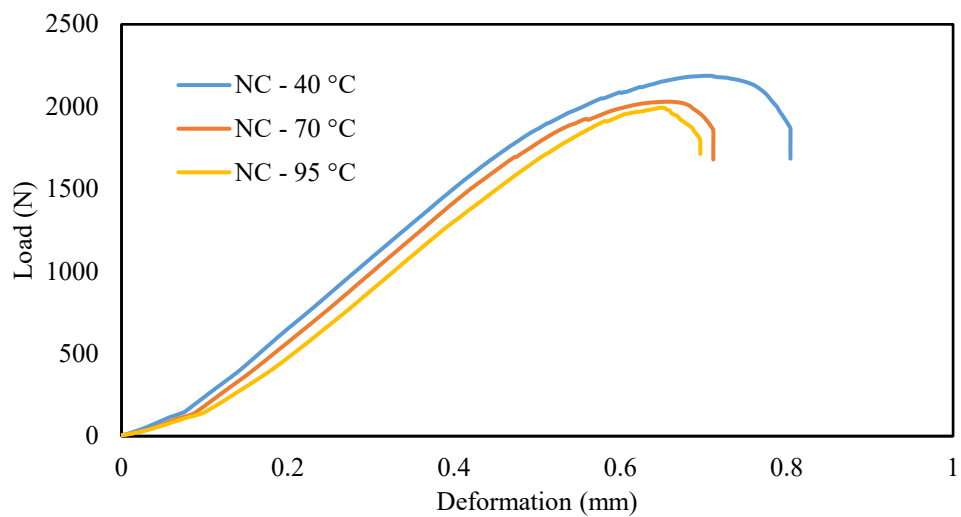
(b)

Figure 65: Load-deformation behavior of samples immersed at various temperature for the exposure of 10 months (a) Compacted samples (b) Non-compacted samples

4.7 Differential Scanning Calorimetry (DSC) Test

Figures 66 and 67 present the DSC curves for the compacted and non-compacted samples immersed at 40°C, 70°C and 95°C for the duration of 10 months. Four samples were tested for each condition. The curves show the reproducibility of the results.
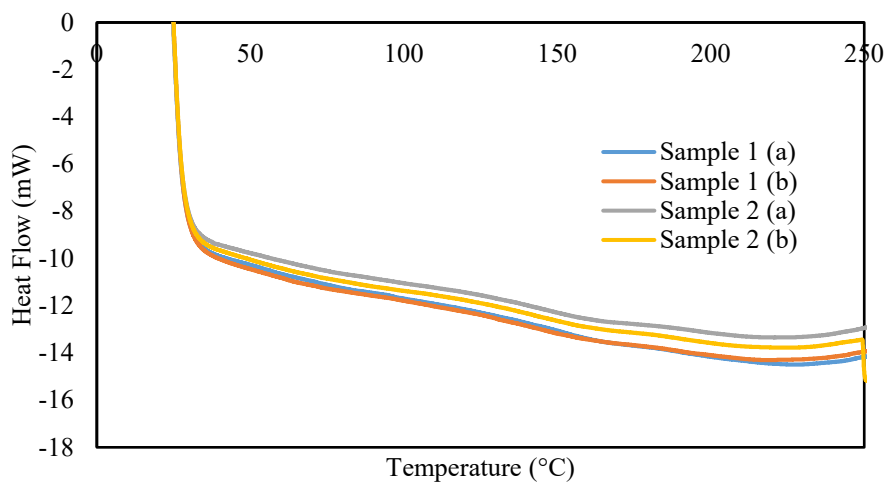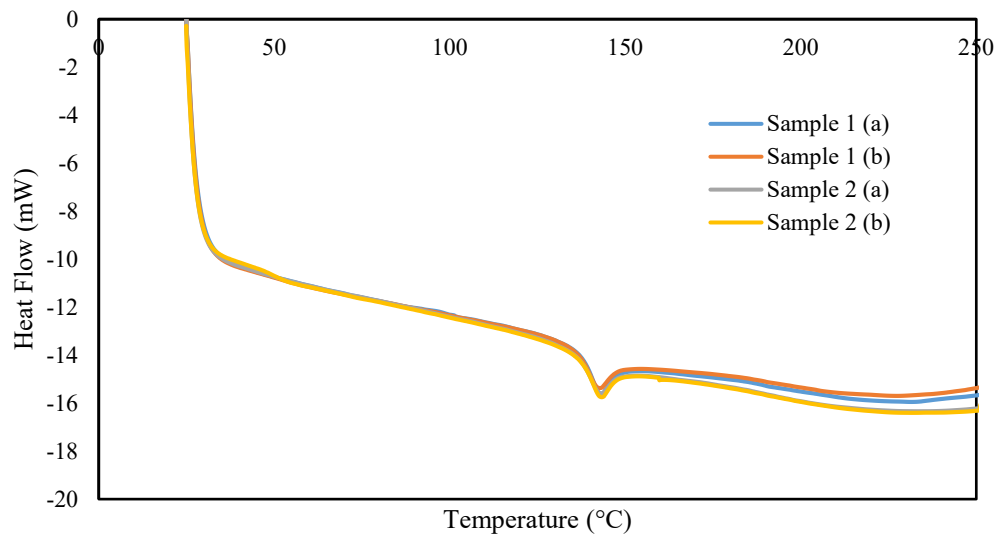

(a)
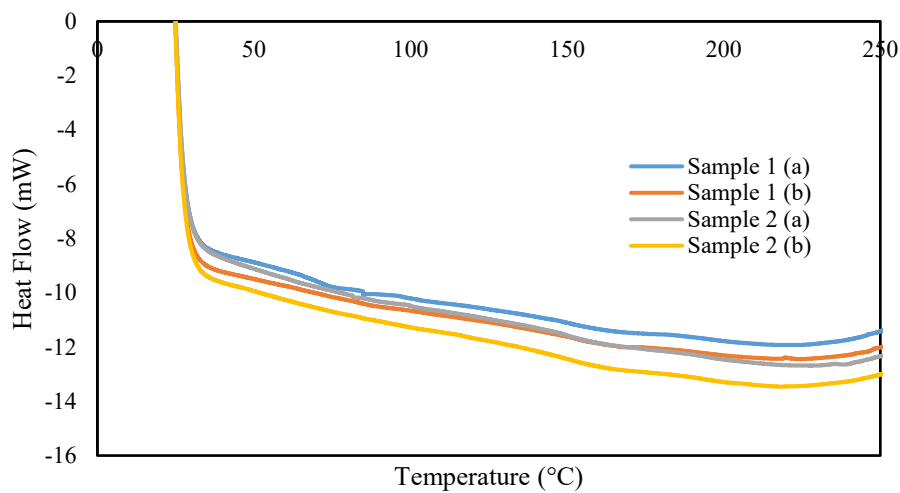
(b)

Figure 66: Heat flow vs temperature behavior of compacted samples immersed for the exposure of 10 months at (a) 40°C (b) 70°C (c) 95°C

(c)

Figure 66: Heat flow vs temperature behavior of compacted samples immersed for the exposure of 10 months at (a) 40°C (b) 70°C (c) 95°C (Continued)

(a)

Figure 67: Heat flow vs temperature behavior of non-compacted samples immersed for the exposure of 10 months at (a) 40°C (b) 70°C (c) 95°C
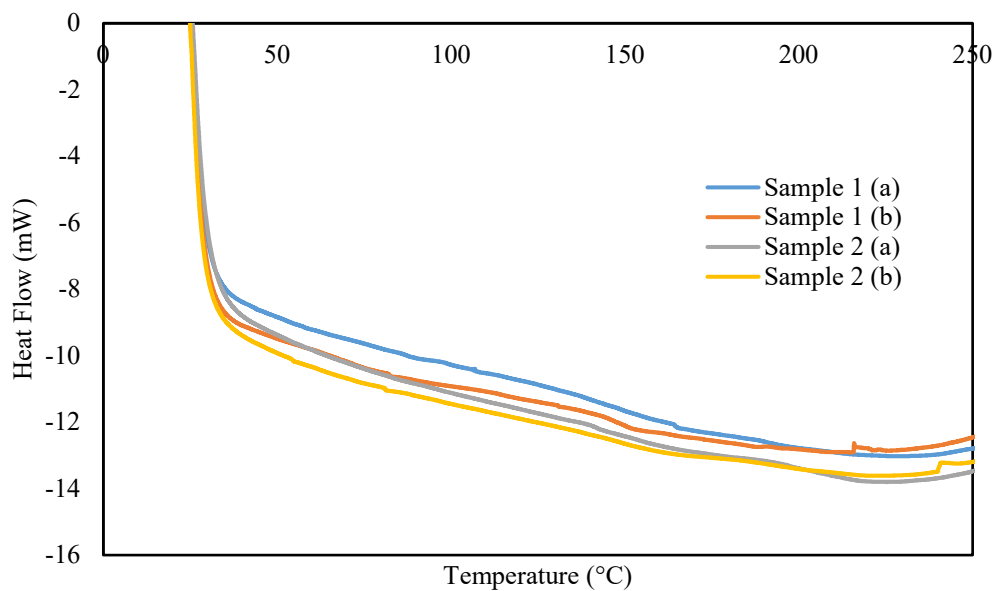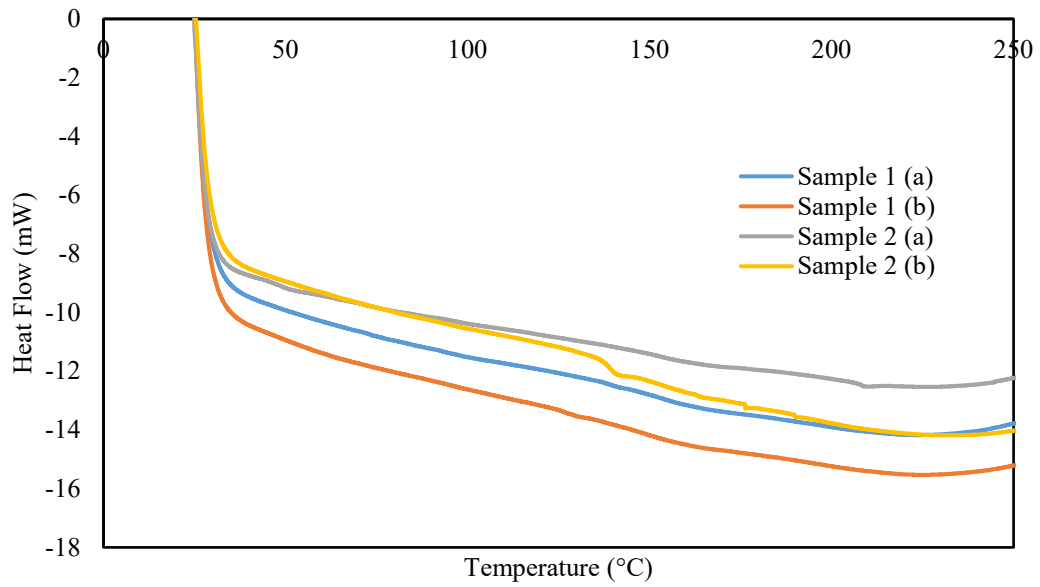
(b)

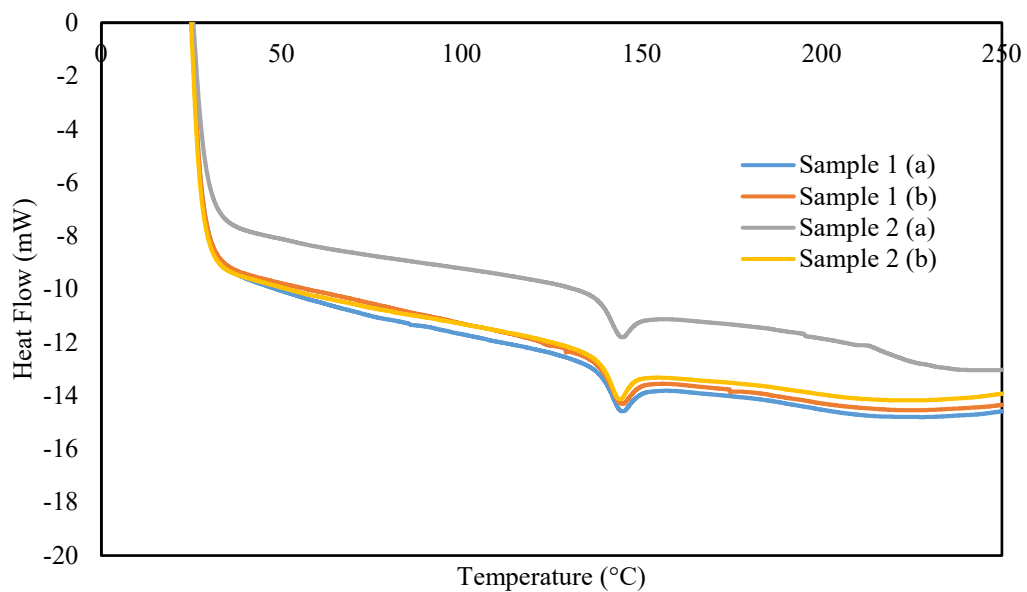
(c)

Figure 67: Heat flow vs temperature behavior of non-compacted samples immersed for the exposure of 10 months at (a) 40°C (b) 70°C (c) 95°C (Continued)

Figure 68 represents the DSC curves of compacted and non-compacted samples for the control samples and specimens immersed at 40°C, 70°C and 95°C. The

DSC results shows, the glass transition temperatures (Tg) of control compacted and control non-compacted samples was 203.27 and 204.5 respectively. To analyse the effect of time and temperature, the Tg was compared for the composite immersed for the duration of 10 months at 40°C, 70°C and 95°C. The Tg of both compacted and non-compacted samples significantly reduced with time at different exposure temperatures. The immersion had the same effect on both type of the samples and only slight variation was observed. Figure 68 (a) shows that the Tg of compacted samples reduced to 149.7°C, 150.4°C and 142.6°C after immersion period of 10 months at 40°C, 70°C and 95°C. Similarly, Figure 68 (b) shows that the Tg of non-compacted samples reduced to 150.7°C, 150.3°C and 142.1°C after immersion period of 10 months at 40°C, 70°C and 95°C.

The shift in Tg could be due to the combined effect of high temperature and water aging on the resin. The value of the Tg is related to the degree of polymerisation, or degree of cross-linking after curing, since a high Tg value suggests a high extent of curing of the resin. The presence of hydrophilic groups in epoxy due to presence of hydroxyl groups, which can also react with water molecules to form weak hydrogen bonds, is known to cause degradation due to moisture uptake [52] at 90C. This indicates that the absorbed water acts as a plasticizer by increasing the mobility of the chains and decreases Tg.

Thermal degradation presents the upper limit to the service temperature of plastics as much as the possibility of mechanical property loss. As such it can be explained as a molecular deterioration caused by overheating. At high temperatures, the components of the long chain backbone of the polymer can begin to separate

(molecular scission) and react with one another to change the properties of the polymer [53].
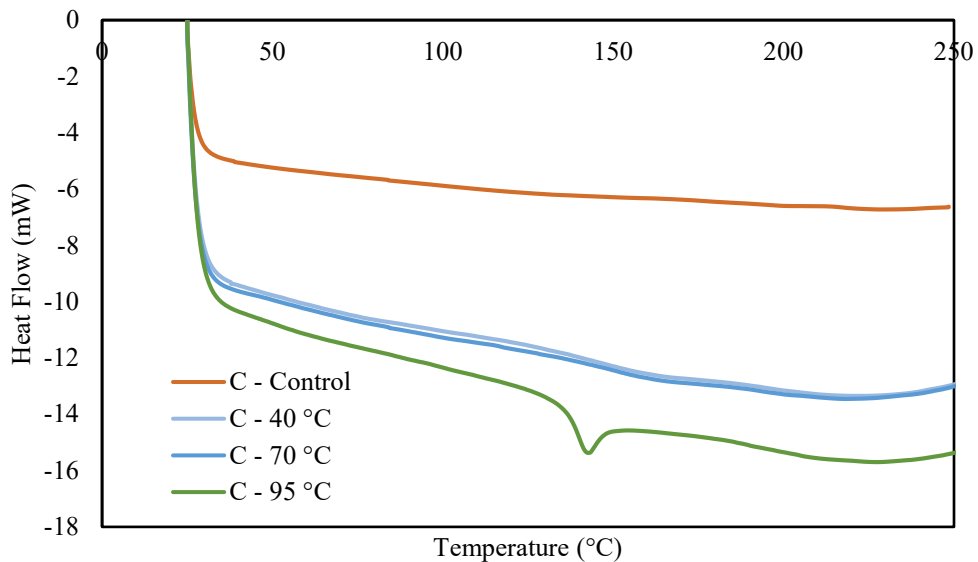
(a)
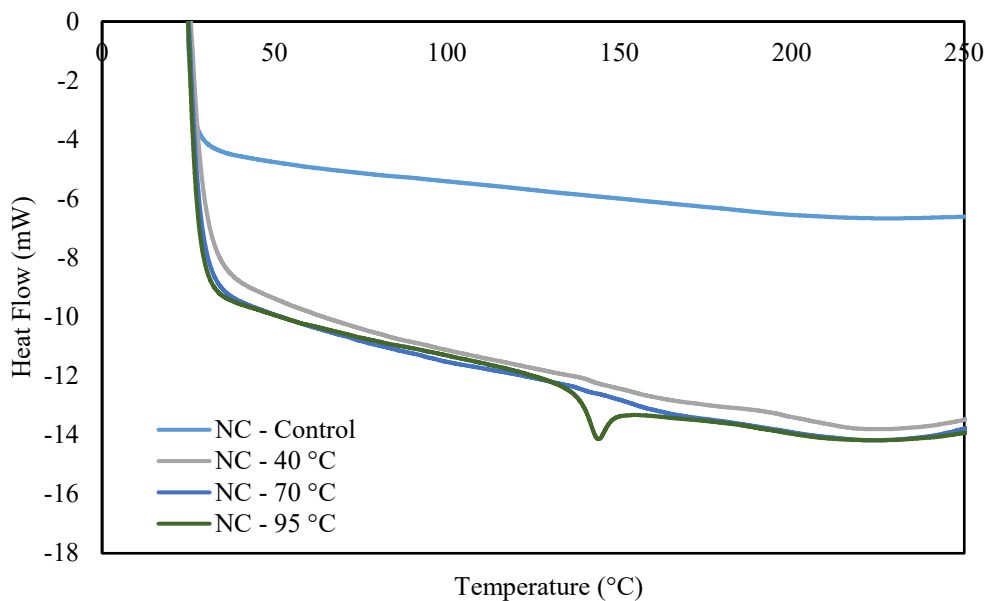
(b)

Figure 68: Heat flow vs temperature behavior of samples immersed at 40°C, 70°C and 95°C for the exposure of 10 months (a) Compacted (b) Non-Compacted

4.8 Dynamic Mechanical Analysis (DMA) Test

Figure 69 presents the storage modulus vs temperature curves for the compacted samples immersed at 40°C, 70°C and 95°C for the duration of 10 months. Three samples were tested for each condition.
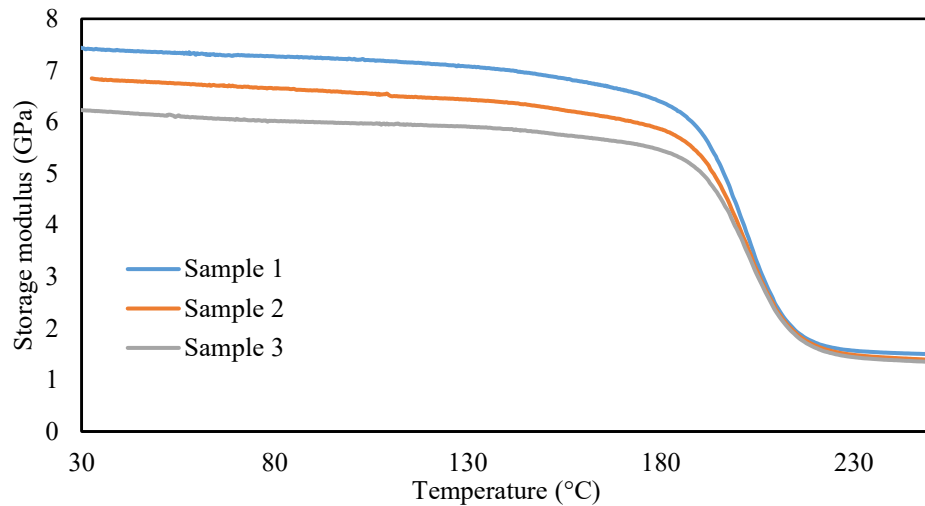
(a)
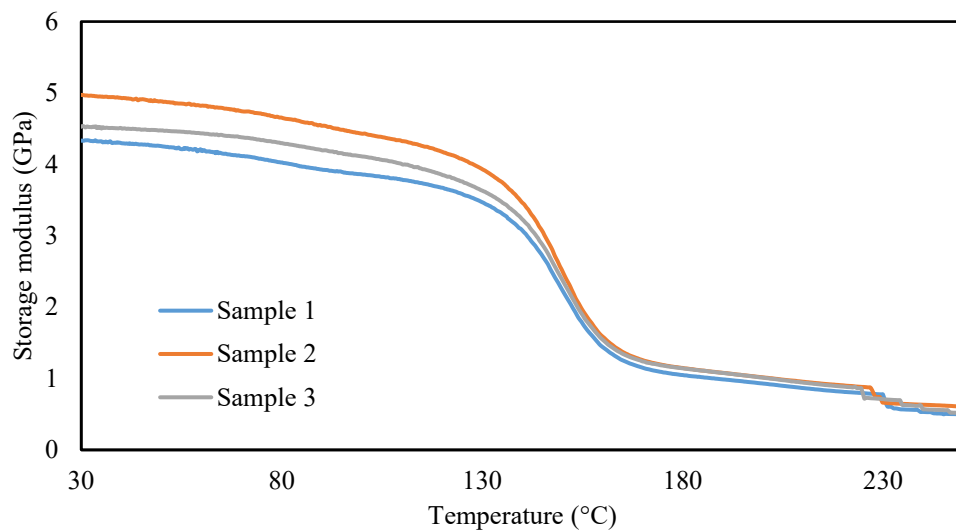
(b)

Figure 69: Storage modulus vs temperature behavior of compacted samples immersed for the exposure of 10 months at (a) Control samples (b) 40°C (c) 70°C (d) 95°C

(c)

(d)

Figure 69: Storage modulus vs temperature behavior of compacted samples immersed for the exposure of 10 months at (a) Control samples (b) 40°C (c) 70°C (d) 95°C (Continued)

Figure 70 presents the loss modulus vs temperature curves for the compacted samples immersed at 40°C, 70°C and 95°C for the duration of 10 months. Three

samples were tested for each condition. The presented curves indicated the reproducibility of the results.
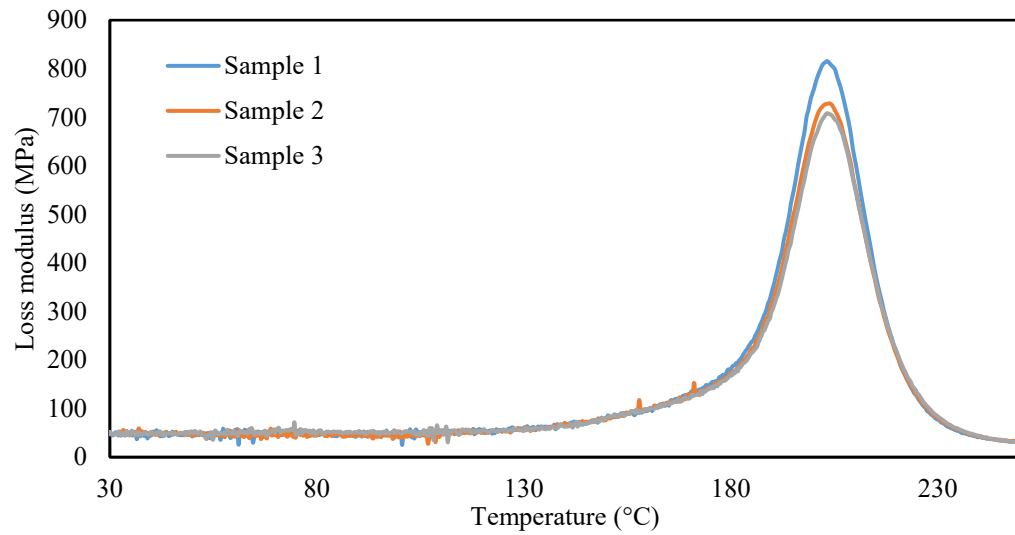
(a)
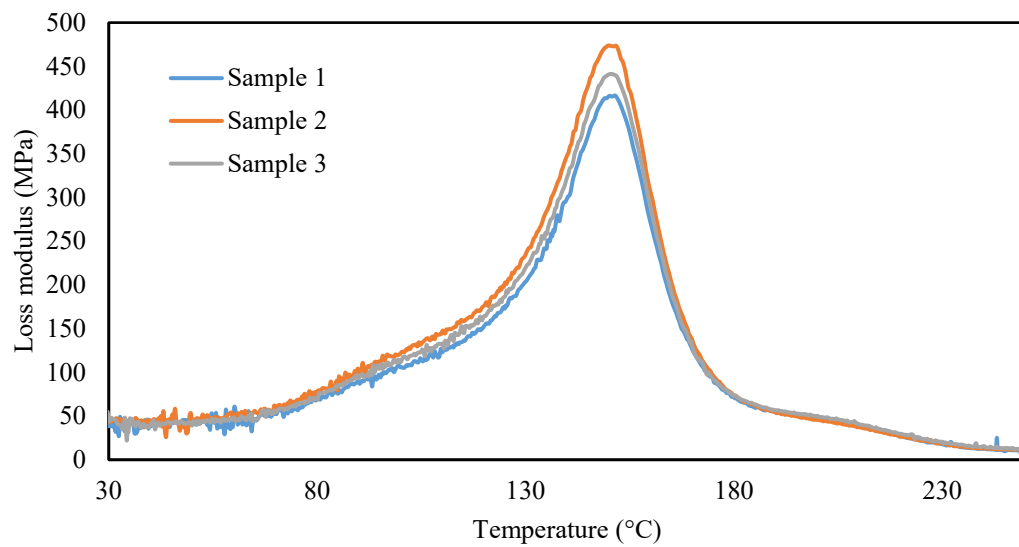
(b)

Figure 70: Loss modulus vs temperature behavior of compacted samples immersed for the exposure of 10 months at (a) Control samples (b) 40°C (c) 70°C (d) 95°C
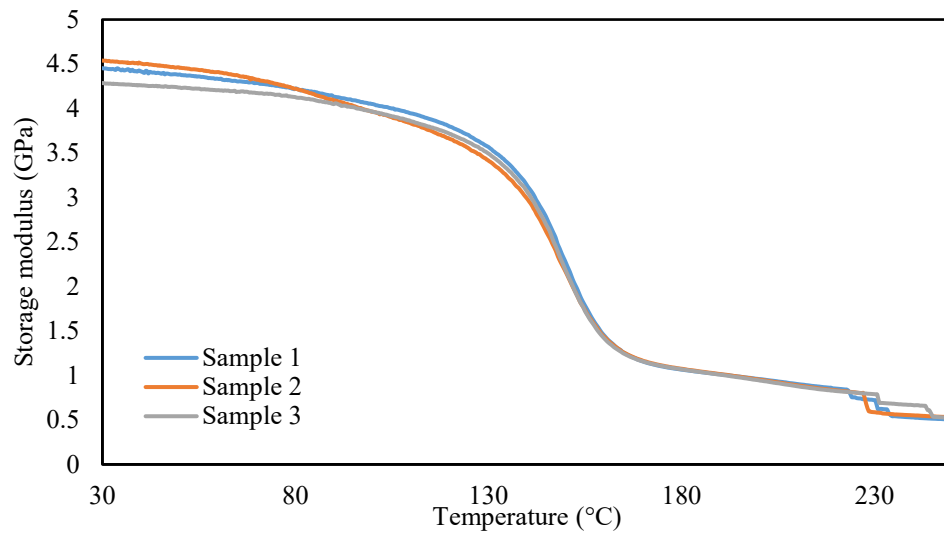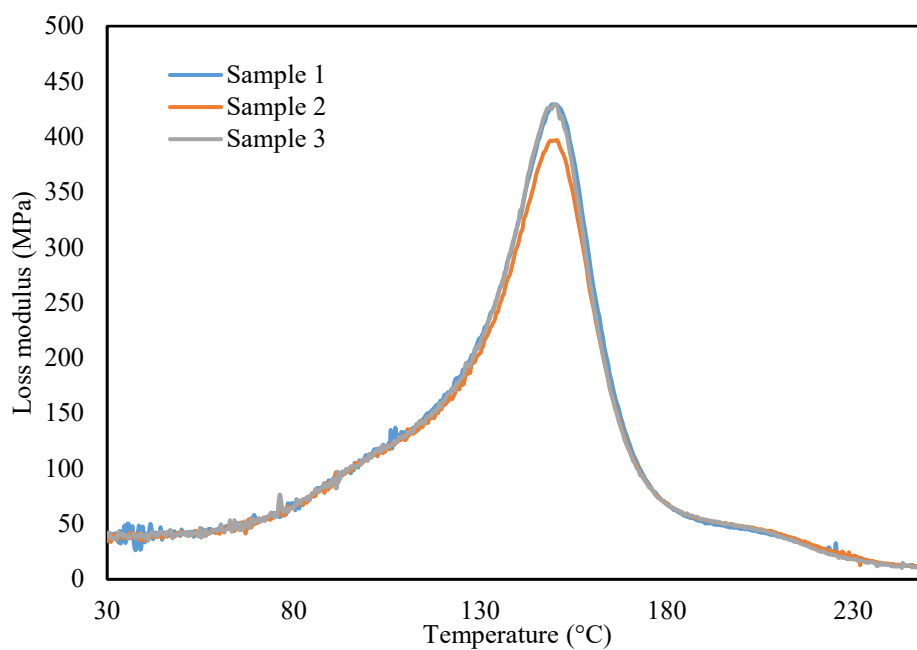
(c)
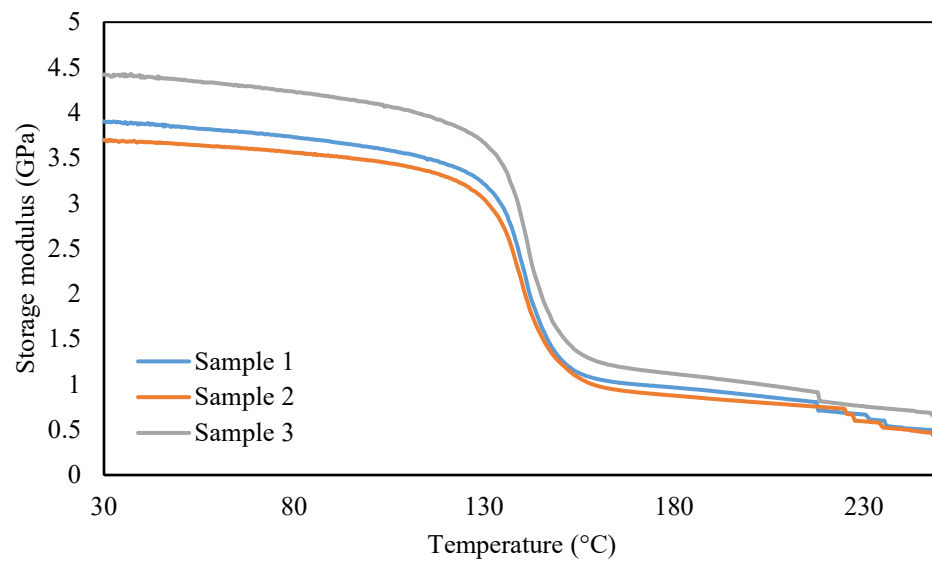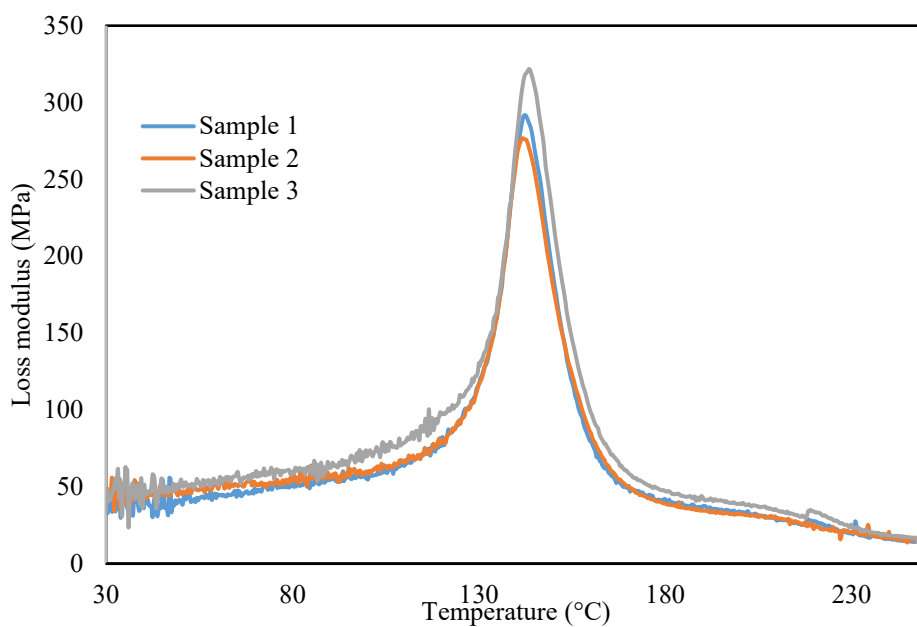

(d)

Figure 70: Loss modulus vs temperature behavior of compacted samples immersed for the exposure of 10 months at (a) Control samples (b) 40°C (c) 70°C (d) 95°C (Continued)

Figures 71 (a) and (b) represent the storage modulus versus temperature curves for the comparison of compacted and non-compacted sample immersed at 40°C, 70°C and 95°C. These samples were compared with the control sample for analyzing the effect of time and temperature on the durability of the samples.
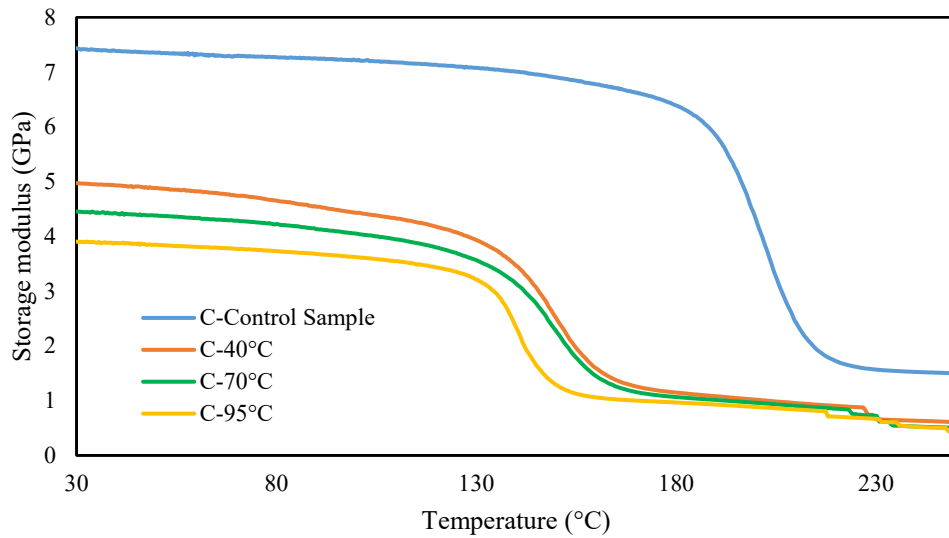
(a)
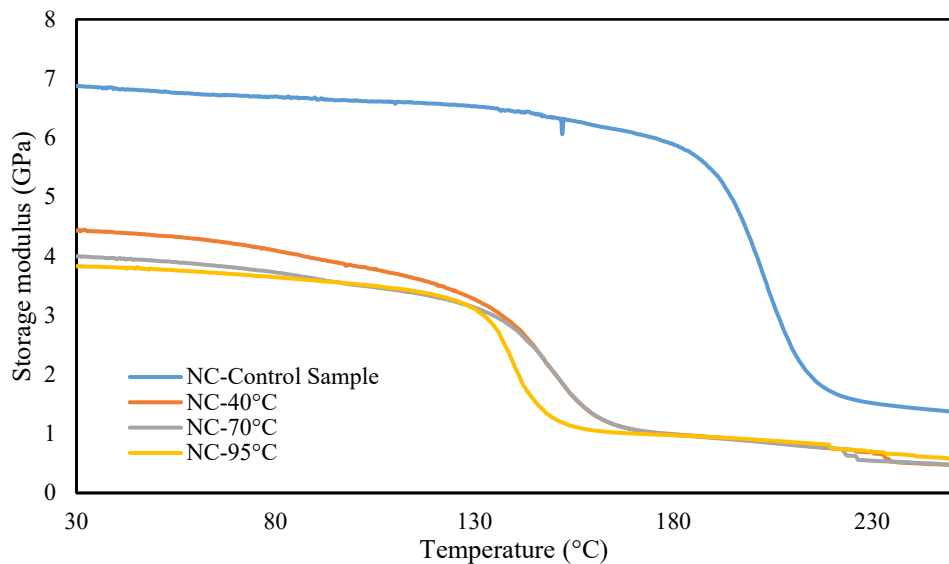
(b)

Figure 71: Storage modulus vs temperature behavior of control samples and samples immersed at 40°C, 70°C and 95°C for the exposure of 10 months (a) Compacted (b) Non-compacted

Figures 72 (a) and (b) represent the loss modulus versus temperature curves for the comparison of compacted and non-compacted sample immersed at 40°C, 70°C and 95°C. These samples were compared with the control sample for analyzing the effect of time and temperature on the durability of the samples.
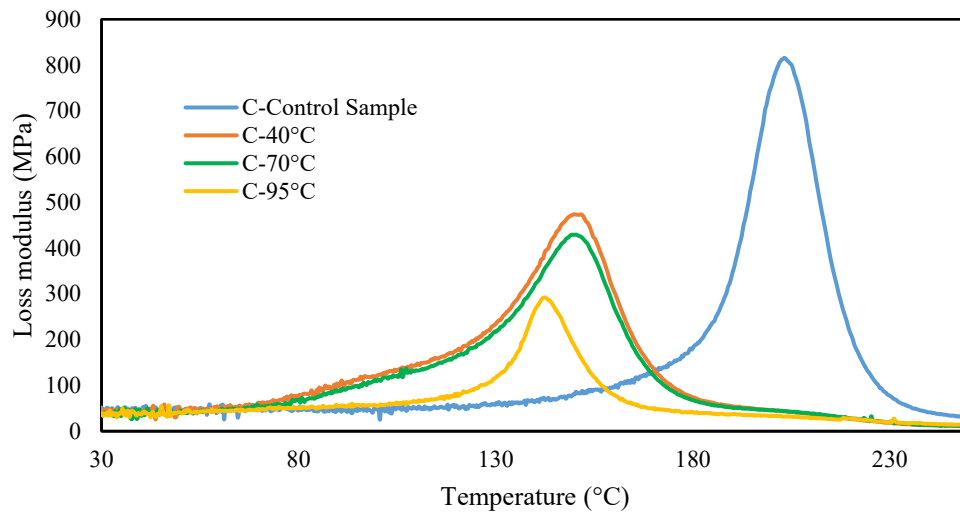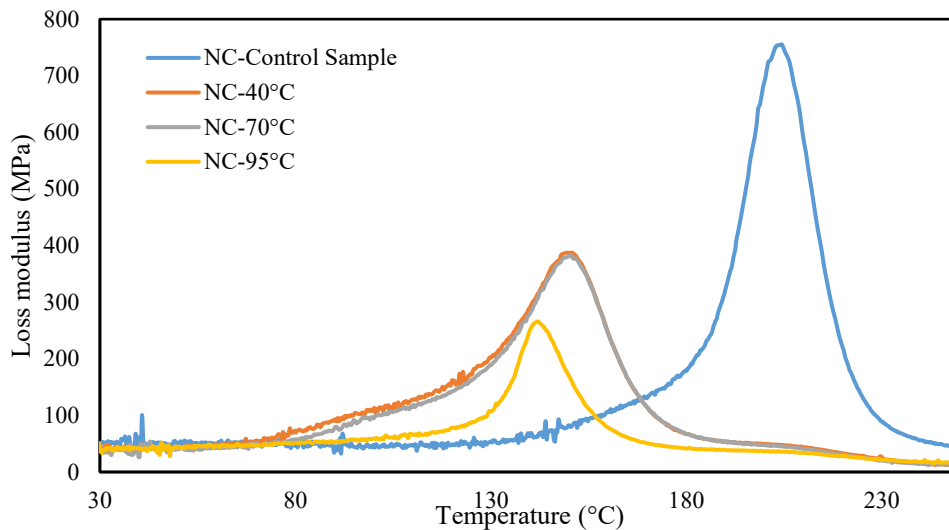

(a)

(b)

Figure 72: Los modulus vs temperature behavior of control samples and samples immersed at 40°C, 70°C and 95°C for the exposure of 10 months (a) Compacted (b) Non-compacted

(a)

(b)
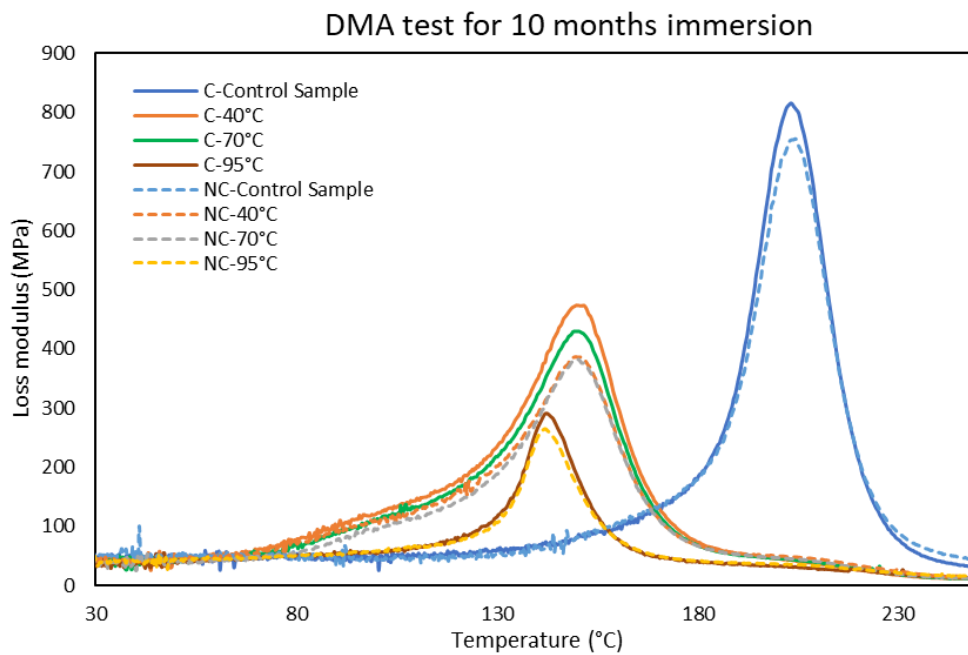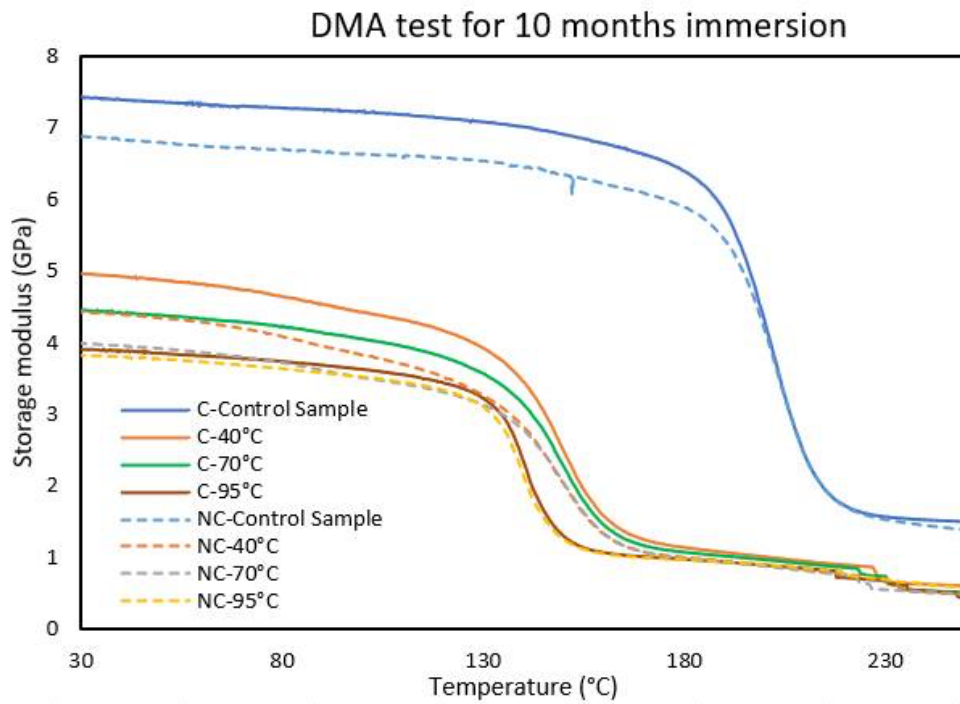
Figure 73: Comparison between compacted and non-compacted (a) Storage modulus (b) Loss modulus

Figures 73 (a) and (b) represent the storage modulus and loss modulus versus temperature curves for the comparison of compacted and non-compacted sample immersed at 40°C, 70°C and 95°C for the duration of 10 months. These samples compared with the control sample for analyzing the effect of time and temperature on the durability of the samples.

A typical DMA curve of the control compacted and non-compacted specimen is shown in Figure 73, together with a DMA scan of specimen aged for 10 months in water at 40°C, 70°C and 95°C. The storage modulus and loss modulus are plotted against temperature. Figure 73 (a) shows, the compacted specimens have improved modulus as compared to the non-compacted samples. The control compacted and non-compacted samples are stable up to 193.8°C and 194.7°C after which glass transition begins. The storage modulus of both type of composites reduced with immersion at different temperatures for the duration of 10 months. The storage modulus of compacted samples was 7.44 GPa for the control, 4.99 GPa, 4.46 GPa, and 3.92 GPa for the samples immersed at 40°C, 70°C and 95°C respectively for the period for 10 months, whereas for the non-compacted samples it was 6.92 GPa for the control, 4.45 GPa, 4.02 GPa and 3.84 GPa for the similar conditions. It was observed that compacted samples immersed at 70°C have almost same storage modulus as non-compacted samples immersed at 40°C. The storage modulus reduced steeply after glass transition temperature, as expected, and found to be almost same for both groups.

As shown in Table 4, the glass transition temperature Tg for all conditioned samples lie between 142.6°C and 150.7°C in the loss modulus traces, whereas it was 203.3°C and 204.5°C for compacted and non-compacted samples respectively, as indicated by the peaks in Figure 73 (b). It was observed that control compacted sample

(815.74 MPa) had higher loss modulus as compared to control non-compacted sample (755.03 MPa). For samples immersed at 40°C, the loss modulus was reduced by 42% and 49% for compacted and non-compacted samples respectively, after the immersion of 10 months. The glass transition temperature dropped significantly to 142°C for the samples immersed at 95°C. The loss modulus reduced to 291.36 MPa and 265.97 MPa for compacted and non-compacted samples respectively.

Table 4: Glass transition temperature and loss modulus values from the DMA test

Sample	T_g (°C)	Loss Modulus (MPa)
C	203.275	815.7456898
C - 40°C	149.7875	473.7730742
C - 70°C	150.425	429.1999919
C - 95°C	142.6375	291.3645
NC	204.5	755.0328957
NC - 40°C	150.775	387.2813
NC - 70°C	150.375	383.0472328
NC - 95°C	142.05	265.9731717

The decrease of the glass transition temperature (T_g) is the result of the plasticizing effect of the absorbed moisture that induces plastic deformation in the matrix [11], [12], and could be due to the due to the disruption of the hydrogen bonds in the epoxy resin [25]. This effect is generally reversible when the absorbed water is removed, however exposure to water at elevated temperatures can cause irreversible impacts, due to the chemical degradation of the matrix and to the deteriorative effect

on the fiber/resin interface [12], [28] which increases internal voids and promotes microcrack formation [12].

4.9 Scanning Electron Microscopy (SEM) Analysis

The fractured surfaces of tested samples were analysed using a Scanning Electron Microscope (SEM). Figure 74 and 75 represent the cross-section of the fiber of non-compacted and compacted specimen immersed at different temperatures for the period of 9 months. Control samples of non-compacted and compacted specimen show strong bonding between the fiber and the matrix as shown in Figures 74 (a) and 75 (a) respectively. Non-compacted samples immersed at 40°C has no effect on the durability of the fibre and matrix, whereas slight effect was observed on the samples immersed at 70°C, as shown in Figures 75 (b) and (c) respectively. At elevated temperature of 95°C, the slight separation of the fibre and matrix flow was observed as shown in Figure 74 (d), moreover circular voids are observed indicating the occurrence of fiber pull out due to weakening of the interfacial bonding. Compacted samples immersed at 40°C and 70°C had almost no effect on the durability of the composite, as shown in Figures 75 (b) and 75 (c). Slightly loose bonding observed for the samples immersed at 95°C as shown in Figure 75 (d) however, the fiber, itself, remained unaffected. This is an indication of matrix disintegration due to the hydrolysis reaction which is accelerated in hot environment, thus leading to a non-uniform distribution of loads among the fibers [48], [54].
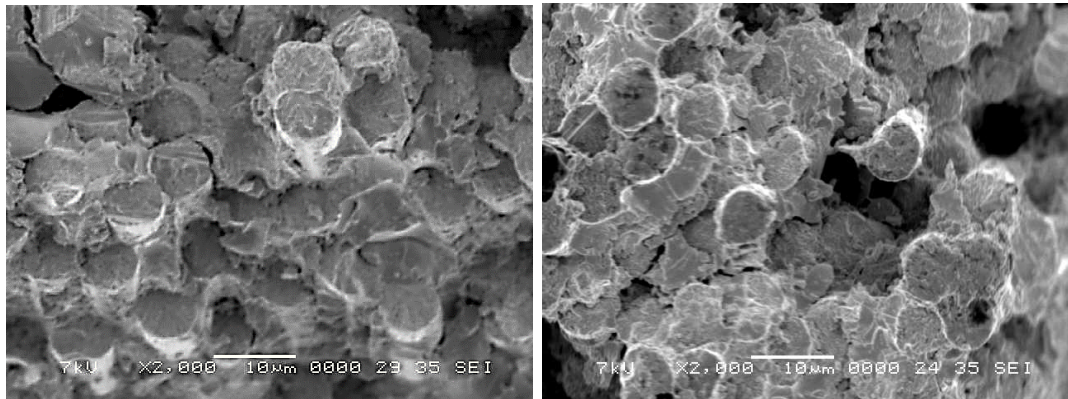
(a)

(b)
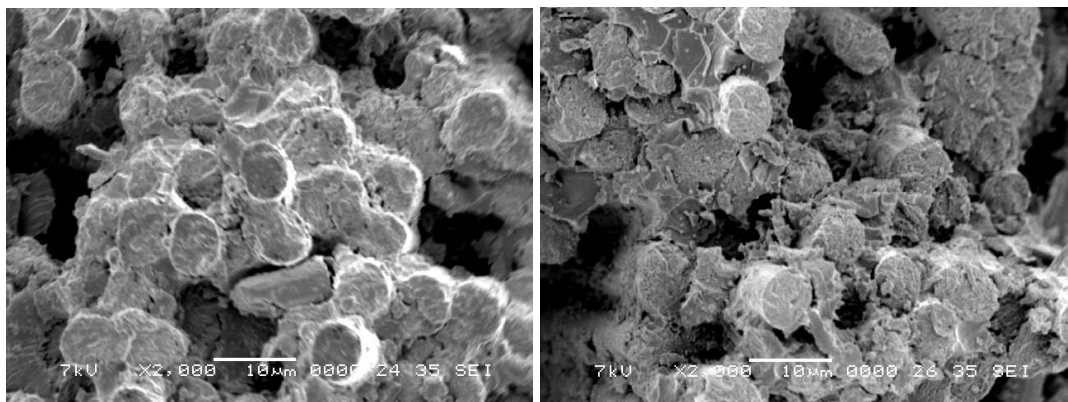
(c)

(d)

Figure 74: SEM of fractured surface of non-compacted samples (a) Control (b) 40°C (c) 70°C (d) 95°C

(a)   (b)

(c)   (d)
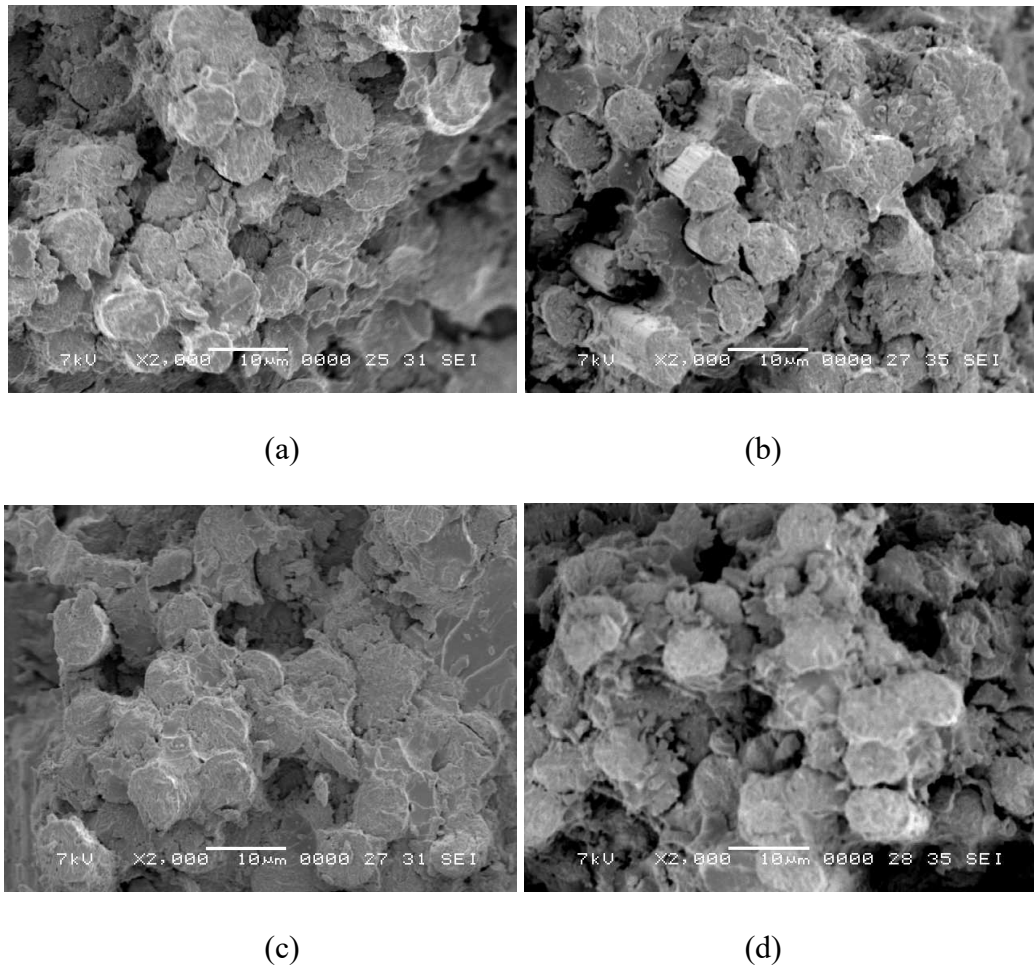
Figure 75: SEM of fractured surface of compacted samples (a) Control (b) 40°C (c) 70°C (d) 95°C

As a woven type composite is used in this study, the orientation of the fiber bonding between the vertical (90°) and horizontal (0°) fibres was also observed as shown in Figures 76 and 77. The bonding between the vertical and horizontal fibre was intact for the control sample of compacted and non-compacted. The bonding between the non-compacted fibres at the interface reduced with the increase of temperature from 40°C to 95°C as shown in Figures 76 (b), (c) and (d). The effect of the temperature was significantly lower in the compacted samples immersed at different temperatures, as shown in Figure 77 (b), (c) and (d).

(a)

(b)

(c)

(d)

Figure 76: Effect of water immersion on the interface of the fibers of non-compacted samples (a) Control (b) 40°C (c) 70°C (d) 95°C
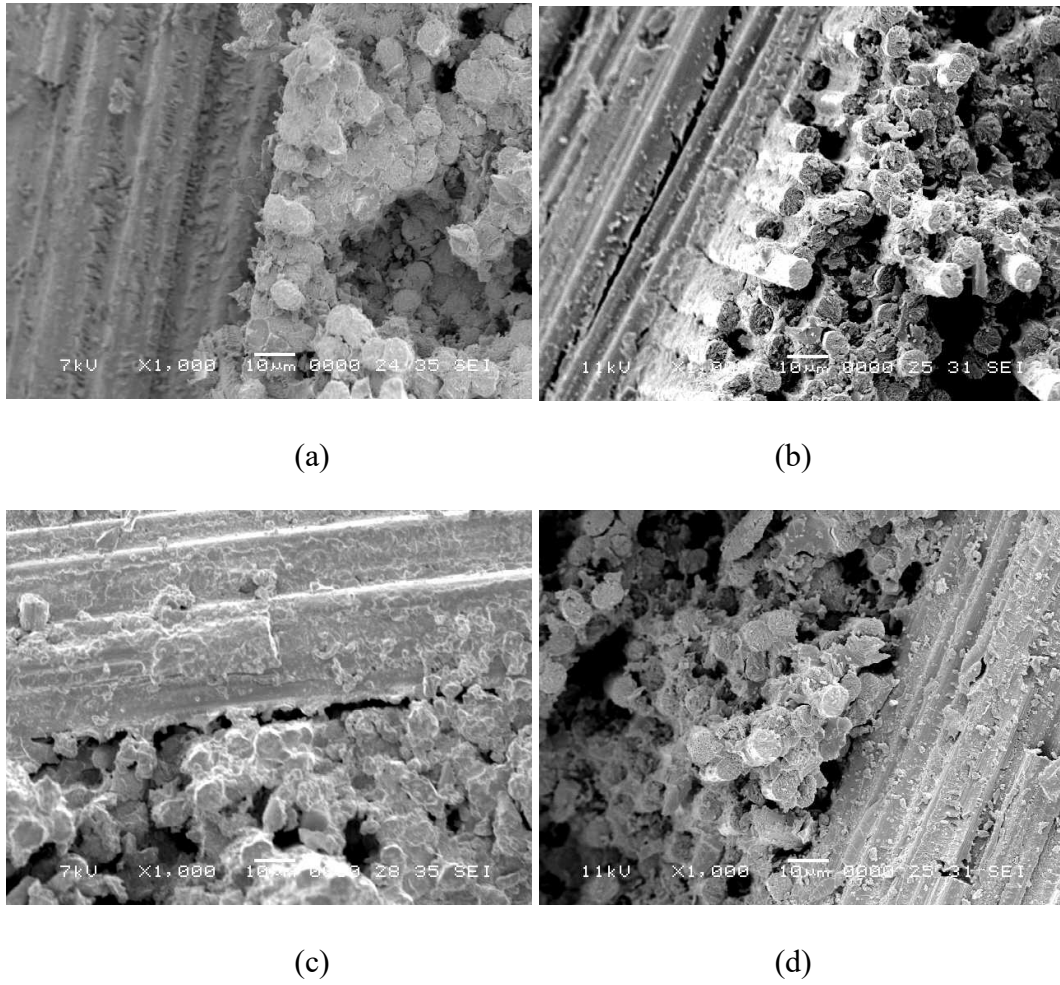
(a)

(b)

(c)

(d)
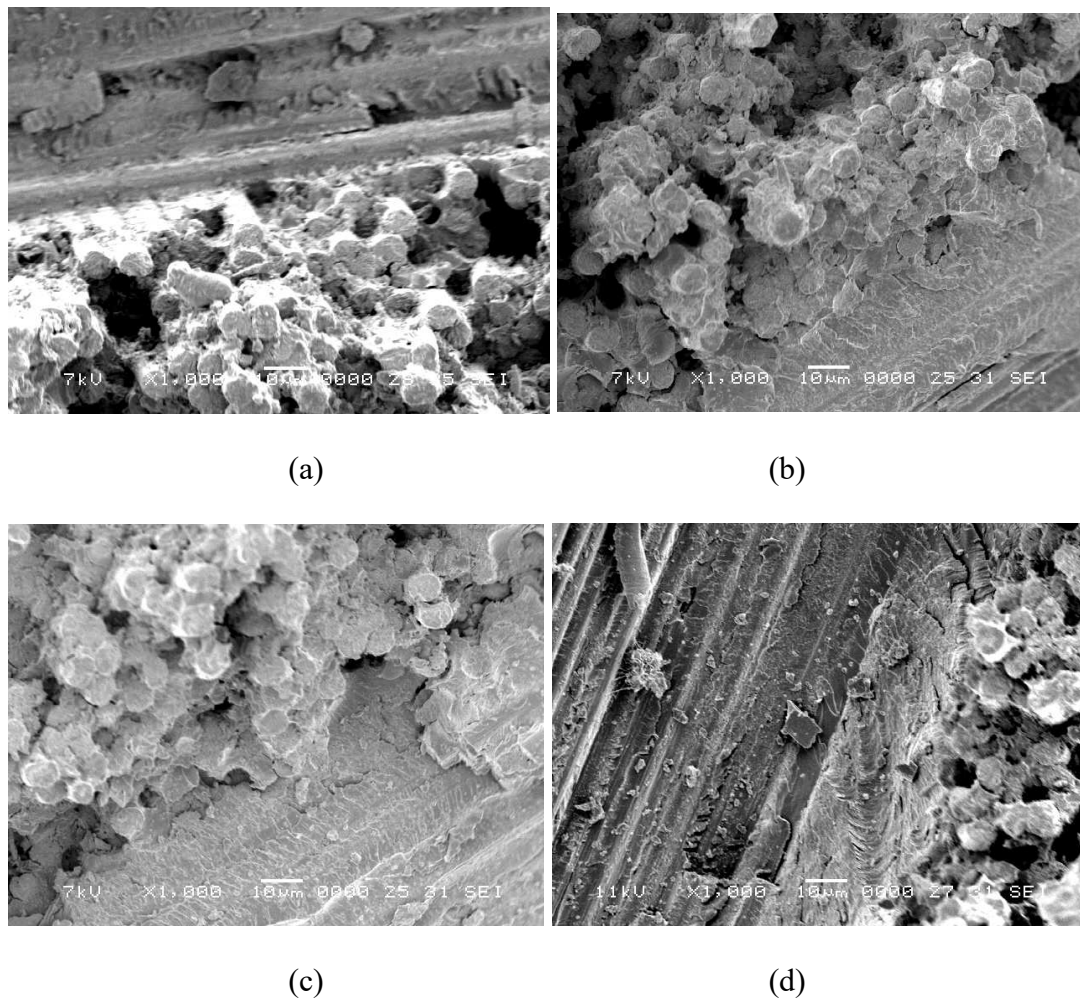
Figure 77: Effect of water immersion on the interface of the fibers of compacted samples (a) Control (b) 40°C (c) 70°C (d) 95°C

Chapter 5: Conclusion

In this research, the impact of different environmental conditions on the thermomechanical behavior of compacted and non-compacted carbon/epoxy plain weave woven laminated composites was investigated. Compacted and non-compacted samples were fabricated consisting of 12 composite layers and were immersed in water for different period of times at different exposure temperatures of 40°C, 70°C, and 95°C. The durability of the composite material was investigated by conducting mechanical, thermal, microstructural and physical tests. Results indicated an insignificant difference on the thermomechanical properties between compacted and non-compacted specimens at the immersion temperatures of 40°C and 70°C, but slight degradation was observed at the immersion temperature of 95°C. Results suggest that in-process compaction and application of edge/surface breathing for the twelve-ply monolithic laminate may be required at high temperature applications, while it may not be necessary for lower temperature applications.

The major findings of the experimental testing of the project are as follows:

- The void volume fraction of compacted control samples, C1 and C2, had a void content of 0.085% and 0.052% respectively, while the non-compacted control samples, NC1 and NC2 had slightly higher values of 0.139% and 0.460% respectively. Although the non-compacted control group showed a slightly higher void content than the compacted control group, both groups were accepted as indicated by the NDT results in accordance with the 6 dB drop method.

- Absorption of water increased gradually with immersion time for all samples. The highest increase of weight was by 2.52% and 2.82% for compacted and non-compacted samples, respectively immersed at the highest exposure temperature

of 95°C after the immersion of 9 months. It was observed that higher temperatures accelerated the absorption process.

- The tensile strength of the samples reduced gradually with time and immersion temperature. However, non-compacted samples immersed at 95°C displayed the highest decrease in the strength from 593 MPa to 504.8 MPa. Similar behavior observed for three-point flexural test where flexural strength reduced by 3 % and 7.6% for compacted and non-compacted samples respectively immersed at 95°C for the period of 10 months.

- The interlaminar shear strength of the compacted samples reduced by 10.3%, 12.4%, and 17.3% whereas it reduced by 11.3%, 12.6% and 17.2% for non-compacted samples after the immersion of 10 months at 40°C, 70°C and 95°C respectively.

- The immersion had the same effect on both type of the samples and only slight variation was observed. Tg of compacted samples reduced from 203.3°C to 149.8°C, 150.4°C and 142.6°C after immersion period of 10 months at 40°C, 70°C and 95°C. Similarly, the Tg of non-compacted samples reduced from 204.5°C to 150.8°C, 150.4°C and 142.1°C after immersion period of 10 months at 40°C, 70°C and 95°C.

- SEM results showed no effect on the durability of compacted and non-compacted samples immersed at 40°C and 70°C. However, at 95°C, slight separation of the fibre and matrix was observed with loose bonding at fibre/matrix interface.

Recommendations:

- Based on the test performed on the twelve-ply composite specimen, results indicated an insignificant difference on the thermomechanical properties between compacted and non-compacted specimens at the immersion temperatures of 40°C and 70°C, however slight degradation was observed at the immersion of 95°C, therefore it would be economical for the company to consider not applying compaction for a twelve-ply flat panel when used at practical temperature applications.

- Extend this study to consider composite panels having higher number of plies (more than 12 layers), and more complex geometries.

- Extend this study to consider evaluating the long-term impact of sub-zero temperatures on the composite material.

References

[1]   M. K. Hossain, K. A. Imran, M. V. Hosur, and S. Jeelani, "Degradation of mechanical properties of conventional and nanophased carbonepoxy composites in seawater," *J. Eng. Mater. Technol. Trans. ASME*, vol. 133, no. 4, pp. 1–6, 2011, doi: 10.1115/1.4004691.

[2]   S. R. Patel, "Durability of advanced woven polymer matrix composites for aerospace applications,", M.A.thesis, Virginia Polytechnic Institute and State University, 1999.

[3]   W. G. Roeseler, B. Sarh, M. U. Kismarton, J. Quinlivan, J. Sutter, and D. Roberts, "Composite structures: the first 100 years," in *16th International Conference on Composite Materials*, Kyoto, Japan, 2007.

[4]   J. Lowe, "Aerospace applications," *Des. Manuf. Text. Compos.*, pp. 405–423, 2005, doi: 10.1533/9781845690823.405.

[5]   S. Rana and R. Fangueiro, *Advanced composites in aerospace engineering*, vol. 2023. Elsevier Ltd, 2016.

[6]   "Glossary of composite terms | Fibre Glast." https://www.fibreglast.com/product/glossary-of-terms-in-composites/Learning_Center (accessed Sep. 02, 2020).

[7]   M. P. Thompson, "How vacuum bags really work: The myth of volatiles and breathers," *Int. SAMPE Tech. Conf.*, vol. 30, pp. 201–212, 1998.

[8]   M. H. Al Kuwaiti and A.-H. I. Mourad, "Thermomechanical characteristics of compacted and non-compacted plain weave woven laminated composites," in *Volume 3A: Design and Analysis*, Jul. 2017, pp. 1–6, doi: 10.1115/PVP2017-65764.

[9]   "Vacuum bagging." https://www.fibreglast.com/category/Vacuum_Bagging (accessed Oct. 02, 2020).

[10]   P. D. Mangalgiri, "Composite materials for aerospace applications," *Bull. Mater. Sci.*, vol. 22, no. 3, pp. 657–664, 1999, doi: 10.1007/BF02749982.

[11]   B. C. Ray, "Temperature effect during humid ageing on interfaces of glass and carbon fibers reinforced epoxy composites," *J. Colloid Interface Sci.*, vol. 298, no. 1, pp. 111–117, 2006, doi: 10.1016/j.jcis.2005.12.023.

[12]   S. Akbar and T. Zhang, "Moisture diffusion in carbon/epoxy composite and the effect of cyclic hygrothermal fluctuations: Characterization by Dynamic Mechanical Analysis (DMA) and Interlaminar Shear Strength (ILSS)," *J. Adhes.*, vol. 84, no. 7, pp. 585–600, 2008, doi: 10.1080/00218460802255434.

[13]   S. Koshima, S. Yoneda, N. Kajii, A. Hosoi, and H. Kawada, "Evaluation of strength degradation behavior and fatigue life prediction of plain-woven carbon-fiber-reinforced plastic laminates immersed in seawater," *Compos. Part A Appl. Sci. Manuf.*, vol. 127, no. August, p. 105645, 2019, doi: 10.1016/j.compositesa.2019.105645.

[14]   F. Almudaihesh, K. Holford, R. Pullin, and M. Eaton, "The influence of water absorption on unidirectional and 2D woven CFRP composites and their mechanical performance," *Compos. Part B Eng.*, vol. 182, no. November 2019, p. 107626, 2020, doi: 10.1016/j.compositesb.2019.107626.

[15]   P. Hubert and A. Poursartip, "Aspects of the compaction of composite angle laminates: An experimental investigation," *J. Compos. Mater.*, vol. 35, no. 1, pp. 2–26, 2001, doi: 10.1177/002199801772661849.

[16]   M. H. H. Al-Kuwaiti and A.-H. I. Mourad, "Effect of different environmental conditions on the mechanical behavior of plain weave woven laminated composites," in *Procedia Engineering*, 2015, vol. 130, doi: 10.1016/j.proeng.2015.12.285.

[17]   "Compositeslab." http://compositeslab.com/composites-101/what-are-composites/ (accessed Oct. 02, 2020).

[18]   "Polymers for aerospace structures," *Introd. to Aerosp. Mater.*, pp. 268–302, 2012, doi: 10.1533/9780857095152.268.

[19]   S. Erden and K. Ho, "Fiber reinforced composites," *Fiber Technol. Fiber-Reinforced Compos.*, pp. 51–79, 2017, doi: 10.1016/B978-0-08-101871-2.00003-5.

[20]   L. A. Khan, A. Nesbitt, and R. J. Day, "Hygrothermal degradation of 977-2A carbon/epoxy composite laminates cured in autoclave and Quickstep," *Compos. Part A Appl. Sci. Manuf.*, vol. 41, no. 8, pp. 942–953, 2010, doi: 10.1016/j.compositesa.2010.03.003.

[21]   P. Sun, Y. Zhao, Y. Luo, and L. Sun, "Effect of temperature and cyclic hygrothermal aging on the interlaminar shear strength of carbon fiber/bismaleimide (BMI) composite," *Mater. Des.*, vol. 32, no. 8–9, pp. 4341–4347, 2011, doi: 10.1016/j.matdes.2011.04.007.

[22]   J. M. F. De Paiva, S. Mayer, and M. C. Rezende, "Evaluation of mechanical properties of four different carbon/epoxy composites used in aeronautical field," *Mater. Res.*, vol. 8, no. 1, pp. 91–97, 2005, doi: 10.1590/s1516-14392005000100016.

[23]   B. Vieille, J. Aucher, and L. Taleb, "Comparative study on the behavior of woven-ply reinforced thermoplastic or thermosetting laminates under severe environmental conditions," *Mater. Des.*, vol. 35, pp. 707–719, 2012, doi: 10.1016/j.matdes.2011.10.037.

[24] P. N. B. Reis, M. A. Neto, and A. M. Amaro, "Effect of the extreme conditions on the tensile impact strength of GFRP composites," *Compos. Struct.*, vol. 188, no. August 2017, pp. 48–54, 2018, doi: 10.1016/j.compstruct.2018.01.001.

[25] Y. Li, R. Li, L. Huang, K. Wang, and X. Huang, "Effect of hygrothermal aging on the damage characteristics of carbon woven fabric/epoxy laminates subjected to simulated lightning strike," *Mater. Des.*, vol. 99, pp. 477–489, 2016, doi: 10.1016/j.matdes.2016.03.030.

[26] H. N. Narasimha Murthy, M. Sreejith, M. Krishna, S. C. Sharma, and T. S. Sheshadri, "Seawater durability of epoxy/vinyl ester reinforced with glass/carbon composites," *J. Reinf. Plast. Compos.*, vol. 29, no. 10, pp. 1491–1499, 2010, doi: 10.1177/0731684409335451.

[27] S. R. Patel and S. W. Case, "Durability of hygrothermally aged graphite/epoxy woven composite under combined hygrothermal conditions," *Int. J. Fatigue*, vol. 24, no. 12, pp. 1295–1301, 2002, doi: 10.1016/S0142-1123(02)00044-0.

[28] A. Kootsookos and A. P. Mouritz, "Seawater durability of glass- and carbon-polymer composites," *Compos. Sci. Technol. TA - TT -*, vol. 64, no. 10, pp. 1503–1511, 2004, doi: 10.1016/j.compscitech.2003.10.019 LK - https://uaeu.on.worldcat.org/oclc/4929268601.

[29] *Accelerated aging of materials and structures*. Washington, D.C.: National Academies Press, 1996.

[30] Y. Weitsman, "Moisture in composites: sorption and damage," in *Composite Materials Series*, vol. 4, Elsevier, 1991, pp. 385–429.

[31] H. Jeong, "Effects of voids on the mechanical strength and ultrasonic attenuation of laminated composites," *J. Compos. Mater.*, vol. 31, no. 3, pp. 276–292, 1997, doi: 10.1177/002199839703100303.

[32] M. De Almeida, M. Cerqueira, and M. Leali, "The influence of porosity on the interlaminar shear strength of carbon / epoxy and carbon / bismaleimide fabric laminates," *Compos. Sci. Technol.*, vol. 61, pp. 2101–2108, 2001, [Online]. Available: https://ac.els-cdn.com/S0266353801001579/1-s2.0-S0266353801001579-main.pdf?_tid=a852931f-85dd-4c79-8ddb-35d52901e7b2&acdnat=1522153499_6e5d8b7a6cea0e20b7b173e9d627909b.

[33] P. A. Olivier, B. Î. Mascaro, P. Margueres, and F. Collombet, "CFRP with voids: Ultrasonic characterization of localized porosity, acceptance criteria and mechanical characteristics," in *16th International Conference on Composite Materials*, Kyoto, Japan, 2007.

[34] P. Olivier, J. P. Cottu, and B. Ferret, "Effects of cure cycle pressure and voids on some mechanical properties of carbon/epoxy laminates," *Composites*, vol. 26, no. 7, pp. 509–515, 1995, doi: 10.1016/0010-4361(95)96808-J.

[35] S. F. M. de Almeida and Z. dos S. N. Neto, "Effect of void content on the strength of composite laminates," *Compos. Struct.*, vol. 28, no. 2, pp. 139–148, 1994, doi: 10.1016/0263-8223(94)90044-2.

[36] M. L. Costa, S. F. M. De Almeida, and M. C. Rezende, "Critical void content for polymer composite laminates," *AIAA J.*, vol. 43, no. 6, pp. 1336–1341, 2005, doi: 10.2514/1.5830.

[37] L. Liu, B. M. Zhang, D. F. Wang, and Z. J. Wu, "Effects of cure cycles on void content and mechanical properties of composite laminates," *Compos. Struct.*, vol. 73, no. 3, pp. 303–309, 2006, doi: 10.1016/j.compstruct.2005.02.001.

[38] L. D. Bloom, M. A. Napper, C. Ward, and K. Potter, "On the evolution of the distribution of entrapped air at the tool/first ply interf'ace during lay-up and debulk," *Adv. Manuf. Polym. Compos. Sci.*, vol. 1, no. 1, pp. 36–43, 2015, doi: 10.1179/2055035914Y.0000000005.

[39] "Strata." https://www.mubadala.com/en/what-we-do/aerospace/strata (accessed Sep. 13, 2020).

[40] "Cycom 970 epoxy resin." Accessed: Sep. 02, 2020. [Online]. Available: https://www.e-aircraftsupply.com/MSDS/101733cytec CYCOM 970 tds.pdf.

[41] E. Cajon, "Hillside composites , LLC unidirectional vs . standard vs . quasi-isotropic plate hillside composites , LLC." [Online]. Available: https://cdn.shopify.com/s/files/1/0089/8813/1428/files/Standard_vs_Quasi_Iso tropic_vs_Uni_Directional_Carbon_Fiber_Plate.pdf?1042.

[42] A.-H. Mourad, H. Fouad, and R. Elleithy, "Impact of some environmental conditions on the tensile, creep-recovery, relaxation, melting and crystallinity behaviour of UHMWPE-GUR 410-medical grade," *Mater. Des.*, vol. 30, no. 10, pp. 4112–4119, 2009.

[43] A.-H. I. Mourad, "Thermo-mechanical characteristics of thermally aged polyethylene/polypropylene blends," *Mater. Des.*, vol. 31, no. 2, pp. 918–929, 2010.

[44] "Standard test method for tensile properties of polymer matrix composite materials ," ASTM Standard D 3039/D 3039M, 2002.

[45] "Standard test method for flexural properties of unreinforced and reinforced plastics and electrical insulation materials," ASTM Standard D 790-03, 2015.

[46] S. Rao, M. Al Kuwaiti, V. Barber, A. Abusafieh, and W. J. Cantwell, "Effect of dwell time on the properties of composite materials," in 17th European Conference on Composite Materials, Munich, Germany, 2016.

[47] M. Xie, Z. Zhang, Y. Gu, M. Li, and Y. Su, "A new method to characterize the cure state of epoxy prepreg by dynamic mechanical analysis," *Thermochim. Acta*, vol. 487, no. 1–2, pp. 8–17, 2009.

[48] A.-H. I. Mourad, B. M. Abdel-Magid, T. El-Maaddawy, and M. E. Grami, "Effect of seawater and warm environment on glass/epoxy and glass/polyurethane composites," *Appl. Compos. Mater.*, vol. 17, no. 5, pp. 557–573, 2010.

[49] P. Biswal, Pranab Reddy, B.N.Srinivasa M.Baruah, "Manufacturing aspects of fabrication of composite reference standard for NDT ultrasonic inspection," *AeroNDT*, no. Composite, pp. 3–5, 2016, [Online]. Available: https://www.ndt.net/article/aero2016/papers/PranabBiswal_BNSrinivasaReddy_PratimMBaruah.pdf.

[50] J. D. H. Hughes, "The carbon fibre/epoxy interface—a review," *Compos. Sci. Technol.*, vol. 41, no. 1, pp. 13–45, 1991.

[51] J. D. Garcia-Espinel, D. Castro-Fresno, P. Parbole Gayo, and F. Ballester-Muñoz, "Effects of sea water environment on glass fiber reinforced plastic materials used for marine civil engineering constructions," *Mater. Des.*, vol. 66, no. PA, pp. 46–50, 2015, doi: 10.1016/j.matdes.2014.10.032.

[52] A. J. Kinloch, *Adhesion and adhesives: science and technology*. London, Chapman and Hall, 1987.

[53] M. Kawagoe *et al.*, "Microspectroscopic evaluations of the interfacial degradation by absorbed water in a model composite of an aramid fibre and unsaturated polyester," *Polymer (Guildf).*, vol. 40, no. 6, pp. 1373–1380, 1999.

[54] M. Robert, P. Cousin, and B. Benmokrane, "Durability of GFRP reinforcing bars embedded in moist concrete," *J. Compos. Constr.*, vol. 13, no. 2, pp. 66–73, 2009.

List of Publications

Al-Kuwaiti, M. H., and A. H. I. Mourad. "Thermomechanical Characteristics of Compacted and Noncompacted Plain Weave Woven Laminated Composites." *American Society of Mechanical Engineers, Pressure Vessels and Piping Division (Publication) PVP*, vol. 3A-2017, 2017, doi:10.1115/PVP2017-65764.

Al-Kuwaiti, M. H. H., and A. H. I. Mourad. "Effect of Different Environmental Conditions on the Mechanical Behavior of Plain Weave Woven Laminated Composites." *Procedia Engineering*, vol. 130, 2015, pp. 638–43, doi:10.1016/j.proeng.2015.12.285.